2004

Determination of the equivalent thickness of base layer of flexible pavement reinforced by geogrid.

Md Badruzzaman
University of Windsor

DETERMINATION OF THE EQUIVALENT THICKNESS OF BASE LAYER OF FLEXIBLE PAVEMENT REINFORCED BY GEOGRID

By

Md. Badruzzaman

A Thesis

Submitted to the Faculty of Graduate Studies and Research through

The Department of Civil and Environmental Engineering

In Partial Fulfillment of the Requirements for the

Degree of Master of Applied Science at the

University of Windsor

Windsor, Ontario, Canada

2004

Your file Votre référence
ISBN: 0-612-92488-2
Our file Notre référence
ISBN: 0-612-92488-2

I hereby declare that I am the sole author of this document.

I authorize the University of Windsor to borrow or photocopy of this document to other institution or individuals for the purpose of research activities.

_____

(Md. Badruzzaman)

ABSTRACT

This thesis presents a numerical analysis for the determination of the equivalent thickness of a homogeneous base layer of an unreinforced multilayered system subjected to the repetitive loadings of a constant value. The system demonstrates the same performance as the analogous multilayered system does which contains the geogrid inclusion as reinforcement in the placement of interest of the base layer.

The constitutive model adopted in the analysis is the modification of the small displacement theory of elastic continuum. Employing the proposed constitutive model the permanent modulus in each homogeneous isotropic layer of the unreinforced multilayered systems is determined for each sequent loading. It is done by the implementation of the Finite Element Method with respect to spatial variables. The same approach is used in analysis of reinforced multilayered systems in which geogrid is placed. In numerical simulation, the layer with geogrid inclusion is considered to be made of homogeneous material.

For each single loading the difference of displacements at arbitrary but corresponding control points of the unreinforced and reinforced system is defined as the first variation of the displacement. Based on the given variation of permanent displacement it is possible to determine the increment of the thickness of the layer of interest being the part of the unreinforced multilayered system that should be superposed to the original thickness of

the layer of unreinforced system. This yields the same deformations as the reinforced multilayered system does.

The performances of both systems (i.e., unreinforced and reinforced) are described in terms of unrecoverable deformations that are conducted in the framework of sensitivity theory. To preserve the unrecoverable features of deflections, the geometry of the problem is to be updated after each load application. The required performance functionals of the unreinforced and the reinforced systems are formulated based on the virtual work principle. To perform the required operation, the adjoint system is introduced. The difference of these two performance functionals due to variation of the boundary's shifts of the base layer is investigated. This is done by introducing the concept of functional with moving ends.

ACKNOWLEDGEMENTS

I would like to acknowledge my deepest gratitude and indebtedness to Dr. B.B. Budkowska, Professor, Department of Civil & Environmental Engineering, University of Windsor, for her keen interest in the research and her encouragement, sincere guidance, friendly supervision and valuable suggestion at every stage of my work. Without her continuous help, this research would not be possible to be accomplished within such a short period. So I wish to express my special thanks and respect to Dr. B.B. Budkowska.

In addition, I also would like to thank to Dr. Madugula, as internal reader from the Department of Civil & Environmental Engineering as well as Dr. Zamani, as external reader from the Department of Mechanical, Automative and Materials Engineering for their valuable suggestions during the evaluation of this thesis and the oral defense.

Lastly, I wish to thank my friends for their continuous support and encouragement during the entire progress of the work. Also, the gratitude is extended to my respectful parents for their continuous support and encouragement.

TABLE OF CONTENTS

LIST OF FIGURES

LIST OF TABLES

E_P = resilient modulus of permanent deformation

G_P = shear modulus of permanent deformation

ν = Poisson's ratio

σ_z, σ_r, σ_θ, τ_{rz} = the stress components (vertical, radial and circumferential normal stresses, shear stress respectively)

ε_r, ε_z, ε_θ, γ_{rz} = the permanent strain components (radial, vertical and circumferential normal, shear strain respectively)

ε_{ij} = strains of the primary system caused by application of load q

$\overline{\sigma_{ij}}$ = stresses of the adjoint system caused by the $\bar{1}$ applied to the point 1

v = displacement in the z direction

r = displacement in the r direction

ρ_{min} = minimum density

ρ_{max} = maximum density

C_u = uniformity co-efficient.

CHAPTER I

INTRODUCTION

1.1 General

The purpose of the pavement design is to carry the traffic load safely, conveniently and most economically over its design life without allowing any unacceptable deterioration and with its low maintenance cost. The design process consists of two different phases. First one is the determination of the thickness of the pavement layers having certain mechanical properties and the second one is the determination of the materials composition, which will provide these properties. The problem of the pavement design can be minimized by ensuring that the traffic loads are well distributed so that the stresses and strains developed at all layers of the pavement are within the capabilities of the materials strength at each layer.

Depending upon the mode of supporting and distributing loads, pavements are classified into three categories. They are flexible pavement, rigid pavement, and composite pavement. The topic of this research is only limited to discussion about the flexible pavement in detail and other two pavements will not be discussed.

Flexible pavements are able to resist only very small tensile stresses, whereas rigid pavement can take appreciable tensile stresses. A semi–flexible pavement possesses appreciable flexural strength but its modulus of elasticity is lower than that of concrete. The essential difference between rigid and flexible pavement is the manner in which they distribute the load over the subgrade. The design principle of flexible pavement is that

surface load is dissipated by carrying it deep into the ground through successive layer of granular materials. Hence the strength of a flexible layer is a result of building up thick layers and thereby distributing the load over the subgrade rather than by the bending action. The thickness design of the flexible pavement is influenced primarily by the strength of the subgrade.

Because of its rigidity and high tensile strength, a rigid pavement tends to distribute the load over a relatively wide area of soil and a major portion of the structural capacity is supplied by the slab itself. Rigid pavements are used for heavier loads and are constructed over relatively poor subgrade. But this subgrade should be uniform for the satisfactory performance since the load is taken up by the bending action of the slab. On the contrary, in the flexible pavements, a high quality, well-compacted subgrade is essential.

Flexible pavement is also called the asphalt pavement, which is generally constructed from bituminous and granular materials. There are three types of construction methods that are available for flexible pavements. They are conventional flexible pavement, full-depth asphalt pavement and contained rock asphalt mat (CRAM). Their geometrical configuration is illustrated in Figures 1.1 to 1.3. In this research we are interested to discuss about the conventional flexible pavement and the other two will not be focused in this research.

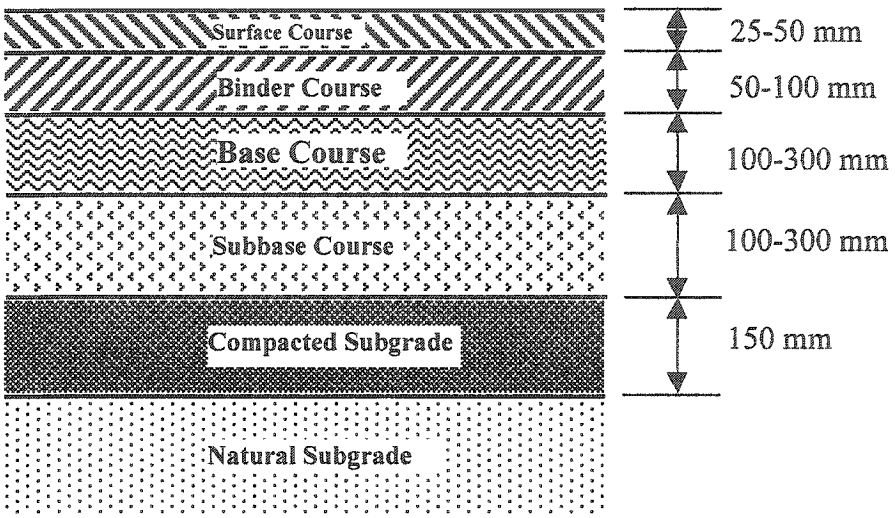

Figure 1.1 Typical cross section of a conventional pavement

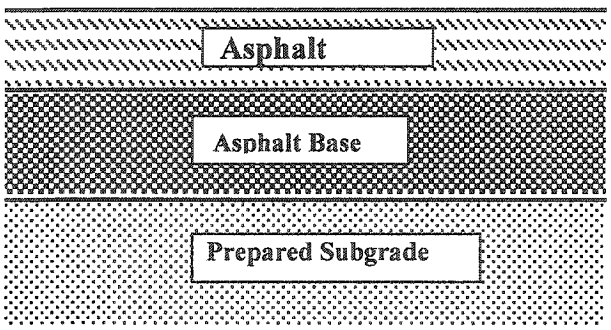

Figure 1.2 Typical cross section of a full-depth asphalt pavement

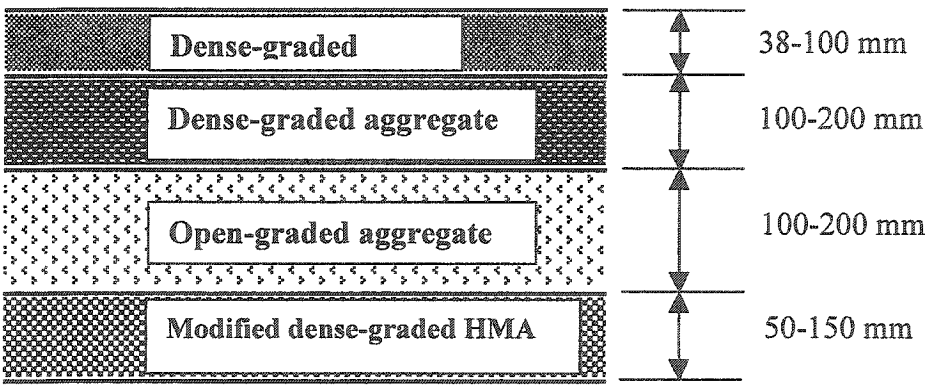

Figure 1.3 Typical CRAM cross-sections

Conventional flexible pavements are layered systems where the basic principle is that better materials are put on top due to high intensity of stress and inferior materials are put on the bottom for low intensity. This design principle results in the most economical design by using the local materials where it is readily available in a large quantity. From Figure 1.1, we can see that conventional flexible pavement consists of surface course, binder course, base course, subbase course, compacted subgrade and natural subgrade. Based on the necessity or economy some of the courses may be omitted. This thesis is strictly based on the laboratory experiment done by Moghaddas-Nejad and Small, 1996 (30), (where the number given in brackets throughout this thesis refer to References), which is limited to the three-layer conventional flexible pavement system. The three layers are described below:

Generally ***surface course*** is the top course of a bituminous pavement (asphalt pavement) and must be able to carry the high stress induced by traffic without unacceptable deformations and should provide a smooth and skid-resistant riding surface. Surface course should be flexible so that it will not fail if consolidation of the subgrade or base course takes place.

Base course is the main structural layer in the pavement whose purpose is to distribute the traffic loads so that the stresses and strains developed by them are within the capacity of the base materials. Hence it possesses high resistance to deformation in order to withstand the high pressure imposed upon it.

Subgrade is the lowest and foundation layer of the flexible pavement system and must be capable to support all the loads, which come on to the pavement. The performance of the pavement may be effected by the subgrade characteristics such as strength, drainage, and compaction. The strength can be increased by compaction or in some cases by stabilization.

Transportation engineers and managers continuously seek or are made aware of new products, materials and systems, which will " improve" pavements and bridges. "Improve" is a general term which may imply a reduced immediate or long term cost, an extension of service life, or a reduction of implementation (design/construction) time. Many new products and systems are proposed to provide a combination of these advantages. Geosynthetics are not a new material to the civil engineering or highway engineering. Since the earliest installations in the late 1950s, over 100 unique civil engineering applications have been successfully and routinely implemented. The success of geosynthetics can be traced to the following advantages: cost savings compared to conventional solutions, ease of construction, improved short term and long term performance, and ease of design and specification by knowledgeable users.

Normally in the investigation the general pavement variables considered are as follows: (1) pavement thickness, (2) type and stiffness of the geosynthetic reinforcement, (3) location of the reinforcement within the aggregate base, (4) quality of different components of pavement materials as defined by their permanent resilient modulus and permanent deformation characteristics, (5) slip at the interface between the geosynthetic

and surrounding materials, (6) pre-rutting the geosynthetic as a simple means of removing slack and providing a prestrecthing effect, and (7) prestressing the geosynthetic.

Potential improvement in performance is evidenced by an overall reduction in permanent deformation and hence the improvement in rutting and fatigue life of the pavement surface. Generally, for the laboratory test, pavement performance is assessed primarily by the permanent deformation induced by the traffic loads, including the total amount of surface rutting, and also the individual rutting in the base and subgrade. On the other hand, for the analytical studies, equivalent pavement designs are developed for geosynthetic reinforced structural sections and compared to similar sections without reinforcement. Finally an analytical procedure is used to evaluate the effects of geosynthetic reinforcement on permanent deformations.

In most flexible pavement systems, the stiffness of each layer is greater than that of the layer below and smaller than that of the layer above. According to this principle the weakest materials are placed in subgrade, the lowest layer of the pavement.

In general the load-distribution capacity of individual layers is a function of both their thickness and the mechanical stiffness of the materials in them. The overall thickness of the pavement as well as that of the individual layers depends on the traffic to be carried, the climate, the quality of subgrade, and the mechanical properties of the materials in the pavement layers.

The design principle of pavement system depends fundamentally on layers of materials; its rigidity, thickness and resistance to stresses induced by traffic volume. A general methodology for pavement design includes material properties, traffic volumes and climate information. Generally, flexible pavement design methods are classified into five categories: empirical method with or without a soil strength test, limiting shear failure method, limiting deflection method, regression method based on the pavement performance or load test, and mechanistic–empirical method. Besides these, some other methods such as serviceability, reliability and dynamic loading are also incorporated to the flexible pavement design in accordance to American Association of State Highway and Transportation Officials, AASHTO (5). All the design methods have their specific advantages and disadvantages, which limit their application under certain circumstances.

This research was carried out based on the technical literature (Moghaddas-Nejad and Small, 1996 (30)), which exclusively demonstrates the flexible pavement, more exactly the conventional flexible pavement with three-layered system as an experimental tool.

There are four design factors in flexible pavement: traffic and loading, environment, materials and failure criteria. Basically in flexible pavement design (e.g. for mechanistic empirical method), three principal types of distress are considered. They are fatigue cracking, rutting and low temperature cracking. In general the causes of failure in reinforced and unreinforced pavements are: 1) the accumulation of vertical permanent deformation throughout the structure (rutting), and 2) fatigue cracking of bound layers.

Fatigue is based on the horizontal tensile strain at the bottom of the surface layer where the failure criteria are related to the allowable number of load repetitions. Structural definition of fatigue is a cyclic time-dependent loading or straining of a material. This is associated with the resilient (recoverable) response of the pavement to transient loading. After a few thousand-load (allowable number) repetitions the resilient (recoverable) strains are of concern in the behavior of a pavement structure built on a reinforced or unreinforced granular layer. The allowable number of load repetitions in the field is much greater than that obtained from laboratory results mainly due to the difference in geometric and loading conditions and therefore it results in fatigue cracking. It's intensity also depends on the aging process of the road structure (infrastructure).

Rutting is one of the important failure criteria that generally occurs only on flexible pavements as a result of load repetition (number of passes) and is indicated by the permanent deformations or rut depth along the wheel paths. As a result rutting influences the performance of the pavement and then affecting the design life of the flexible pavement. There are two design methods available to control the rutting. One is to limit the vertical compressive strain on the top of subgrade and the other is to limit the rutting to a tolerable amount. Rutting can be reduced to a tolerable amount by limiting the vertical compressive strain, if the quality of the surface and base courses are well controlled according to design specifications or some specific standards.

Over the years, rut depth has been considered in assessing the quality of road sections and whether to take maintenance actions. Typically a rut 12 mm deep would require routine

maintenance, and a rut of 19 to 25 mm deep would require an overlay. In regions where softer binders are used, typically where great temperature differences occur, rutting may be the dominating distress, as well as a good indicator of the state of the road.

Crack propagation through a pavement base is one of the main causes of pavement deterioration. This can appear due to the environmental distress resulting from the movement in a subgrade as result of thermal expansion or shrinkage. The movement in a subgrade may create a discontinuity in the base layer. As aging occurs, the asphalt layer becomes more brittle and susceptible to cracking. The cracked asphalt–bound layer cannot provide as adequate load distribution on the granular courses and growth accelerates. The use of geosynthetics inclusions increase the tensile strength, which will have significant influence on the behavior of the pavement surface under traffic loading and environmental movements.

Thermal cracking includes both temperature cracking (mainly in most parts of Canada and some parts of USA) and thermal fatigue cracking. Low temperature cracking is due low temperature in winter (below -23^0C) and fatigue cracking can occur when the asphalt becomes hardened due to aging.

The main focus of this research is related to the rutting failure criteria of the flexible pavement, which is more fully described later.

1.2 The Need for Research

The life of a pavement is an important agenda for a national economy, as a large proportion of pavement maintenance budget is spent each year solely on the repairs of pavement defects associated with cracking. A good pavement must provide a smooth riding profile, withstand large traffic volumes and transmit the stresses efficiently to the underlying subgrade support. But after a certain number of service years, pavement defects (cracking) appear at the surface due to repeated traffic loading, local environmental distress and aging. The traditional flexible pavement rehabilitation using the overlay method is expensive and rarely provides a durable solution as the cracks rapidly propagate through the new asphalt layer forming the so-called "reflective cracks" (Rigo, 1993 (38)). Hence this overlaying method, which has to be used after only short period of usage in the rehabilitation period, is expensive on it. So the advent of any materials or new technology might be the alternative to costly overlaying method in the pavement construction.

Research and development on the use of geogrids and geotextiles inclusions in pavement base layers have been used and are ongoing also. Geosynthetics (geogrid and geotextiles only) have been used for unpaved and paved roads to fulfill one or more of the basic functions of reinforcement, separation, filtration, and drainage. An interlayer of geosynthetics placed below the asphalt top and/or compacted base fundamentally helps to stress transfer and control crack propagation from underneath as a stress absorbing membrane (Rigo, 1993 (38)). These inclusions have the potential to extend pavement life by reinforcing and inhibiting reflection of cracks.

1.3 Objective of the Research

The objective of this research is to determine the equivalent thickness of a homogenous base layer of an unreinforced multilayered system subjected to the repetitive loadings of a constant value. The system demonstrates the same performance as the analogous multilayered system does which contains the geogrid inclusion as reinforcement in the placement of interest of the base layer. It is obvious, that the deformability of the top pavement surface depends on the place where the geogrid insertion is introduced. The research also refers to previous investigations of similar type that have been conducted on geogrid reinforcement in flexible pavement.

The performances of both systems (i.e., unreinforced and reinforced) are described in terms of unrecoverable deformations. The investigations are conducted in the framework of sensitivity theory. They employ the concept of functional with moving ends. The constitutive model adopted in the analysis is the modification of the small displacement theory of elastic continuum, which incorporates the unrecoverable features of deformation. This is achieved by introducing the modulus of permanent deformation, which is related to the current state of deformation. The simulation of unrecoverable deformation is executed by application of the geometry updating during each unloading process.

The data on deformability of the systems (unreinforced and reinforced) investigated are provided from the experimental studies published in the technical literature (Moghaddas-Nejad and Small, 1996 (30)). They are focused on monitoring of cumulative permanent

displacements of selected control points of multilayered systems subjected to repetitive loadings of a constant value. Employing the proposed constitutive model the permanent modulus in each homogeneous isotropic layer of the unreinforced multilayered systems is determined for each subsequent loading. It is done by the implementation of the Finite Element Method with respect to spatial variables. The same approach is used an analysis of reinforced multilayered systems in which geogrid is placed. In numerical simulation, the layer with geogrid inclusion is considered to be made of homogeneous material, which is based on homogenization approach.

The placement of geogrid in the selected layer results in decrease of permanent displacement of monitored points. The inclusion of geogrid into frictional coarse material results in development of the stronger layer. This is due to the fact that relatively stiffer geogrid element possesses openings allowing for interlocking and inter-penetration of the aggregate particles of the base layer. The application of repetitive loading results in development of the composite layer. The proposed theoretical approach can be implemented to measure the performance of the reinforced base layer for the geogrid placement at the different level of the base layer, which results in development of different equivalent layer of unreinforced transportation system.

For each single loading the difference in displacements at arbitrary but corresponding control points of the unreinforced and reinforced system is defined as the first variation of the displacement. Based on the given variation of permanent displacement it is possible to determine the increment of the thickness of the layer of interest being the part of the

unreinforced multilayered system that should be superposed to the original thickness of the layer of unreinforced system. This yields the same deformations as the reinforced multilayered system does.

The required performance functional of the unreinforced and the reinforced systems are formulated based on the virtual work principle. To perform this operation, the adjoint system is introduced. The difference of these two performance functionals due to the variation of the boundary's shifts of the base layer is investigated. This is done by the concept of functional with moving ends, which is discussed later.

Bearing in mind that the variations of the performance functional are equal to the work of the unit load on the differences of the permanent deformations at the control point, which are known from experimental studies, the variations of the shifts of boundaries of the layer can be determined.

1.4 Structure of the Thesis

The contents of this thesis are arranged into six chapters. This thesis includes the following:

Chapter I: This chapter contains general discussion on flexible pavement, the need for research, objective of the research and thesis organization.

Chapter II: It contains the general discussion on geogrid as base reinforcement in flexible pavement and some possible problems for geogrid inclusion in the base layer. It also reviews the literature relevant to the theme of the study and the definitions and terminology mostly used in the flexible pavement.

Chapter III: This chapter includes the deflection data collection and retrieving procedures of flexible pavement based on the accumulated number of traffic passes. This data modeling of laboratory results include the testing program, regression analysis of the data and development of a set of polynomial deflection equation based on the accumulated number of passes.

Chapter IV: This chapter describes the theoretical formulation based on the functional with moving ends and its application in this thesis to determine the equivalent base thickness of unreinforced section comparing to the reinforced section (geogrid inclusion in the middle of the base layer as well as at the base-subgrade interface).

Chapter V: This chapter includes the numerical analysis and results. Numerical investigations are done with the aid of Finite Element Method (FEM) and its application software ABAQUS.

Chapter VI: This chapter includes the conclusion and recommendation regarding the potential benefits of geogrid inclusion in the base layer of flexible pavement or any other suitable position in the flexible pavement.

Appendices: These include various sample calculations, relevant tables and figures, ABAQUS input file, CAE results and other related sources.

The outline of the whole thesis is as follows:

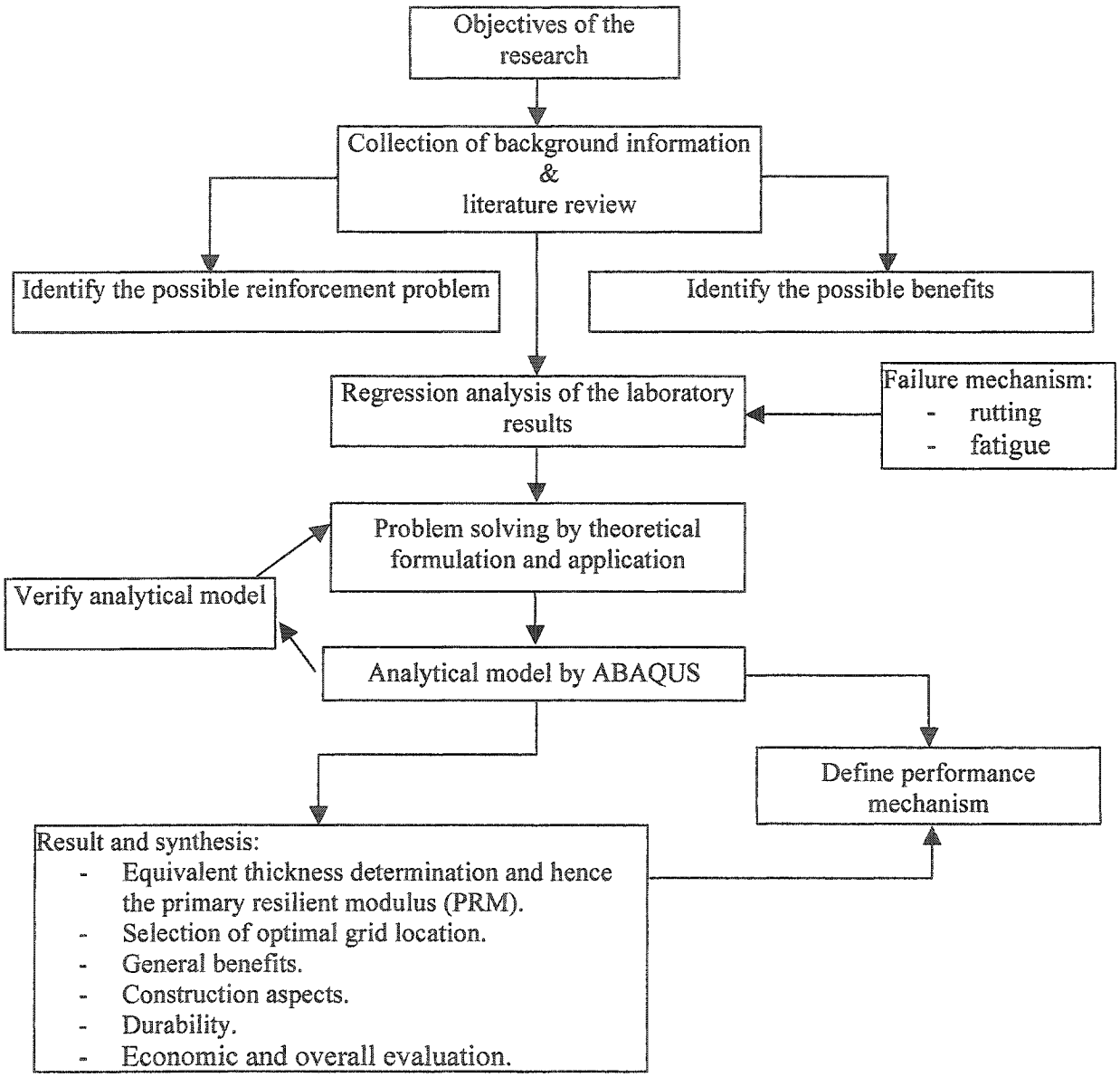

Figure 1.4 General approach used in evaluating geogrid reinforcement of flexible pavements

CHAPTER II

LITERATURE REVIEW AND BACKGROUND INFORMATION

2.1 Introduction

In general terms, the rationale for technological development is to provide a new means and offer new solutions which at least ensure a sustainable development being economically and functionally superior to the existing. The economical assessment of new technological products can be done in many ways. Practically many researchers had already put their effort to mitigate the rutting failure criteria as well as to improve the performance of the flexible pavement. One of them is the geosynthetic inclusion into the frictional base material as reinforcement like what steels do for concrete. Geosynthetics can be defined as a variety of synthetic polymer materials that are specially fabricated to geotechnical applications, which are generally characteristics of high-density polyethylene, polypropylene or polyester. As a consequence geosynthetic (i.e. geogrids and geotextiles) have been studied and used for more than 15-20 years as reinforcement in the base course layer of flexible pavements. The benefits of geosynthetic application lies in the possibility (most of the cases) of reducing the thickness of the base course layer such that a roadway of equal service life results or in extending the service life of the roadway. But this fabric application have been limited for the most part to high deformation systems in which surface deflections of 75 mm or greater are allowable, e.g., haul and access roads over soft ground.

The first alternative is beneficial if the cost of the geosynthetic is less than the combined cost of the replaced base course material and any construction related costs associated

with a reduced base thickness (such as excavation, relocation of utilities and purchase of right of way). The second alternative is beneficial when maintenance and replacement costs are offset by the cost of geosynthetic inclusion into the base layer. Generally both alternatives are attractive in areas where the quality gravel sources are not in adequate supply, especially in urban areas where these types of sources have become depleted, or in environmentally sensitive areas where the sitting of gravel quarries is not permitted.

2.2 Geosynthetics used in Flexible Pavement

Geosynthetics are man-made materials for the purpose of improving the qualities of soil. The application of geosynthetics to flexible pavement structures serves many reasons. They are specified as follows:

- Substantial decrease of deformations of the system
- Increase of comfort of service that the transportation system provides to the users.
- Increase of the safety of the system
- Increase of durability of the system
- Extension of the service life of the system.

Geosynthetcis can be classified into several categories based on the structure and function:

- Geogrids
- Geotextiles

- Geonets
- Geocomposites
- Geocells
- Geomembranes

Geotextiles, geomembranes and geogrids are the three principal categories of geosynthetics. Geotextiles are textile fabrics providing filtration, separation or reinforcement of soil. Geomembranes are impermeable sheets used in such places as landfills to prevent the vertical movement of fluids. The most significant purpose of geogrid is soil reinforcement. Geogrids and geotextiles are generally used in the most road construction. Geotextiles were first examined for use as reinforcement in paved roads in the early 1980's (Brown et al., 1982 (13); Ruddock et al., 1982 (39)), while geogrids were first studied in the late 1980's (Barker 1987 (8); Haas et al., 1988 (25); Barksdale et al., 1989 (11)).

The focus of this research is reinforcement applications in the roadway construction. Therefore, separation and filtration functions provided by the geotextiles will not be discussed in this research and the reinforcement application of the geogrid will be discussed elaborately in this research. The reinforcement application of the geotextile will be discussed shortly and the reason for doing that is also discussed here. There are a lot of differences regarding the reinforcement application for geogrids and geotextiles, which should be clearly understood at first.

2.3 Geogrid used as base reinforcement in the flexible pavement

Geogrids are made of high strength plastic (i.e., high-density polyethylene or polypropylene) and are formed in grid like configuration. Grids can be manufactured with opening sizes compatible with typical base course maximum particle sizes i.e., 25 to 110 mm. According to rib spacing and the applied stress conditions, geogrids are of two types: (1) uniaxial geogrid and (2) biaxial geogrid. They are shown in Figure 2.1

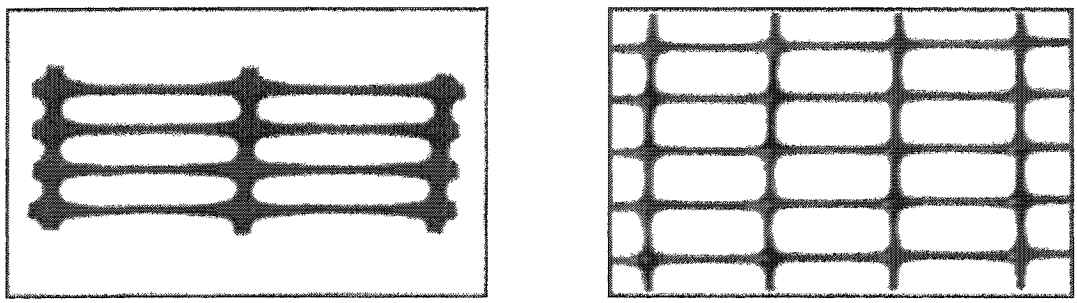

Uniaxial geogrid Biaxial geogrid

Figure 2.1 Types of geogrids

Uniaxial geogrids are designed to endure stress in one direction. This type of geogrids is stronger than biaxial geogrids, but can only be applied in situations where stresses occur in a single direction (unless two uniaxial grids are placed at right angles to each other). On the other hand, biaxial geogrids can take stresses in two directions, but they don't have as much tensile strength in either direction as a uniaxial geogrid does in its direction of application. Both types of grids provide the most efficient means for carrying tensile stresses transmitted through the base course.

Recent developments in geogrid technology, however, suggest that the interlock and tensile modulus characteristics of certain grid products might be beneficial as reinforcement within the granular base of low-deformation systems, such as flexible pavements, as well as high deformation systems. This was clearly demonstrated in the University of Waterloo research program done by Abdel Halim, 1993 (2), which is subsequently discussed.

With some similar properties to TENSAR biaxial geogrids, such as modulus or ultimate tensile strength, geotextiles do not provide the same mechanisms of reinforcement nor equivalent performance in base reinforcement and subgrade improve applications. Geogrids provide improvement to roadways through four primary mechanisms:

- Interlock;
- Reinforcement;
- Confinement;
- Separation;

and provide secondary-benefiting functions as well. These mechanisms are more fully discussed in Table 2.1.

Table 2. 1 Geogrid Improvement Mechanisms

MECHANISM	FUNCTION	BENEFIT
Interlock	Primary	- Provides interlocking of aggregate at the placement of interface and results the sufficient rigidity and strong geometry. - Prevents lateral movement of the aggregate - This mechanism is a function of the gradation and angularity of the base aggregate and the geometry of the geogrid.
Reinforcement	Primary	Provides tensile strength, with high modulus in the tension zone, of the aggregate base course
Confinement	Primary	Provides a uniform confinement plane below the aggregate and prevents or limits the amount of subgrade rutting upheaval of subgrade into the aggregate base
Separation	Primary	Prevents aggregate base course from punching down into the subgrade, thus maintaining effective aggregate thickness
Filtration	Secondary	Water draining from the separated subgrade and confined aggregate will not transport fines if aggregate meets soil filter gradation requirements for the subgrade
Tensioned Membrane	Secondary	Will be mobilized at very low strains if a thin aggregate section is used and rutting of subgrade occurs

(Source: www.tensarcorp.com, (43))

Interlock or positive bond between the reinforcement and the aggregate particles is required to truly reinforce the granular base of flexible pavements. Because an unbound base cannot take tension, the function of the interlock or bond is to mobilize the strength of the reinforcement and impart this resisting force to the base. Interlocking effectively transmits the shear stresses from the base material to the grid, thereby increasing the shearing capacity of the base. This requires, however, sufficient shear strains to mobilize this effect. This effect also reduces lateral movement of the aggregate base and base deterioration, which is especially pronounced for weak base materials. The interlocking between the grid and the base materials also prevents, to some degree, migration of fines into the base and base material into the subgrade. In addition to possessing the appropriate physical properties to interlock with the base layer, a pavement reinforcing material should possess the following mechanical properties:

1) High tensile modulus to resist stretching under load;
2) Dimensional stability to resist radial stresses without deforming, warping, or stretching;
3) Elastic response under dynamic loading;
4) Resistance to plastic strain with repeated load applications; and
5) Inertness and durability.

Geogrids perform as a structural reinforcement layer within the aggregate base when it is interlocked and possesses a high initial and secant modulus. Typically geogrid is placed at the bottom (thickness < 250 mm) or at the mid height (thickness>= 250 mm) of the

aggregate base. It is obvious that the deformability of the top pavement surface depends on the place where the geogrid insertion is introduced. The aggregate interlocked in the grid provides confinement of the underlying subgrade. This mechanism prevents the subgrade from moving up into the base aggregate layer due to rutting and integrity and thickness of base is maintained throughout this mechanism. Separation of the aggregate base and subgrade i.e., punching of aggregate into subgrade, can be maintained by the aggregate grid interlock. The grid structure and integrity must be such as to provide long term interlock under dynamic loads to maintain the confinement and separation. The geogrid also influences the subgrade soil behavior. Rather than an improvement in subgrade properties, geogrids improve subgrades through a change in the boundary conditions acting on the subgrade. If sufficient deformations occurs the geogrid becomes concaved and begins to act as a tensioned membrane. The normal stress supported on the top side of grid will then be greater than that on its bottom side, thereby reducing the vertical stress acting on the subgrade.

The potential benefits resulting from the application of geogrid inclusions into the base course include a significant decrease in the short- term permanent deformations (rutting), increase in tensile strength, reduction of fatigue cracking, increase in durability of the pavement structure and lowering the life-cycle cost of the pavement structure. The significant reduction of the permanent deformation is possible mainly due to the confinement and interlocking of the composite base material. Development of the stronger layer is due to the fact that relatively stiffer geogrid element possesses openings allowing for interlocking and inter-penetration of the aggregate particles of the base

layer. The application of repetitive loading results in development of the composite layer. The proposed theoretical approach can be implemented to measure the performance of the reinforced base layer for the geogrid placement at the different levels of the base layer, which results in development of different equivalent layer of unreinforced transportation system. The mechanism of stress transfer from the soil to the geogrid insertion depends primarily on the geometric properties of the inclusions and the improved load distribution on the subgrade layer causing a reduction of subgrade deformations. The possible savings can be assessed by taking into account the fact that the mitigation of deformation can be obtained by placing the geogrid in the granular base layer which results the significant reduction of base thickness. Considerable savings can also be generated due to lowering the labor expenditures, smaller spending for transport of heavy bulk material and offset any construction related costs associated with a reduced thickness (such as excavation, relocation of utilities and purchase of right-of way). Benefits are also seen when maintenance and replacement costs are offset by the cost of geosysnthetic. A cost analysis (Anderson, P. and Killeavy, M. 1989, (6)) showed a cost of \$ 19.88/m^2 for the reinforced section and \$20.40/m^2 for the unreinforced section.

2.4 Geotextiles used in roadways

Geotextiles provide improvement to roadways through one primary mechanism:

- Separation

and can provide secondary-benefiting functions as shown in Table 2.2. For more than a decade geotextile fabrics have been used for subgrade stabilization of soft foundation

soils. In subgrade stabilization, the separation function of the fabric is the key to performance. It prevents granular base materials from punching into soft foundation soils under the wheel or track loads of construction vehicles. Because base punching or localized shear failure is prevented, the subgrade can develop its full bearing capacity. When the soil shear strength is quite low (< 48 kPa) and the subgrade is prone to deep rutting, then this separation function can provide an increase in subgrade load capacity. On the other hand, these benefits diminish when subgrade shear strength increases (> 48 kPa).

Table 2.2 Geotextile Improvement Mechanisms

MECHANISM	FUNCTION	BENEFIT
Separation	Primary	Prevents subgrade and aggregate base course from mixing, thus maintaining effective aggregate thickness.
Filtration	Secondary	Prevents subgrade water, draining to the aggregate base, from transporting fines.
Reinforcement – Tensioned Membrane	Possible Secondary	May provide support through deflected membrane if deep ruts develop in the subgrade.
Drainage	Possible Secondary	Provides lateral, in-plane drainage (applicable to nonwoven geotextile only).

(Source: www.tensarcorp.com (43))

The primary failure mode of unreinforced aggregate sections is the lateral sliding/ displacement of the aggregate under load. With regard to lateral displacement, geotextiles provide little benefit due to the poor frictional characteristics. Interlock of the aggregate is not possible with geotextile sheets. Therefore the interlock, confinement and structural reinforcement benefits are not possible to achieve through the use of geotextiles and finally it can be concluded that geotextiles are not suitable for reinforcement; they can be used for filtration, drainage and separation purposes for roadway construction.

2.5 Some problems – when geosynthetic is inserted in the base layer

There are some general reasons why the engineers don't want to use or have confidence in geosynthetics:

1) The respective industry's inability to communicate with the pavement community;
2) Misunderstanding the unique aspects of each pavement use (separation, stabilization and reinforcement);
3) Failure to clearly define performance criteria for temporary and permanent pavements;
4) Failure to document and demonstrate the long-term benefits of using geosynthetics; and
5) Failure to define how, where and when geosynthetics work in "high-type" pavement applications.

Although, the principle for flexible pavement of layered system may look simple, a number of uncertainties may arise when geosynthetics are inserted in the base layer under environmental distress. The designs are difficult, as there are no simple rules in the codes for a reinforced flexible pavement. The key to optimizing geogrid potential is proper design. Proper design requires appropriate layer thickness and selection of optimum geogrid location. No benefits are expected when a single layer of grid is placed within the zone of compression, such as near the interface of surface-base layer. Through the field experience it is also found that if the base is very thick, second layer of geogrid may be placed at some middle location to retard the rate of permanent deformation within the base itself.

From the practical viewpoint, regarding the placement of the polymer grid in road material, the interlocking effect can be expected but much of the working of the membrane tension effect in polymer grids cannot, especially immediately after the completion of the pavement. Therefore, laying of the polymer grid must be carried out so as to induce as much interlocking effect as possible.

2.6 Literature Review

In recent years, several laboratory and full–scale trials have been carried out to study the reinforcement potential of geogrids in both unpaved (high deformation) and paved (low deformation) roads. Regarding this several reliable design methods have been developed. Despite the vast amount of information available and increased experience with geotextiles and geogrids, many failures still occur because of a lack of understanding of

how these materials affect the properties of the basic engineering materials (e.g., subgrades, engineering fills, and pavement materials) or how reinforcement affects the load response of the structure.

Even a review of the literature can be confusing because various studies indicate everything from inferior to superior performance of reinforced paved and unpaved roads compared with unreinforced structures. Several studies report conflicting observations about the optimum location for reinforcement, which ranges from the base-subgrade interface to a location near the top of the base. Variables that might result in apparent discrepancies in test results include type of structure; subgrade type and strength; failure criteria; static versus dynamic load; shape, size and magnitude of load; and type and location of reinforcement.

Smith et al., 1994 (40) performed both a detailed literature review of several laboratory and field studies of geosynthetic-reinforced flexible pavements and a laboratory study to evaluate the effectiveness of using geotextiles and geogrids in flexible pavements. Full-scale field studies regarding the flexible pavements having geosynthetic-reinforced unstabilized granular bases have been conducted by Ruddock et al., 1982 (39), Barker, 1987 (8), and Pappin, 1975 (33).

Most of the researchers agree that geosynthetics improve the performance of flexible pavements. The effect of a geogrid is to restrict the lateral movement of the granular subgrade, and this, in turn, reduces lateral deformation of the pavement under repeated

tire loading. (Moghaddas-Nejad and Small, 1996 (30); Chan et al., 1989 (19); Omoto et al., 1992 (32); and Miura et al., 1990 (29)).

Al-Qadi et al., 1994 (3) performed laboratory scale repeated load tests in a concrete test tank to compare separation and reinforced functions of geotextiles and geogrids and to prepare for the construction of field test sections. Cyclic circular plate loading tests (where the load was cycled using a constant amplitude until a certain rut depth was achieved) were performed on pavement sections consisting of subgrade base and HMA (hot mixed asphalt) pavement. A loading pressure of 552 kPa was applied to a 30 cm diameter plate, corresponding to an applied force of 40 kN (9 kips) at a loading rate of 0.5 Hz. The sections were reinforced with geotextiles and/or geogrids placed between the subgrade and base level. The pavement surface was instrumented with LVDTs while applied load was measured.

Al-Qadi et al., 1994 (3), 1997(4) and Smith et al., 1994 (40) studies state that the improvement mechanisms associated with geogrids and geotextiles were different. The geotextile-reinforced sections performed better than the geogrid reinforced sections with regard to rut development. The geotextile section carried 2-3 times the number of load repetitions than the geogrid sections with the same control sections. In terms of service life, similar results were obtained.

Al-Qadi et al., 1994 (3) demonstrated that when separation and filtration were the main problems associated with a pavement design, geotextiles offered superior improvement as

compared to geogrids. If the improved performance of the geotextile sections was due to separation and filtration functions, then it would be expected that the performance of the geogrid sections would be no worse than the control sections and perhaps better to a much lesser extent than the geotextile sections due to the same functions. These results tend to suggest that the differences in layer properties between the sections was greater than that which could be accounted for by the parameters used to define these properties and/or the analysis technique used to compare sections was not able to account for the property differences observed. Base course soil used contained particles as large as 50 mm, which may have prevented positive interaction with the 25 mm by 33 mm aperture size of the geogrid. Problems have also been encountered with geogrids where the base course soil was sized excessively large, thereby preventing proper interlock. The lack of an appreciable reinforcement function in the studies of Al-Qadi et al., 1994 (3) and Barker, 1987 (8) may be due in part to this characteristic of the base layer soil used. Taken as a whole, these results indicate that the ability of the base layer soil to interlock with the geosynthetic is critical for the function of preventing lateral spread and that geogrids appear to be a more suitable product for meeting this criterion.

Miura et al., 1990 (29) conducted laboratory and field experiments and modeled the test sections using a finite element program to investigate the pavement response (non-uniform settlement) with and without geogrid reinforcement. Laboratory tests were conducted to investigate the structural influence of different design variables, while finite element analyses were performed to illustrate reinforcement mechanisms (deformation analysis). The field tests were performed to demonstrate the reinforcement application.

Model tests were conducted in a concrete box 1.5 m by 1.5 m by 1m deep. A 50 mm AC layer was used. A 200 mm subbase and 150 mm base were compacted on top of the subgrade. For the field-tests, Miura et al., 1990 (29) varied the thickness of the base and subbase between the reinforced and unreinforced sections. The reinforced section contained either 50 or 100 mm less base and/or subbase than the unreinforced section. Biaxially oriented tensar grids SS1, SS2 and SS3 were used as reinforcement. Test results clearly reveal that the reinforcement SS2 is more effective than the other geogrids when placed on subbase. The grids were placed either at the bottom of the base or subbase, or double grids were used at the bottom of the subbase and base or at the bottom and mid-height of the base. Cyclic loads of 200 kPa (29 psi) were applied through a 20 cm diameter plate for 10,000 cycles. In their analysis all the materials composing the pavement were assumed elastic. Young's modulus (50 MPa, 25 MPa, 10 MPa and 2 MPa for asphaltic concrete, base, subbase and clay respectively) and Poisson's ratio ν (0.38, 0.43, 0.43 and 0.47 for asphaltic concrete, base subbase and clay respectively) were used in the numerical analysis.

Performance was determined by measuring a modulus of subgrade reaction for reinforced and non-reinforced sections. The test results indicate that optimal grid position is such that it can develop the greatest tensile force. Also a stiffer grid is more effective since it develops a greater tensile force for an equal strain application. The laboratory test results demonstrated that geogrids of increased stiffness provide for increased levels of improvement. Improvement was closely related to the magnitude of strain measured in the geogrid during loading. The performance of the field sections also improved with the

use of stiffer geogrids, but not to the same extent as that demonstrated in the laboratory results. The laboratory test results show a strong dependency of improvement on the geosysnthetic position within the base and subbase layers. The test results indicate that the way in which the geogrid carries the strain, or load was dependant on the geogrid position and in turn influences the geogrid reinforcement potential. The results also indicate that the geogrid reinforcement potential is not fully realized if it is placed too high within the base layer. In their test it appeared that placing the geogrid 125 mm below the pavement surface (75 mm into the base or middle of the base layer) was not sufficiently deep to realize the reinforcement potential of the geogrid. They also placed the geogrid at different positions and they came to conclusion that may the optimal geogrid position was not unique, but was dependent on the geosysnthetic type and pavement layer mechanical properties. They also stated that if the geogrid is inserted in the proper location then the reinforcement by a one-layer polymer grid is comparable to the bearing function of a 100 mm thickness of base material. The field test results are ambiguous with regard to the effect of geogrid position in the test section.

In his own technical paper Miura, 1988 (28) suggested that the mechanism of the polymer grid for the reinforcement of a pavement base layer was mainly due to the interlocking effect rather than the membrane tension effect. The membrane tension effect of the reinforcement in a base layer will act effectively only when the reinforcement is placed at a slightly tensioned state and in a concave upward shape.

To clarify the function of reinforcement in the pavement, a deformation analysis was carried out. Finite element analysis was performed using three element types for deformation analysis. A truss element capable of tension only was used for the grid. A joint element, representing a discontinuous plane and having a normal and shear stiffness, was used to model the interaction between the grid and the soil. 2-D continuum (triangular) elements were used for the AC (asphalt concrete), base, subbase and subgrade. Isotropic, elastic properties were used for all 2-D elements. Results from reinforced and unreinforced analysis showed little difference. This was said to be due to the FEM taking account of the membrane stretching effect only and not the interlocking effect. But they suggested that the interlocking effect (second mechanism) of a polymer grid plays an important role in suppressing surface settlement of the pavement. No information was given on who developed the model or how the model was developed. Therefore, they suggested that laying of the polymer grid must be carried out so as to induce as much interlocking effect as possible.

Giroud et al., 1985 (23) describe the initial development of a design method for geogrid reinforced unpaved structures. The authors claim that design methods for geotextile-reinforced applications are not suitable because they do not account for the mechanism of interlocking between the grid and soil. The authors also warn that the suggested approaches developed for unpaved roads are not suitable for paved situations due to the fact that tolerable deformation in unpaved roads are much greater (say 75 mm or 150 mm), therefore the mechanisms of failure are different. The paper reviews the

mechanisms through which geogrids can improve the performance of an unpaved structure.

The design method described in their paper is largely empirical and consists of determining unreinforced base layer thickness depending on the number of traffic passes and the strength of the subgrade soil from a design chart. This chart assumes a certain load associated with each pass. The geogrid type is then used to determine the reinforced base thickness reduction ratio. This ratio is as great as 0.75 for applications where the unreinforced base thickness is large (greater than 1 m) corresponding to situations where the subgrade strength is low and the number of traffic passes is large. The ratio is as small as 0.4 for situations where the unreinforced base thickness is relatively small (less than approximately 0.5 m) corresponding to strong subgrade and/or low traffic passes.

Haas et al., 1988 (25) performed comprehensive laboratory experiments at University of Waterloo by using a stationary plate to which a cyclic load (repeated load) was applied and demonstrated the importance of variables such as geogrid placement position, base course thickness and subgrade strength. In general, it was shown that reinforced sections carried three times the number of load cycles as compared to a similar control section, and that reinforcement allowed up to a 50 % reduction in base course thickness. They placed the geogrids in different positions depending on the subgrade strength (CBR value) and the base thickness. When the geogrid was placed at the interface of the AC (asphalt concrete) and base, the section performed slightly worse. The study also showed that maximum rutting reduction benefits of grid reinforcement were evident when grid

was placed within the lower half of the base course of flexible pavements. The principal objectives of the experimental investigations were to develop the equivalency factors for geogrid reinforced granular base sections and hence develop structural design procedures for reinforced flexible pavements and also analyze the grid reinforcement mechanisms in flexible pavements through the use of stress, strain, and deflection measurements.

The test facility at the University of Waterloo consisted of a large rectangular box, 4572 mm x 1829 mm x 914 mm. The load applied to the pavement surface for both types of static and dynamic loadings was 40 kN, which applied a pressure of 552 kPa through the load plate. In their test program they reported that grid reinforcement could increase the number of load cycles carried by a factor of 3. Base thickness reductions of 25 to 50 percent made possible by inclusion of geogrids and the optimum location of grid reinforcement within the granular layer was found to be dependent on granular thickness and subgrade strength. They suggested that the potential benefits are incorporated with the optimum location of grid reinforcement because grid location can dramatically affect the load response of the pavement. They also examined the stress, strain and deformation analysis to indicate how grid reinforcement at the maximum location can effectively interlock with and confine aggregate base, resulting in increased resistance to lateral and vertical deformation.

Haas et al., 1988 (25) indicated that for low deformation systems interlock and confining action is required, while for high deformation systems a tension membrane action is more effective. They also concluded that for better performance a geogrid should be placed at

the base-subgrade interface of thin sections and near the mid point of thicker base layers. If the base is very thick, a second layer of geogrid may be placed at some middle location to retard the rate of permanent deformation within the base itself. For optimum grid reinforcement they proposed placing the grid in a zone of moderate elastic strain (i.e. 0.05% -0.2%) beneath the load center and stated that maximum permanent strain in the grid during its design life should not exceed 1%-2% depending on the rut depth failure criterion. Under these ideal conditions, grid reinforcement behaves elastically and effectively confines aggregate base, thus prolonging the life of the pavement structure. No benefits can be expected when a single layer of grid is placed within the zone of compression, such as near the top of the base layer under an asphalt concrete surface.

Wathugala et al., 1996 (44) described the importance of using elasto-plastic constitutive models for pavement materials in analyzing geosynthetic-reinforced flexible pavements. The effect of stiffness of the geosynthetic reinforcements on pavement behavior was also studied. They analyzed the pavement materials by the finite element method with different constitutive models. They presented six different analyses where Young's modulus for the Case 1, linear elastic models with geosynthetics (Case 1a, E = 1 GPa; Case 1b, E = 100 GPa); Case 2, linear elastic models without geosynthetics; Case 3, elasto-plastic models with geosynthetics (Case 3a, E = 1GPa; Case 3b, E = 100 GPa); and Case 4, elasto-plastic models without geosynthetic on the same pavement under the same load cycle and thereafter they compared among the six analyses. From their study we can conclude that the linear elastic analyses predicted tensile stresses in the crushed limestone base layer although in reality this material cannot withstand tensile stresses. They got a

very close result for the vertical stresses directly under the load for all of the analyses and were little smaller than those predicted by Boussinesq's equations. The linear elastic analyses showed only a small reduction in settlements when geosynthetcis were added. Actually from the theory of elasticity, the linear elastic analyses are not capable of predicting permanent settlements under the cycle load. Empirical relationships relating elastic strains to plastic strains are available for traditional pavements but not for geosynthetic-reinforced flexible pavements. On the other hand, elasto-plastic analyses showed a large reduction in settlements especially with stiffer geogrids and they do not require one to resort to any empirical relationships, which is required for the elastic case.

They also described briefly about the other models used by the other researchers. Some researchers have used nonlinear elastic material properties in the finite element analysis of the flexible pavement. Zaghloul and White, 1993 (48) have successfully used the general-purpose finite element program ABAQUS, 2002 (1) to simulate traditional flexible pavements. In their study they also introduced the Hierarchical Single Surface (HiSS) models for soils. They claimed that these models offer better capabilities in capturing the behavior of granular soil layers than the models available in ABAQUS.

Chan et al., 1989 (19) conducted four large-scale experiments in the Nottingham Pavement Test Facility to investigate the aggregate base reinforcement potentials of geosynthetics (geogrid and woven geotextile) in surfaced pavements. They did an analytical study by using a comprehensive finite element program GAPPS7 to make a comparison between measured and calculated response. They analyzed the problem with

the axisymmetric representation of the pavement. The geosynthetic reinforcement was modeled using a two-dimensional, flexible fabric membrane element, which cannot take bending or compression loading. The fabric element allows slip or separation to occur when appropriate at the interface between it and the adjacent material. Two non-linear, isotropic elastic-plastic models and a linear, cross-anisotropic model were used to idealize the granular base of pavement. The laboratory research was conducted at the University of Nottingham, while the analytical studies were carried out at the Georgia Institute of Technology. They also included the study of parameters that might influence the pavement performance. The parameters are prestressing, prerutting, stiffness, types and locations of geosynthetics. For the laboratory tests they used the hot rolled asphalt and the continuously graded asphaltic concrete mix for the surfacing; rounded sand, gravel and slightly angular and non-flaky dolomitic limestone for granular base with compaction; inorganic, low plasticity silty clay for the subgrade; and a stiff woven geotextile (stiffness at 5 % strain, Sg = 750 kN/m) and a geogrid of lower stiffness as reinforcement of base layer. The tire pressure was 550 kPa and the estimated contact pressure acting on the pavement was 460 and 500 kPa with circular contact areas of 68 and 76 mm radii respectively. The wheel moved at a speed of 3.2 to 4.8 km/h.

From their experimental and analytical studies they conclude: (1) the benefits of using geosynthetics as base reinforcement in flexible pavement depends largely on the quality and thickness of the granular base layer, and the location of the geosynthetics; (2) despite the lower stiffness of geogrid when the geogrid and geotextile are both placed within the granular base layer, the geogrid performs more effectively as reinforcement than the

geotextile; (3) prerutting of high quality granular material resulted in densification and hence improvement in rut resistance while prerutting of weak granular material did not exhibit the same improvement ; (4) prestressing of geosyntheics, with the ensuring of good anchorage, can provide the short term additional improvement on the pavement performance while the long term benefit can be lost due to stress relaxation; and (5) a cross-anisotropic model was a better representation for a granular base than the various isotropic non-linear models.

Moghaddas-Nejad et al., 2003 (31) did a drained repeated load triaxial compression test to investigate the resilient and permanent stress-strain behavior of two granular materials with and without a geogrid (other types of geotextiles were not considered) as reinforcement. These two granular soils were utilized as base and subgrade materials in model reinforced pavement tests (Moghaddas-Nejad and Small, 1996 (30)). The geosynthetic used as reinforcement was a biaxially oriented grid called TENSAR ® SS2. On–sample-measuring method was also used to get the more accurate result of recoverable deformation. A finite element analysis was carried out to obtain the stress conditions of each element beneath a tire (Moghaddas-Nejad et al., 1996 (26)). The pavement consisted of three layers: a wearing course 20-mm thick, a base layer of 50-mm thick, and a 60-mm thick subgrade. A geogrid was modeled by placing membrane elements at the middle of the base layer, and a uniform circular load of 165 kPa and 50 mm diameter was used to simulate the tire load. A low loading frequency (i.e., 0.1 Hz) was used in the tests as repeated loads were applied by a conventional triaxial loading.

The authors developed a new model that predicts permanent deformation in a pavement material at any stress condition and any number of load cycles with and without a geogrid. The model can also be used in design of reinforced and unreinforced strains in the vicinity of a geogrid or in the unreinforced parts of the pavement. In their paper, they also discussed and investigated the effect of geogrid inclusion in reducing the unrecoverable permanent deformation of soils at various combinations of deviator and confining stress. The test results describe that a geogrid can play a significant role in reduction of deformation of the triaxial specimen, and could, therefore, be expected to reduce deformations in the field but, the geogrid does not have any significant influence on the resilient modulus of the two types of soil (sand and fine gravel whether reinforced or reinforced) which were tested.

2.7 Definitions and Terminology

A. Geogrid - a biaxial as well as uniaxial polymeric grid formed by a regular network of integrally connected tensile elements with apertures of sufficient size to allow interlocking with surrounding soil, rock, or earth to function primarily as reinforcement.

B. Multi-Layer Geogrid - a geogrid product consisting of multiple layers of grid which are not integrally connected throughout.

C. Woven Geogrid – a geogrid product formed by weaving discrete strips of polymer into a network. These geogrids usually require a protective coating to protect the polymer from pre-mature degradation.

D. Welded Strip Geogrid – a geogrid product formed by heat bonding (welding) of discrete strips of polymer into a regular network.

E. Traffic Benefit Ratio (TBR) (also known as Traffic Improvement Factor or TIF) - a ratio comparing the performance of a pavement cross-section with a geogrid-reinforced base course to a similar cross-section without geogrid reinforcement, based on the number of cycles to failure, with failure defined as a selected depth of rut.

F Aperture Stability Modulus (also known as Torsional Rigidity or Torsional Stiffness) - resistance to in-plane rotational movement measured by applying a 17.36 lb-inch (20 kg-cm) moment to the central junction of a 9-inch by 9-inch specimen restrained at its perimeter. For multi-layer geogrid products, torsional stiffness testing shall be performed on each layer of grid individually, and results shall not be assumed as additive from single layers to multiple layers.

G Subgrade Improvement – placement of a geogrid immediately over a soft subgrade soil in order to improve the bearing capacity and mitigate deformation of the subgrade soil. The goal of this application may be to reduce undercut

requirements, improve construction efficiency, and reduce the amount of aggregate subbase / base material required, provide a stiff working platform for pavement construction, or combination of these.

H Base Reinforcement – the function of reinforcement is to strengthen by additional assistance, material or support. For the same reason that steel reinforcement is embedded in concrete, reinforcing materials can be incorporated into the base layer of flexible pavements so that the two materials act together to resist forces. Placement of a geogrid beneath or within the aggregate base course of a flexible pavement system to improve the stiffness of the system. The goal of this application may be to reduce the amount of aggregate base material required (reducing initial cost), increase the life of the pavement (reduce life-cycle cost), or a combination of the two.

I Permanent Resilient Modulus – resilient modulus is a fundamental material property that is similar in concept to the modulus of elasticity. Resilient modulus is the elastic modulus based on the recoverable strain under repeated load. It is differ from the modulus of elasticity in that it is determined from a repeated load, triaxial compression test and is based on only the resilient (or recoverable) portion of the strain. Resilient modulus is defined as:

Resilient modulus = (stress amplitude /strain amplitude)

where

stress amplitude = load/area of the specimen

strain amplitude = recoverable deformation

On the other-hand permanent resilient modulus represents the permanent deformation that is based on the unrecoverable plastic strain under repeated load. This concept is very important in the design of flexible pavement. Figure 2.2 shows the straining of a specimen under a repeated load test. Generally as the

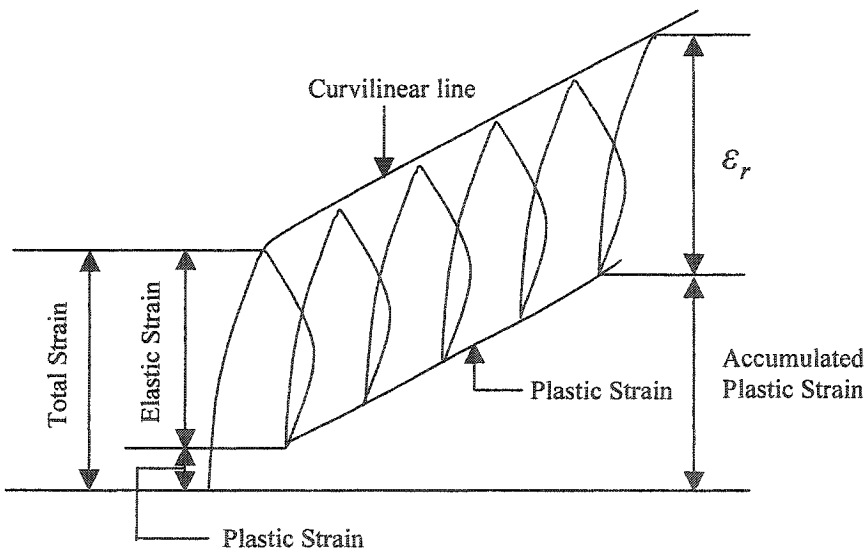

Figure 2.2 Strains under repeated loads

members of load repetitions increase, the permanent deformation decreases. On the other hand, the elastic deformation as indicated as recoverable deformation becomes stable (i.e. for well compacted soil). Permanent deformation rather than

recoverable elastic deformation is studied through the whole research for the analysis of flexible pavement.

J Pre-rutting – in general, prerutting is beneficial because of the additional compactive effect applied to the granular base which results of a denser and stiffer zone at the top of the granular layer. As a result, improved resistance to permanent deformation and less rutting can be achieved. But care must be taken in prerutting weak granular material, which tends to fail in shear rather than densify under the concentrated wheel load to avoid the detrimental effect on the pavement surface.

The purpose of prerutting is to induce a tensile force in the geosynthetic, thereby increasing its reinforcing potential. To carry out prerutting, a moving wheel load (5 kN for sand and 9 kN for crushed dolomitic limestone) is generally applied directly to the surface of the granular base layer of the pavement section.

K Prestressing of geosynthetics - the purpose of prestressing is to reduce the chance of slippage during construction of the upper granular layer. While prestressing has led to better performance in laboratory – scale pavement, its benefit in normal site practice may be difficult to achieve, because of economic and installation problems associated with the use of high stress and permanent anchors.

CHAPTER III

DATA MODELLING OF LABORATORY RESULTS

3.1 Testing Program

The performance of this research is based on the experimental evidence done by Moghaddas-Nejad and Small, 1996 (30). They performed an indoor test track called model test facility, which was carried out, by Wong and Small, 1994 (46) at first. The laboratory set-up was arranged to represent a real life pavement system made in the scale of 1:4. Thus it was a typical three-layer structure which consisted of a 20 mm bitumen wearing course overlying a 40 mm thick base layer of crushed aggregate of basaltic origin that overlaid the subgrade layer of granular soil (silica sand) 2000 mm thick corresponding to the thickness of 80 mm wearing course, 160 mm base and 8000 mm subgrade in the filed. The wearing course is constructed from a proprietary cold-mix bituminous material (pavefix), which consists of a 5 mm maximum size aggregate and a special bitumen binder. Material used for the base layer was a crushed aggregate of basaltic origin consisting mainly of sub angular particles of 5 mm nominal size. Hence the system is identified as conventional flexible pavement. The flexible pavement is reinforced by the inclusion of geogrid in places of interest. One geogrid was used in the experiment and it was a biaxially oriented polymer grid of Tensar SS2 type. Although the geogrid reinforcement used in the tests was not scaled down, it was a product with a relatively small opening size and a small web size. The index characteristics of the pavement layer materials together with the properties of the geogrid are specified in Table 3.1 and 3.2 sections Moghaddas-Nejad and Small, 1996 (30) for a complete description.

Table 3.1 Properties of Granular Materials

	Base material	Subgrade
Property	Uniform fine gravel	Well graded sand
D_{10}	2.0 mm	0.25 mm
D_{60}	4.0 mm	0.37 mm
Minimum density, ρ_{min}	1380 kg/m^3	1440 kg/m^3
Maximum density, ρ_{max}	1490 kg/m^3	1690 kg/m^3
Uniformity co-efficient $C_u = \frac{D_{60}}{D_{10}}$	= 2.0	≈ 2.0

Table 3.2 Properties of Geogrid-Tensar SS2

Property	Longitudinal direction	Transverse direction
Grid opening size	40 mm	28 mm
Grid web size	0.9 mm thick x 3 mm wide	1.2 mm thick x 3 mm wide
Loads at 2% strain	7.0 kN/m	12.0 kN/m
Loads at 5% strain	14.0 kN/m	23.0 kN/m
Approximate peak strain	12.0 %	10.0 %
Mass/area	0.3 kg/m^2	-
Polymer composition	Polypropylene	-

The facility consists of a laboratory scale driven wheel that is guided around an oval-shaped track by an overhead guided rail system. Load was applied by the moving tire (diameter of wheel 230 mm) with an average velocity of 2.67 km/h the movement of which was generated and controlled by the predetermined computer program. The pressure exerted on the laboratory pavement model was considered to be uniformly distributed with the magnitude of 210 kPa (30 psi) acting on a circular area of 24.5 cm^2. The area was considered as circular due to axisymmetric simulation because of load condition.

The pavement model was placed in a steel tank 0.5 m wide and 1.4 m long. It was divided into three horizontal sections, the first one being unreinforced denoted as α-α, followed by section β-β, in which the geogrid was placed at the bottom of the base course, which then was adjacent to section γ-γ that contained geogrid inserted in the midheight of the base layer (shown in Figure 3.1).

Evolution of rutting in each section (α-α, β-β and γ-γ) was monitored by means of 7V linear voltage displacement transducers (LVDTs) that were connected to a data acquisition system. To transmit data from the LVDTs back to the computer through a data rail, an analog to digital signal converter is used. The recorded permanent displacements of points (denoted as 1, 2 and 3) were located at centerlines (with respect to the applied load). Points 1, 2, and 3 in each section were located on the top surface of wearing course (point 1), at the interface of wearing course and base layer (point 2) and

at the interface of base course and subgrade soil (point 3). They are also shown in Figure 3.1.

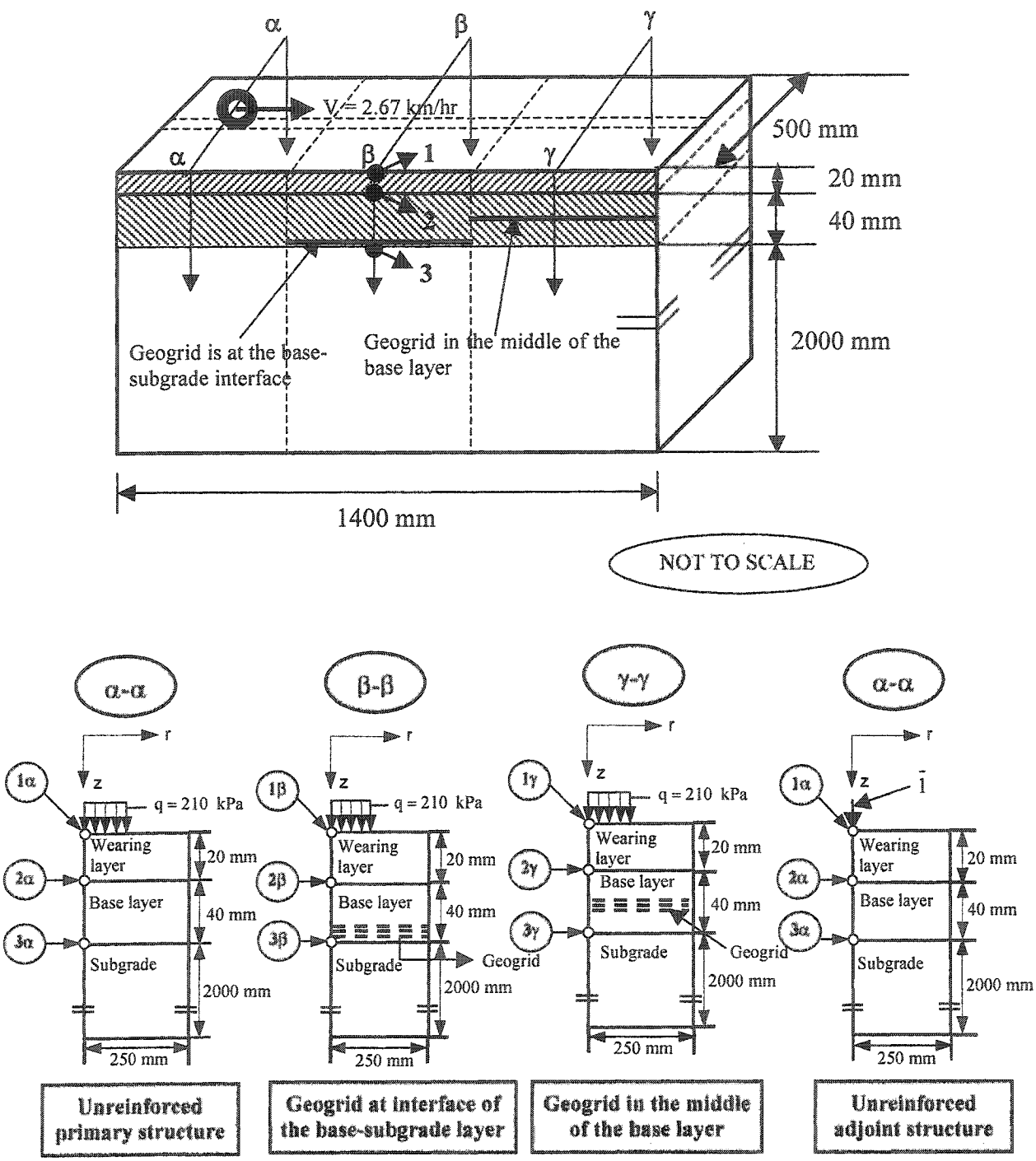

Figure 3.1. Laboratory set-up for simulation of short-term rutting process for unreinforced and reinforced flexible pavement structure.

In fact the points at which the displacement record is monitored, form a set of nine points denoted as (1α, 2α, and 3α); (1β, 2β, and 3β); (1γ, 2γ, and 3γ); where the second letter stands for the appropriate section.

The performance criterion is described by the rut depth and deflection bowl. In numerical analysis contour of deflection bowl is similar to cylinder. Equivalent thickness of a homogenous base layer of the unreinforced system is not determined throughout the experiment but which is determined in this research. This is one of the major objectives of this research.

No information for subgrade strength and stiffness characteristics is available or conducted in the experiment. The experimental results also did not suggest any design method.

3.2 Regression Analysis

3.2.1 Methodology

Traditionally, data is analyzed by the statistical regression analysis. This method is commonly used to develop empirical models by estimating parameters and co-efficient of independent or explanatory variables in mathematical relationships that can explain most of the variations in the dependent or particular variable. A scatter-gram of the data should be reviewed first to estimate the model shape. Analysis of variance should precede regression analysis to identify statistically significant independent variables. Many new analyses and modeling technique have emerged during the last decade.

The modeling of data is a common practice in engineering and science. It consists of determining the parameters of theoretical relations that give the best agreement between theoretical and experimental results. There are four methods available for the modeling of data (i.e., laboratory results):

1) Linear Regression
2) Polynomial Regression
3) Interpolation
4) Non-linear optimization

To study the behavior of mechanical properties of flexible pavement, the test/laboratory results obtained in the test of Moghaddas-Nejad et al., 1996 (30) needs to be re-acquired and modeled to find the theoretical formulas to formulate the problem. The primary step of re-acquiring the test data is to scan and copy the graph presented in the paper. Some key data were determined by measurement and made into tables. In the statistical analysis stage, polynomial regression, one method of non-linear regressions, had been employed to interpret the data and build the corresponding formulas, because it is the best statistical method to analyze the non-linear variables.

Linear regression finds the straight line that best fits a set of data points, thus providing a linear relationship between two variables.

$$y = Ax + B \tag{3.1}$$

where A is the slope, B is the intercept with the y – axis.

But if the test data contain non-linear variables then linear regression is no longer valid and the polynomial regression is superior to linear regression. Linear regression is generalized to non-linear regression by using polynomials of order of m:

$$P(x) = a_0 + a_1 x + \ldots\ldots\ldots\ldots\ldots\ldots + a_{m-1} x^{m-1} + a_m x^m \qquad (3.2)$$

where the (m + 1) coefficients a_m, a_{m-1}, ... , a_1 and a_0 define a polynomial of order m. Equation (3.2) may also be written as:

$$P(x) = \sum_{j=0}^{m} a_j x^j \qquad (3.3)$$

Polynomial regression consists of fitting a set of n data points (x_i, y_i) to a polynomial model. Linear regression is a particular polynomial regression corresponding to m =1, A = a_1, and B = a_0. The accuracy of the fit between the polynomial line and data points is evaluated by the sum E of the squared distances between data points and fitted points.

$$E = \sum_{i=1}^{n} [(P(x_i) - y_i]^2 \qquad (3.4)$$

The fit can be evaluated as best when E is minimum, namely, when E being differentiated with respected to the coefficients a_i (i= 0, 1,……, m) equals to 0. This means, however, the following (m+1) equations are satisfied:

$$\frac{\partial E}{\partial a_j} = 0 \quad for \quad j = 0,1,2,\ldots\ldots\ldots\ldots\ldots\ldots\ldots\ldots,m \tag{3.5}$$

Equation (3.4) implies that

$$\sum_{i=1}^{n}[P(x_i) - y_i]\frac{\partial P(x_i)}{\partial a_j} = 0 \quad for \quad j = 0,1,2,\ldots\ldots\ldots\ldots\ldots,m \tag{3.6}$$

After some algebraic manipulations, Equation (3.6) becomes:

$$\sum_{k=0}^{m}\sum_{i=1}^{n} x_i^{k+j} a_k = \sum_{i=1}^{n} y_i x_i^j \quad for \quad j = 0,1,2,\ldots\ldots\ldots\ldots\ldots, \; m \tag{3.7}$$

Equation (3.7) can be written as:

$$\sum_{k=0}^{m} G_{jk} a_k = H_j \quad for \; j = 0,1,2,\ldots\ldots\ldots\ldots\ldots,m \tag{3.8}$$

where

$$G_{jk} = \sum_{i=1}^{n} x_i^{j+k} \tag{3.9}$$

and

$$H_j = \sum_{i=1}^{n} y_i x_i^j \tag{3.10}$$

The coefficient vector A is denoted as:

$$A = a_k \quad for \;\; k = 0,1,2,\ldots\ldots\ldots\ldots,m \tag{3.11}$$

By using the matrix notation, Equation (3.11) can be summarized as:

$$GA = H \tag{3.12}$$

Hence the polynomial coefficients are therefore:

$$A = G^{-1}H \tag{3.13}$$

where G^{-1} is the inverse matrix of G and $A_j = a_j$. For instance, the quadratic polynomial is

$$A = \begin{bmatrix} a_0 \\ a_1 \\ a_2 \end{bmatrix}, \qquad G = \begin{bmatrix} n & \sum_{i=1}^{n} x_i & \sum_{i=1}^{n} x_i^2 \\ \sum_{i=1}^{n} x_i & \sum_{i=1}^{n} x_i^2 & \sum_{i=1}^{n} x_i^3 \\ \sum_{i=1}^{n} x_i^2 & \sum_{i=1}^{n} x_i^3 & \sum_{i=1}^{n} x_i^4 \end{bmatrix}, \qquad \text{and} \qquad H = \begin{bmatrix} \sum_{i=1}^{n} y_i \\ \sum_{i=1}^{n} x_i y_i \\ \sum_{i=1}^{n} x_i^2 y_i \end{bmatrix} \tag{3.14}$$

and the cubic polynomial is

$$A = \begin{bmatrix} a_0 \\ a_1 \\ a_2 \\ a_3 \end{bmatrix}, \quad G = \begin{bmatrix} n & \sum_{i=1}^{n} x_i & \sum_{i=1}^{n} x_i^2 & \sum_{i=1}^{n} x_i^3 \\ \sum_{i=1}^{n} x_i & \sum_{i=1}^{n} x_i^2 & \sum_{i=1}^{n} x_i^3 & \sum_{i=1}^{n} x_i^4 \\ \sum_{i=1}^{n} x_i^2 & \sum_{i=1}^{n} x_i^3 & \sum_{i=1}^{n} x_i^4 & \sum_{i}^{n} x_i^5 \\ \sum_{i=1}^{n} x_i^3 & \sum_{i=1}^{n} x_i^4 & \sum_{i=1}^{n} x_i^5 & \sum_{i=1}^{n} x_i^6 \end{bmatrix},$$

$$\text{and} \quad H = \begin{bmatrix} \sum_{i=1}^{n} y_i \\ \sum_{i=1}^{n} x_i y_i \\ \sum_{i=1}^{n} x_i^2 y_i \\ \sum_{i=1}^{n} x_i^3 y_i \end{bmatrix} \tag{3.15}$$

The same approach can be applied to acquire the polynomial of higher order.

Now, in practice if the x data contain large number, i.e., H matrix contains huge exponent number then the matrix will be poorly conditioned matrix. To solve the problem we need the concept of logarithmic transformation. Then the basic polynomial equation of order m will be

$$y = a_0 + a_1 x' + a_2 (x')^2 + a_3 (x')^3 + \ldots\ldots\ldots\ldots\ldots\ldots\ldots\ldots\ldots + a_m (x')^m \tag{3.16}$$

where, $x' = \log_{10}(x)$

Therefore, applying the logarithmic transformation for cubic polynomial we get,

$$[G'] = \begin{bmatrix} n & \sum_{i=1}^{n} x_i' & \sum_{i=1}^{n} (x_i')^2 & \sum_{i=1}^{n} (x_i')^3 \\ \sum_{i=1}^{n} x_i' & \sum_{i=1}^{n} (x_i')^2 & \sum_{i=1}^{n} (x_i')^3 & \sum_{i=1}^{n} (x_i')^4 \\ \sum_{i=1}^{n} (x_i')^2 & \sum_{i=1}^{n} (x_i')^3 & \sum_{i=1}^{n} (x_i')^4 & \sum_{i}^{n} (x_i')^5 \\ \sum_{i=1}^{n} (x_i')^3 & \sum_{i=1}^{n} (x_i')^4 & \sum_{i=1}^{n} (x_i')^5 & \sum_{i=1}^{n} (x_i')^6 \end{bmatrix}$$

and

$$[H'] = \begin{bmatrix} \sum_{i=1}^{n} y_i \\ \sum_{i=1}^{n} (x_i') y_i \\ \sum_{i=1}^{n} (x_i')^2 y_i \\ \sum_{i=1}^{n} (x_i')^3 y_i \end{bmatrix} \qquad (3.17)$$

where coefficient matrix

$$[A'] = [G']^{-1}[H'] \qquad \text{where } [A'] = \begin{bmatrix} a_0' \\ a_1' \\ a_2' \\ .... \\ a_m' \end{bmatrix}$$

Besides E, the R^2 values are used to measure the quality of fitting:

$$R^2 = 1 - \frac{\sum_{i=1}^{n}[y_i - P(x_i)]^2}{\sum_{i=1}^{n} y_i^{\,2} - \frac{1}{n}(\sum_{i=1}^{n} y_i)^2} \tag{3.18}$$

R^2 varies from 0 to 1, the best fitting corresponding to R^2=1. With the advent of computer and a lot of powerful application software, the process of finding the polynomial coefficient can be easily accomplished by such software as MATLAB or EXCEL.

In applying MATLAB/EXCEL, several trials have to be done to get the exact solution, depending on what accuracy should be satisfied. Regarding to the present problem, cubic polynomial is always the first and best attempt.

A detailed step-by-step procedure and related calculations is explained in the Appendix A1 to get the polynomial coefficients of a polynomial regression equation by using the MATLAB Program.

3.2.2. Presentation of the Laboratory Results

The laboratory set-up that was previously described and the concept for conducting the experimental research resulted in the outcome on the development of short-term rutting process associated with each section are discussed in this section. Also the assessment of the results performed by means of regression analysis, which provided more accurate retrieval are discussed step by step in this section.

Firstly we have to determine the equations of accumulated permanent deformation for three different conditions namely, unreinforced section (α-α), geogrid at the base subgrade interface (β-β), and geogrid in the middle of the base layer (γ-γ) by means of polynomial regression analysis as a function of number of vehicle passes N. Thus for ***unreinforced cross section (α-α)*** it is possible to express the accumulated permanent displacements as a function of number N of repetitions.

$$V_{1U}(N)[mm] = -0.0491 - 0.3431 \times \log_{10}(N) - 1.7791 \times \log_{10}^{2}(N) + 0.1009 \times \log_{10}^{3}(N) \quad (3.19)$$

$$V_{2U}(N)[mm] = -0.9056 + 2.0629 \times \log_{10}(N) - 2.3229 \times \log_{10}^{2}(N) + 0.2149 \times \log_{10}^{3}(N) \quad (3.20)$$

$$V_{3U}(N)[mm] = 0.2588 + 0.143 \times \log_{10}(N) - 0.572 \times \log_{10}^{2}(N) - 0.0014 \times \log_{10}^{3}(N) \quad (3.21)$$

where V_{1U}, V_{2U}, V_{3U} are the cumulative permanent vertical deflections of the unreinforced section (α-α) of points 1, 2 and 3 respectively.

The corresponding curves are illustrated in Figure 3.2

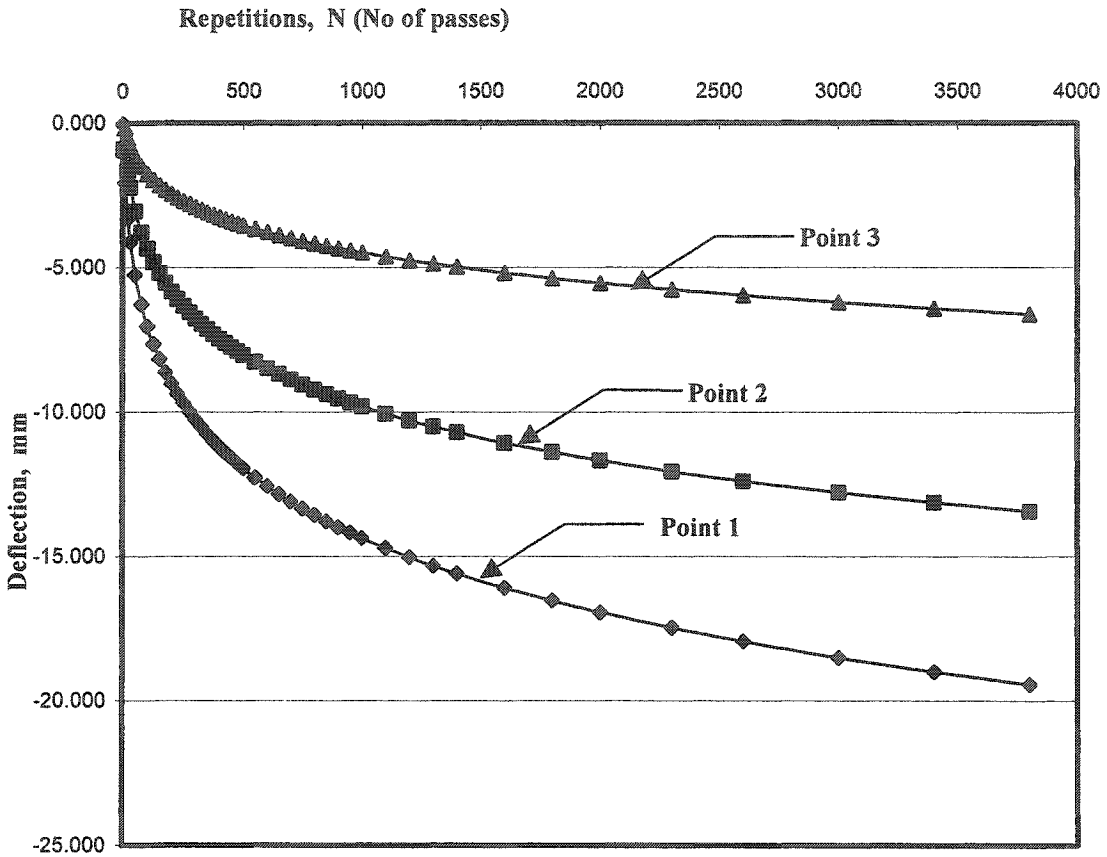

Figure 3. 2 Cumulative permanent deflections V_{iU} of unreinforced pavement system for points i = 1, 2 and 3 resulting from number N of load repetitions

Similarly, we can determine accumulated permanent vertical displacements for ***reinforced section (β-β)*** that contains the geogrid reinforcement at the interface of base layer and subgrade layer. This means that we have:

$$V_{1RI}(N)[mm] = 0.0320 + 0.1161\log_{10}(N) - 1.1322\log_{10}^{2}(N) + 0.0.0390\log_{10}^{3}(N) \qquad (3.22)$$

$$V_{2RI}(N)[mm] = -0.0006 + 0.4359\ \log_{10}(N) - 0.6063\log_{10}^{2}(N) + 0.0186\ \log_{10}^{3}(N) \qquad (3.23)$$

$$V_{3RI}(N)[mm] = -0.0472 + 0.5152\log_{10}(N) - 0.3666\ \log_{10}^{2}(N) + 0.0408\ \log_{10}^{3}(N) \qquad (3.24)$$

where V_{1RI}, V_{2RI}, and V_{3RI} are the cumulative permanent vertical deflections of the reinforced section (β-β) of points 1, 2 and 3 respectively.

The corresponding curves are illustrated in Figure 3.3.

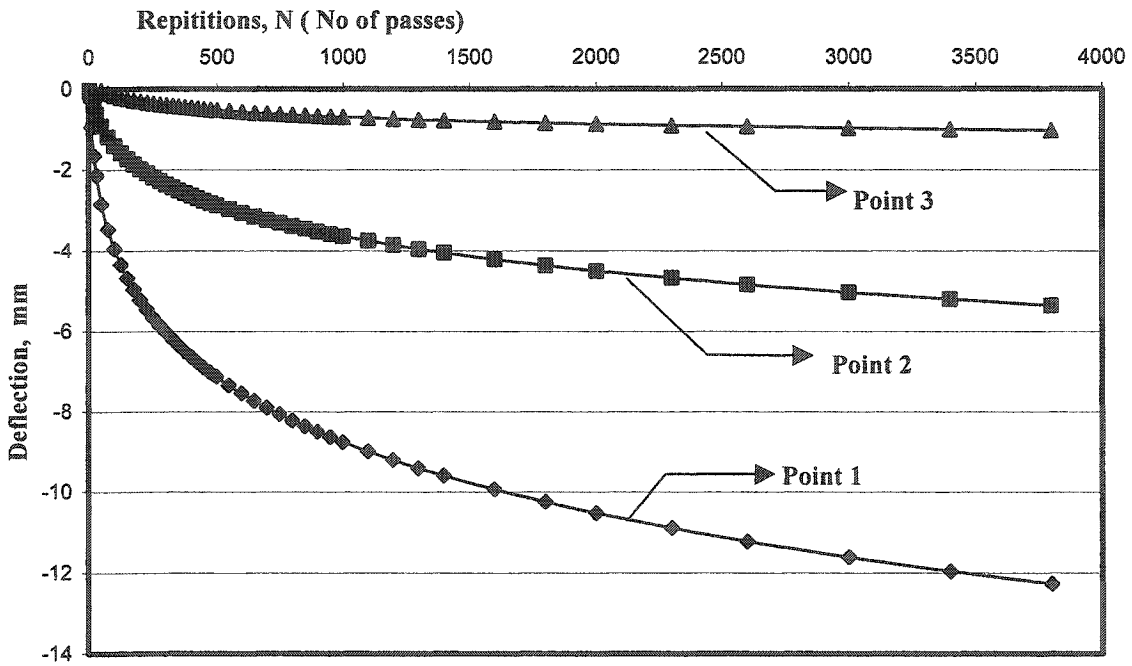

Figure 3. 3. Cumulative permanent deflections V_{iRI} of reinforced pavement system (geogrid at the base-subgrade interface) for points i = 1, 2 and 3 resulting from number N of load repetitions.

Consequently, we can determine the accumulated permanent vertical displacements for ***reinforced section (γ-γ)*** that contains the geogrid reinforcement located in the middle of the base layer. Thus:

$$V_{1RM}(N)[mm] = -0.0207 - 0.0241 \log_{10}(N) - 0.4144 \log_{10}^{2}(N) - 0.0039 \log_{10}^{3}(N) \quad (3.25)$$

$$V_{2RM}(N)[mm] = -0.0024 + 0.7109 \log_{10}(N) - 0.8625 \log_{10}^{2}(N) + 0.1213 \log_{10}^{3}(N) \quad (3.26)$$

$$V_{3RM}(N)[mm] = -0.0198 + 0.4213 \log_{10}(N) - 0.3984 \log_{10}^{2}(N) + 0.0389 \log_{10}^{3}(N) \quad (3.27)$$

where V_{1RM}, V_{2RM}, and V_{3RM} are the cumulative permanent vertical deflections of the reinforced section (γ-γ) of points 1, 2 and 3 respectively.

The corresponding curves are illustrated in Figure 3.4.

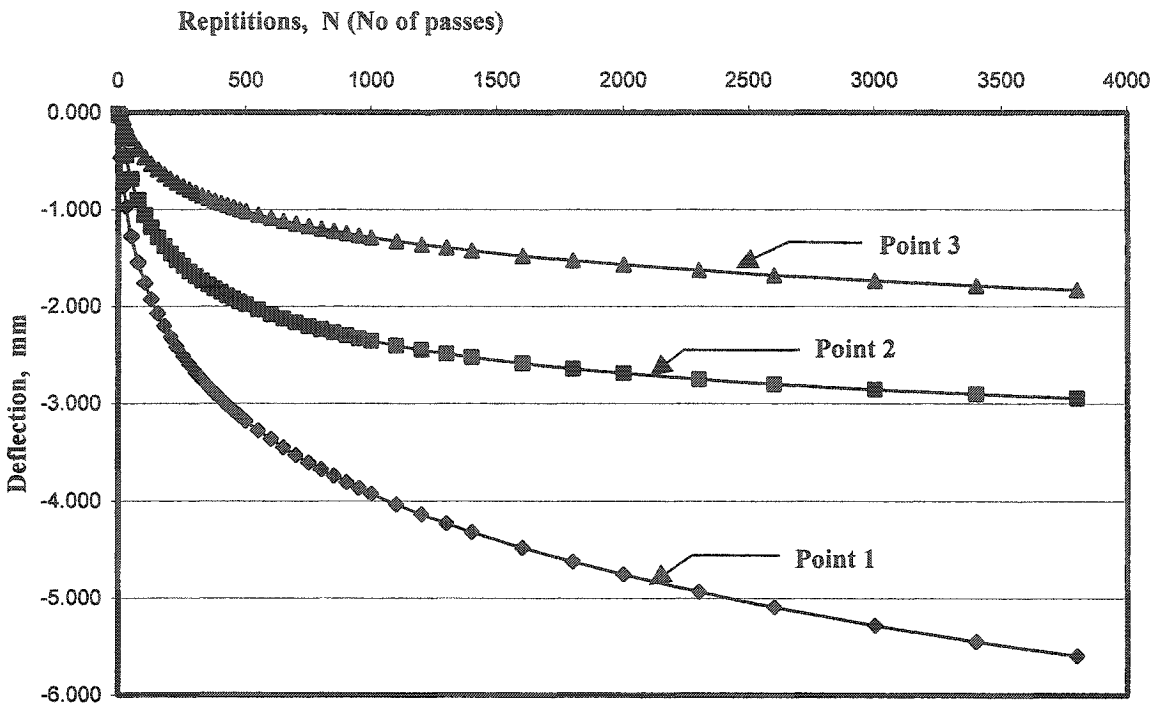

Figure 3. 4. Cumulative permanent deflections V_{iRM} of reinforced pavement system (geogrid in the middle of the base layer) for points i = 1, 2 and 3 resulting from number N of load repetitions.

The described problem is formulated in terms of permanent vertical deformations that are unrecoverable. The laboratory studies conducted on three comparative models provided experimental data on the permanent displacements of characteristic points 1, 2 and 3 of unreinforced, geogrid reinforced at the base subgrade interface and geogrid reinforced in the middle of the base layer, which are shown in Figure 3.2, 3.3 and 3.4 respectively. Typically, for comparative studies both unreinforced and reinforced sections have the same geometry that consists of the same components (wearing course followed by base layer and subgrade layer). In experimental studies three systems are subjected to the same

repetitive loadings of pressure type of constant value acting on the same area. It is worth noting that recoverable deformations were negligible and were not recorded. That's why the investigated systems are characterized by cumulative unrecoverable deformation.

A closer look at the results presented in Figures 3.2 – 3.4 shows that reinforced section that contains the geogrid insertion results in much smaller deformations that is translated to longer durability of the system, safer conditions of driving and better economy of the system. Another advantage of application of geogrid can be associated with reduction of the thickness of the base layer that is considered to be thinner when geogrid holds when compared with the unreinforced section. The requirement imposed on both sections unreinforced (U) and reinforced (R) to provide the same performance and comfort of utilization of transportation system makes the criterion allowing to determine the equivalent thickness of the homogeneous unreinforced base layer. It is postulated that the difference between deflections of unreinforced (U) and reinforced (R) system can be compensated by increasing the thickness of the base layer of unreinforced system.

Equations (3.19)-(3.21) form basis for determination of increment of permanent deformation associated with each consecutive load application. They result in increments of permanent deformation ΔV_{iU} for i = 1, 2 and 3 that can be determined as the difference of accumulated permanent deformations corresponding to the current number of load application N and the cumulative deformations for the previous (N-1) load applications. Thus for ***unreinforced cross section*** ***(α-α)*** Equations. (3.19)-(3.21) for (N-1) have the following forms:

$$V_{1U}(N-1)[mm] = -0.0491 - 0.3431 \times \log_{10}(N-1) - 1.7791 \times \log_{10}^{2}(N-1) + 0.1009 \times \log_{10}^{3}(N-1) \quad (3.28)$$

$$V_{2U}(N-1)[mm] = -0.9056 + 2.0629 \times \log_{10}(N-1) - 2.3229 \times \log_{10}^{2}(N-1) + 0.2149 \times \log_{10}^{3}(N-1) \quad (3.29)$$

$$V_{3U}(N-1)[mm] = 0.2588 + 0.143 \times \log_{10}(N-1) - 0.572 \times \log_{10}^{2}(N-1) - 0.0014 \times \log_{10}^{3}(N-1) \quad (3.30)$$

The suitable subtractions of Equations (3.19)-(3.21) and Equations (3.28)-(3.30) give the increments of permanent deformation Δ_{iU} for i = 1, 2 and 3 associated with each load application N that are presented as follows:

$$\Delta_{1U}(N)[mm] = V_{1U}(N) - V_{1U}(N-1) = -0.3431 \log_{10}\left(\frac{N}{N-1}\right) - 1.7791 \log_{10}^{2}\left(\frac{N}{N-1}\right) + 0.1009 \log_{10}^{3}\left(\frac{N}{N-1}\right) \quad (3.31)$$

$$\Delta_{2U}(N)[mm] = V_{2U}(N) - V_{2U}(N-1) = 2.0629 \log_{10}\left(\frac{N}{N-1}\right) - 2.3229 \log_{10}^{2}\left(\frac{N}{N-1}\right) + 0.2149 \log_{10}^{3}\left(\frac{N}{N-1}\right) \quad (3.32)$$

$$\Delta_{3U}(N)[mm] = V_{3U}(N) - V_{3U}(N-1) = 0.143 \log_{10}\left(\frac{N}{N-1}\right) - 0.572 \log_{10}^{2}\left(\frac{N}{N-1}\right) - 0.0014 \log_{10}^{3}\left(\frac{N}{N-1}\right) \quad (3.33)$$

It is worth noting that Equations (3.28)-(3.30) have to satisfy the condition that for N = 1

$$V_{1U}(N-1) = V_{2U}(N-1) = V_{3U}(N-1) = 0 \quad (3.34)$$

Similar analysis of deformability can be conducted for reinforced section RI (geogrid reinforced at the interface of base and subgrade layer) and RM (geogrid reinforced in the middle of the base layer) of the flexible pavement. The relationships of Equations (3.25)-(3.27) are also valid for N-1 load applications, thus similarly to Equations (3.28)-(3.30), they are now written for ***reinforced section (β-β)*** with geogrid located at the interface of base layer and subgrade layer. Thus:

$$V_{1RI}(N-1)[mm] = 0.0320 + 0.1161\log_{10}(N-1) - 1.1322\log_{10}^{2}(N-1) + 0.0.0390\log_{10}^{3}(N-1) \quad (3.35)$$

$$V_{2RI}(N-1)[mm] = -0.0006 + 0.4359\log_{10}(N-1) - 0.6063\log_{10}^{2}(N-1) + 0.0186\log_{10}^{3}(N-1) \quad (3.36)$$

$$V_{3RI}(N-1)[mm] = -0.0472 + 0.5152\log_{10}(N-1) - 0.3666\log_{10}^{2}(N-1) + 0.0408\log_{10}^{3}(N-1) \quad (3.37)$$

The analogous condition to Equation (3.34) is valid for the set of Equations (3.35)-(3.37) too, which is expressed as for N = 1:

$$V_{1RI}(N-1)\ [mm] = V_{2RI}\ (N-1)[mm] = V_{3RI}\ (N-1)[mm] \quad (3.38)$$

The increment of permanent deformation Δ_{iRI} at points i =1, 2 and 3 of ***reinforced section (β-β)*** can be determined based on properly performed subtractions of Equations (3.22)-(3.24) and Equations (3.35)-(3.37), which result in the following outcomes:

$$\Delta_{1RI}(N)[mm] = V_{1RI}(N) - V_{1RI}(N-1)$$
$$= 0.1161 \log_{10}\left(\frac{N}{N-1}\right) - 1.1322 \log_{10}^{2}\left(\frac{N}{N-1}\right) + 0.039 \log_{10}^{3}\left(\frac{N}{N-1}\right) \quad (3.39)$$

$$\Delta_{2RI}(N)[mm] = V_{2RI}(N) - V_{2RI}(N-1)$$
$$= 0.4359 \log_{10}\left(\frac{N}{N-1}\right) - 0.6063 \log_{10}^{2}\left(\frac{N}{N-1}\right) + 0.0186 \log_{10}^{3}\left(\frac{N}{N-1}\right) \quad (3.40)$$

$$\Delta_{3RI}(N)[mm] = V_{3RI}(N) - V_{3RI}(N-1)$$
$$= 0.5152 \log_{10}\left(\frac{N}{N-1}\right) - 0.3666 \log_{10}^{2}\left(\frac{N}{N-1}\right) + 0.0408 \log_{10}^{3}\left(\frac{N}{N-1}\right) \quad (3.41)$$

The relationships of Equations (3.25)-(3.27) are also valid for N-1 load applications, thus similarly to Equations (3.28)-(3.30), they are now written for ***reinforced section (γ-γ)*** with geogrid located in the middle of the base layer. Thus we have:

$$V_{1RM}(N-1)[mm] = -0.0207 - 0.0241 \log_{10}(N-1) - 0.4144 \log_{10}^{2}(N-1) - 0.0039 \log_{10}^{3}(N-1)$$

(3.42)

$$V_{2RM}(N-1)[mm] = -0.0024 + 0.7109 \log_{10}(N-1) - 0.8625 \log_{10}^{2}(N-1) + 0.1213 \log_{10}^{3}(N-1) \quad (3.43)$$

$$V_{3RM}(N-1)[mm] = -0.0198 + 0.4213 \log_{10}(N-1) - 0.3984 \log_{10}^{2}(N-1) + 0.0389 \log_{10}^{3}(N-1) \quad (3.44)$$

The analogous condition to Equation (3.34) is valid for the set of Equations (3.42)-(3.44) too, which is expressed as for N = 1:

$$V_{1RM}(N\text{-}1)\ [mm] = V_{2RM}\ (N\text{-}1)[mm] = V_{3RM}\ (N\text{-}1)[mm] \quad (3.45)$$

The increment of permanent deformation Δ_{iRM} at points i =1, 2 and 3 of ***reinforced section (γ-γ)*** can be determined based on properly performed subtractions of Equations (3.25)-(3.27) and Equations (3.42)-(3.44), which result in the following outcomes:

$$\begin{aligned}\Delta_{1RM}(N)[mm] &= V_{1RM}(N) - V_{1RM}(N-1) \\ &= -0.241 \log_{10}\left(\frac{N}{N-1}\right) - 0.4144 \log_{10}^{2}\left(\frac{N}{N-1}\right) - 0.0039 \log_{10}^{3}\left(\frac{N}{N-1}\right)\end{aligned} \quad (3.46)$$

$$\begin{aligned}\Delta_{2RM}(N)[mm] &= V_{2RM}(N) - V_{2RM}(N-1) \\ &= 0.7109 \log_{10}\left(\frac{N}{N-1}\right) - 0.8625 \log_{10}^{2}\left(\frac{N}{N-1}\right) + 0.1213 \log_{10}^{3}\left(\frac{N}{N-1}\right)\end{aligned} \quad (3.47)$$

$$\Delta_{3RM}(N)[mm] = V_{3RM}(N) - V_{3RM}(N-1)$$
$$= 0.4213 \log_{10}\left(\frac{N}{N-1}\right) - 0.3984 \log_{10}^{2}\left(\frac{N}{N-1}\right) + 0.0389 \log_{10}^{3}\left(\frac{N}{N-1}\right) \quad (3.48)$$

The increments of permanent deflections of point 1 for unreinforced system Δ_{1U} and reinforced systems Δ_{1RI} and Δ_{1RM} corresponding to each single load application N are shown in Figure 3.5

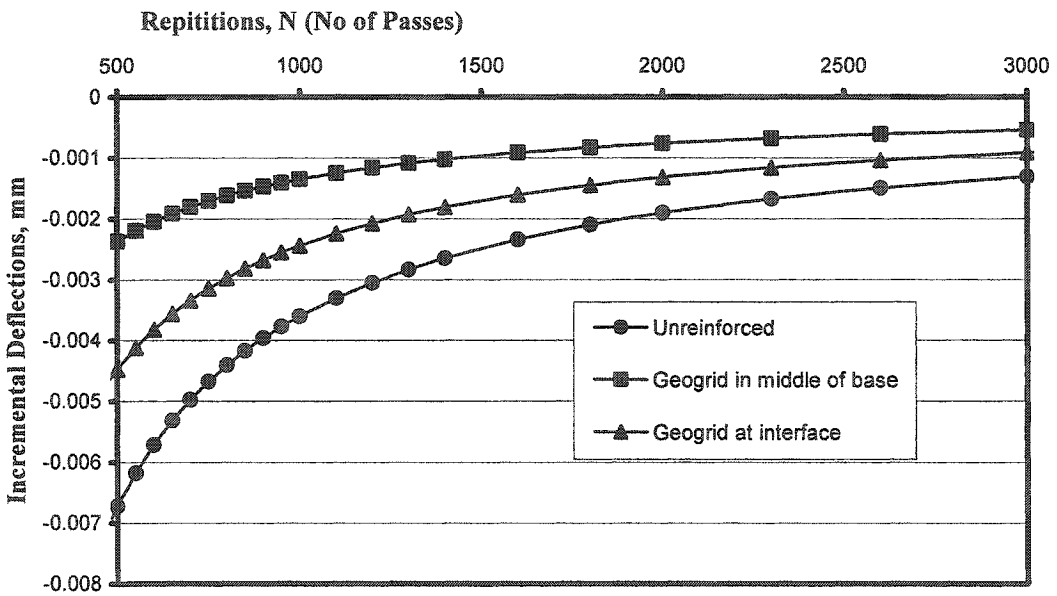

Figure 3.5. Distributions of permanent deformations of unreinforced Δ_{iU} and reinforced Δ_{iR} pavement systems generated by sequential number N of load application.

It is evident that $\Delta_{iR} < \Delta_{iU}$ which justifies the purpose of the geogrid insertion in the base layer. The superiority of the performance of the reinforced system over the unreinforced

one is expressed in terms of the decrement of deflections associated with each single load application N. It is assessed by means of $\delta i(N)$ for points i = 1, 2 and 3 as:

$$\delta 1(N) = \Delta_{1U}(N) - \Delta_{1R}(N) \tag{3.49}$$

$$\delta 2(N) = \Delta_{2U}(N) - \Delta_{2R}(N) \tag{3.50}$$

$$\delta 3(N) = \Delta_{3U}(N) - \Delta_{3R}(N) \tag{3.51}$$

Employing the above formulas, the results in terms of $\delta i(N)$ as the functions of the number of load applications N for unreinforced and reinforced cross section with geogrid at the base subgrade interface are the following:

$$\begin{aligned}\delta 1_{(U\text{-}RI)}(N)[mm] &= \Delta_{1U}(N) - \Delta_{1RI}(N) \\ &= -0.4592 \log_{10}\left(\frac{N}{N-1}\right) - 0.6469 \log_{10}^{2}\left(\frac{N}{N-1}\right) + 0.0619 \log_{10}^{3}\left(\frac{N}{N-1}\right)\end{aligned} \tag{3.52}$$

$$\begin{aligned}\delta 2_{(U\text{-}RI)}(N)[mm] &= \Delta_{2U}(N) - \Delta_{2RI}(N) \\ &= 1.627 \log_{10}\left(\frac{N}{N-1}\right) - 1.7166 \log_{10}^{2}\left(\frac{N}{N-1}\right) + 0.1963 \log_{10}^{3}\left(\frac{N}{N-1}\right)\end{aligned} \tag{3.53}$$

$$\begin{aligned}\delta 3_{(U\text{-}RI)}(N)[mm] &= \Delta_{3U}(N) - \Delta_{3RI}(N) \\ &= -0.3722 \log_{10}\left(\frac{N}{N-1}\right) - 0.2054 \log_{10}^{2}\left(\frac{N}{N-1}\right) - 0.0422 \log_{10}^{3}\left(\frac{N}{N-1}\right)\end{aligned} \tag{3.54}$$

where $\delta 1_{(U\text{-}RI)}$, $\delta 2_{(U\text{-}RI)}$, $\delta 3_{(U\text{-}RI)}$ are the differences between the increments of permanent deformations of unreinforced and reinforced cross section with geogrid at the base-subgrade interface of points 1, 2 and 3 respectively.

The results of Equations (3.52)-(3.54) are presented in Figure 3.6.

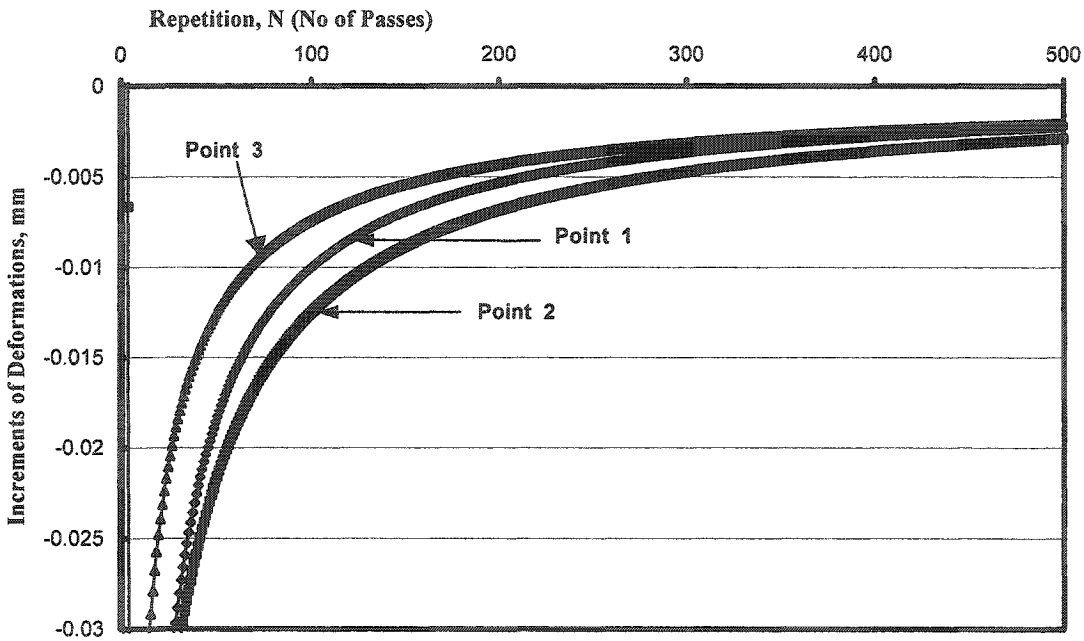

Figure 3.6. Distributions of the differences of the permanent deformations of $\delta 1(N)$, $\delta 2(N)$ and $\delta 3(N)$ of unreinforced and reinforced pavement systems (i.e., geogrid at the interface of base-subgrade layer) generated by the sequential number of load application N.

Similarly for the unreinforced and geogrid in the middle of the base layer we have:

$$\delta 1_{(U-RM)}(N)[mm] = \Delta_{1U}(N) - \Delta_{1RM}(N)$$
$$= -0.1021 \log_{10}\left(\frac{N}{N-1}\right) - 1.3647 \log_{10}^{2}\left(\frac{N}{N-1}\right) + 0.1048 \log_{10}^{3}\left(\frac{N}{N-1}\right)$$

(3.55)

$$\delta 2_{(U-RM)}(N)[mm] = \Delta_{2U}(N) - \Delta_{2RM}(N)$$
$$= 1.352 \log_{10}\left(\frac{N}{N-1}\right) - 1.4604 \log_{10}^{2}\left(\frac{N}{N-1}\right) + 0.0936 \log_{10}^{3}\left(\frac{N}{N-1}\right)$$

(3.56)

$$\delta 3_{(U-RM)}(N)[mm] = \Delta_{3U}(N) - \Delta_{3RM}(N)$$
$$= -0.2783 \log_{10}\left(\frac{N}{N-1}\right) - 0.1736 \log_{10}^{2}\left(\frac{N}{N-1}\right) - 0.0403 \log_{10}^{3}\left(\frac{N}{N-1}\right)$$

(3.57)

where $\delta 1_{(U-RM)}$, $\delta 2_{(U-RM)}$, $\delta 3_{(U-RM)}$ are the differences between the increments of permanent deformations of unreinforced and reinforced cross section with geogrid in the middle of the base layer of points 1, 2 and 3 respectively.

The results of Equations (3.39)- (3.41) are presented in Figure 3.7.

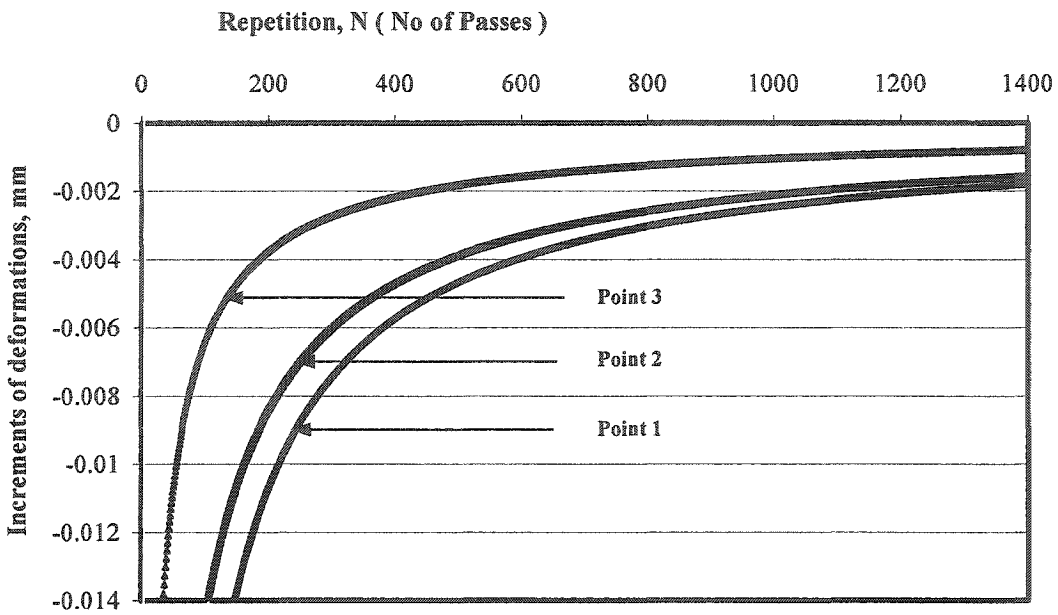

Figure 3.7. Distributions of the differences of the permanent deformations of $\delta 1(N)$, $\delta 2(N)$ and $\delta 3(N)$ of unreinforced and reinforced pavement systems (i.e., geogrid in the middle of the base layer) generated by the sequential number of load application N.

CHAPTER IV

PROBLEM FORMULATION

4.1 Introduction

Particular instances of problems involving the concept of a functional were considered more than 300 years ago, and in fact, the first important results in this area are due to Euler (1707 – 1783). Nevertheless, up to now, the " Calculus of functional" still does not have methods of a generality comparable to the methods of classical analysis (i.e., the ordinary " Calculus of Functions"). The most developed branch of the " Calculus of functionals" is concerned with finding the maxima and minima of functionals, and is called the " Calculus of Variations".

The Calculus of Variations is assuming an increasingly important role in the field of analysis, physics and engineering. It is at present a powerful method for the solution of problems in dynamics and statics of rigid bodies, general elasticity, the theory of plates and shells, vibration optics, quantum mechanics, optimization of orbits and controls etc.

4.2 Definitions and Terminology related to Functionals

4.2.1 Functional

A functional is defined as a quantity or function, which depends upon the entire course or path of one or more functions rather than on a number of discrete variables. The domain of a functional is a set or collection of admissible functions, which belongs to a function space or class rather than to a region in coordinate space. According to Euler, functionals

can be regarded as "functions of infinitely many variables". (i.e., the values of the function y (x) at separated points.)

For example the length of a curve y = y (x) defined over the close interval $x_0 \le x \le x_1$, or more compactly $[x_0, x_1]$ is given by the integral:

$$L = L(y) = \int_{x_0}^{x_1} \sqrt{1+(y')^2}\,dx = \int_{x_0}^{x_1} F(x, y')dx$$

where, $y' = \dfrac{dy}{dx}$

Thus the value of L depends on the path or form of the function y (x), called the *argument function*. In order that the above integral exist, it is sufficient that y (x) be taken as an arbitrary continuous function with a piecewise continuous derivative. Symbolically L = L (y) expresses the dependence of L on y.

Functionals may also depend upon the behavior of more than one function. Suppose two admissible functions y (x) and z (x) are continuously differentiable on the closed segment $[x_0, x_1]$. y (x) and z(x) have specified values at x_0 and x_1; that is:

$y(x_0) = y_0$, $y(x_1) = y_1$, $z(x_0) = z_0$ and $z(x_1) = z_1$

Therefore a functional of y and z is:

$$J(y,z)=\int_{x_0}^{x_1} F(x,y,z,y',z')dx$$

where F is a continuous function of its five arguments x, y, z, y', z'. By choosing different functions, we obtain different functionals.

4.2.2 Function Spaces

Geometric language is useful when studying functionals. Thus, we shall regard each function y(x) belonging to some class as a point in some space, and spaces whose elements are functions will be called function spaces.

In the study of functions of a finite number n of independent variables, it is sufficient to consider a single space, i.e., n-dimensional Euclidean space. However, in the case of function spaces, there is no such " universal space". In fact the nature of the problem under considerations determines the choice of functions. For example, if we are dealing with a functional of the form:

$$\int_a^b F(x,y,y')\,dx\,,$$

it is natural to regard the functional as defined on the set of all functions with a continuous first derivative, while in the case of a functional of the form

$$\int_a^b F(x, y, y', y'')\,dx$$

the appropriate function space is the set of all functions with two continuous derivatives. Therefore, in studying functionals of various types, it is reasonable to use various function spaces.

4.3 Theoretical Formulation of the Functional with Moving Ends

The general formula for the functional is the form of:

$$J_1(y_1, \ldots\ldots, y_n) = \int_{x_0}^{x_1} F(x, y_1, \ldots\ldots, y_n, y_1', \ldots\ldots, y_n')dx \qquad (4.1)$$

when Equation (4.1) depends on a single function y which is continuously differentiable on the closed segment $[x_0, x_1]$ and then Equation (4.1) reduces to:

$$J(y) = J_1(y) = \int_{x_0}^{x_1} F(x, y, y')dx \qquad (4.2)$$

when F is a continuous function of its three arguments x, y, y' for the first functional J_1 defined in Equation (4.2) where y (x) has specific values at end points x_0 and x_1; that is:

$$y(x_0) = y_0 \quad ; \quad y(x_1) = y_1 \qquad (4.3)$$

Now, we assume that the end points of the curves for which Equation (4.2) is defined such that $F(x,y,y')$ can move in an arbitrary way. For example, suppose that we are given the functional:

$$J(y+h) = J_2(y) = \int_{x_0+\delta x_0}^{x_1+\delta x_1} F(x,\, y+h,\, y'+h')\, dx \tag{4.4}$$

When F is a given explicit function of x, (y + h), $(y'+h')$ and $[x_0 + \delta x_0]$, $[x_1 + \delta x_1]$ are fixed end points for the second functional J_2 defined in Equation (4.4) where [y (x)+h (x)] have specific values at end points $[x_0 + \delta x_0]$ and $[x_1 + \delta x_1]$; that is:

$$y(x_0+\delta x_0) = y_0 + \delta y_0 \quad ; \quad y(x_1+\delta x_1) = y_1 + \delta y_1 \tag{4.5}$$

The boundary conditions of integrands at $F(z,y,y')$ and $F(z,y+h,y'+h')$ are shown in Figure 4.1. The difference between y and [y + h (x)] is very small. The first variation δJ of functionals given by Equations (4.2) and (4.4) is sought. It is worth noting that functional (4.2) and (4.4) are defined within different boundaries at end points (Gelfand and Fomin, 1963 (22)).

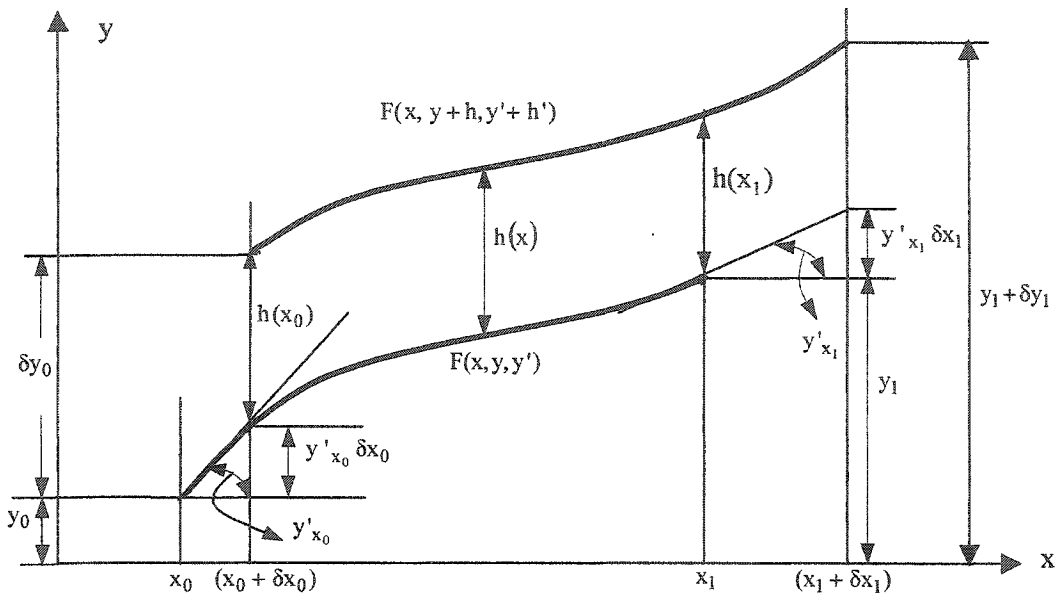

Figure 4.1. The functions $F(x,y,y')$ and $F(x,y+h,y'+h')$ for which the functionals J_1 and J_2 are formulated.

The subtraction of Equation (4.4) from Equation (4.2) results in the first variation of δJ of functional J [y], which is given as:

$$\delta J = J_2 - J_1 = J(y+h) - J(y) = \int_{x_0+\delta x_0}^{x_1+\delta x_1} F(x,y+h,y'+h')\,dx - \int_{x_0}^{x_1} F(x,y,y')\,dx \qquad (4.6)$$

By taking into account the required modifications of the integrand's boundaries we get:

$$\delta J = \int_{x_0}^{x_1} [F(x,y+h,y'+h') - F(x,y,y')]dx - \int_{x_0}^{x_0+\delta x_0} F(x,y+h,y'+h')\,dx + \int_{x_1}^{x_1+\delta x_1} F(x,y+h,y'+h')dx$$

(4.7)

In Equation (4.7) the first two integrals can be expanded by means of Taylor's series, which results the first two integrals of Equation (4.8). By means of Taylor's mean value theorem with respect to last two integrals of Equation (4.7) we can get (neglecting the terms of order higher than one):

$$\delta J = \int_{x_0}^{x_1} [F_y\, h(x) + F_{y'}\, h'(x)]dx - F(x,y,y') \Big|_{x=x_0} \delta x_0 + F(x,y,y') \Big|_{x=x_1} \delta x_1 \tag{4.8}$$

Integrating by parts the second term under first integral results in:

$$\begin{aligned} \delta J &= \int_{x_0}^{x_1} F_y h(x)dx + F_{y'} h(x)\Big|_{x_0}^{x_1} - \int_{x_0}^{x_1} \frac{d}{dx} F_{y'} h(x)dx - F(x,y,y')\Big|_{x=x_0} \delta x_0 + F(x,y,y')\Big|_{x=x_1} \delta x_1 \\ &= \int_{x_0}^{x_1} (F_y - \frac{d}{dx} F_{y'}) h(x)dx + F_{y'}\, h(x)\Big|_{x_0}^{x_1} - F(x,y,y')\Big|_{x=x_0} \delta x_0 + F(x,y,y')\Big|_{x=x_1} \delta x_1 \end{aligned} \tag{4.9}$$

Equation (4.7) demonstrates that δJ can be determined by means of integrand F, its derivative and their values at boundaries $x = x_0$ and $x = x_1$. The second term of Equation (4.7) contains increment of function y equal to h (x) that is not defined for $x = x_0$ and $x = x_1$. However it can be determined by means of given δy_0 and δy_1 and its derivative y' at $x = x_0$ and $x = x_1$ respectively. Thus:

$$h(x_0) = \delta y_0 - y'_{x_0} \delta x_0 \tag{4.10}$$

$$h(x_1) = \delta y_1 - y'_{x_1} \delta x_1 \tag{4.11}$$

The explicit application of relationships of Equations (4.10) and (4.11) will be evident, if Equation (4.9) will be reshaped to the following form:

$$\delta J = \int_{x_0}^{x_1} (F_y - \frac{d}{dx} F_{y'}) h(x) dx + F_{y'} \Big|_{x_1} h(x_1) - F_{y'} \Big|_{x_0} h(x_0) - F(x,y,y') \Big|_{x=x_0} \delta x_0 + F(x,y,y') \Big|_{x=x_1} \delta x_1 \tag{4.12}$$

Substituting Equations (4.10) and (4.11) into Equation (4.12) gives:

$$\begin{aligned} \delta J = \int_{x_0}^{x_1} (F_y - \frac{d}{dx} F_{y'}) h(x) dx + F_{y'} \Big|_{x=x_1} (\delta y_1 - y'_{x_1} \delta x_1) - F_{y'} \Big|_{x=x_0} (\delta y_0 - y'_{x_0} \delta x_0) \\ - F(x,y,y') \Big|_{x=x_0} \delta x_0 + F(x,y,y') \Big|_{x=x_1} \delta x_1 \end{aligned} \tag{4.13}$$

Rearranging Equation (4.13) with suitably combine the terms associated with shifts of boundaries δx_0 and δx_1, it is arrived at:

$$\delta J = \int_{x_0}^{x_1} [(F_y - \frac{d}{dx} F_{y'}) h(x)] dx + (F - F_{y'} y') \Big|_{x_1} \delta x_1 - (F - F_{y'} y') \Big|_{x_0} \delta x_0 + F_{y'} \Big|_{x_1} \delta y_1 - F_{y'} \Big|_{x_0} \delta y_0 \tag{4.14}$$

Equation (4.14) represents sensitivity of δJ due to the changes of δx_0 and δx_1. Also Equation (4.14) can be considered as the basis that defines first variation of energy potential due to the shifts of boundaries δx_0 and δx_1.

4.4 Application of Functional with Moving Ends for the Assessment of the Equivalent Thickness of Base Layer

For our defined problem we are interested to apply the sensitivity theory for the assessment of equivalent base layer. By definition, sensitivity analysis is considered to be conducted in any field when the starting solution is known (i.e., $F(x, y, y')$. This means that, when the starting solution for any kind of problem is given, i.e., all initial material characteristics, the state of deformation of the system and required constitutive relation are known.

The theoretical basis for the evaluation of the energy potential J_1 of permanent deformations of unreinforced pavement system is provided by the virtual work principle. The energy potential J_1 can be assessed of deformation Δ_{iU} caused by each single number N of load application. To determine Δ_{iU} the virtual work principle is used and for the implementation of virtual work principle the primary structure and the adjoint structure are introduced. The primary structure is subjected to the original loading, while the adjoint structure is subjected to the virtual unit loading at the point of interest, i.e., where the displacements are monitored at control points in the laboratory experiments. Adjoint structure is constructed in the same way as the primary structure, i.e., it satisfies the same constitutive laws and deforms in the same way as the primary system does. The mathematical form of the virtual work theorem gives:

$$\bar{1}v = \int_{V=Volm} (\varepsilon_{ij}\overline{\sigma_{ij}})(dV) \qquad (4.15)$$

where $\bar{1}$ = unit virtual force applied to the point 1 of adjoint structure,

v = the displacement (permanent deformation) caused by the external pressure load q applied on the primary structure at the point where the virtual force is applied on,

ε_{ij} = strains of the primary system caused by application of load q,

$\overline{\sigma_{ij}}$ = stresses of the adjoint system caused by the load $\bar{1}$ applied to the point 1.

The primary pavement system employed in the analysis is considered to be an axisymmetric, which has been discussed in chapter III. It is shown in Figure 4.2.

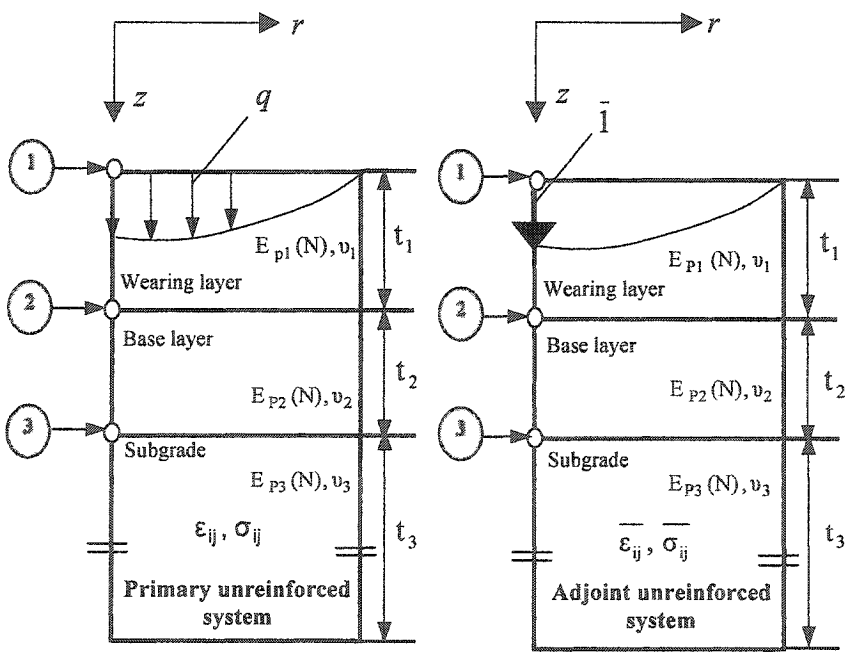

Figure 4.2. Sections of primary and adjoint unreinforced pavement systems

In the studies performed, the dynamic effect (inertia force) is not taken into consideration, therefore the load q applied on the primary system can be considered either as a moving pressure or as a applying pressure q of " pumping type" that is slowly applied and removed without changing the load amplitude. It is postulated that the primary system deforms in permanent fashion (not recoverable), which is characterized by the " modified Hooke's law" and depends on number of each N load application and for which geometry updating is required for the next following step. Now for the purpose of sensitivity analysis to be performed in the virtual work principle, a temporary system called adjoint system is introduced. (Figure 4.2) It is constructed in the same way as the primary structure, i.e., it satisfies the same constitutive laws and deforms in the same way as the primary system does.

Thus for the unreinforced pavement system with unrecoverable deformations (i.e., permanent deformations) and with the associated adjoint system (shown in Figure 4.2), the potential energy of permanent deformation J_1 (i.e., the functional) can be determined by means of permanent deformation Δ_{1U} of point 1. It is given as:

$$J_1(\Delta_1(N)) = \bar{1} \bullet \Delta_{1U}(N) = \iint_A [\int_0^{t_1} \varepsilon_{ij}\, \overline{\sigma_{ij}}\, dz + \int_{t_1}^{t_1+t_2} \varepsilon_{ij}\, \overline{\sigma_{ij}}\, dz + \int_{t_1+t_2}^{t_1+t_2+t_3} \varepsilon_{ij}\, \overline{\sigma_{ij}}\, dz]dA \qquad (4.16)$$

where ε_{ij} = strains of the primary system when the load q is applied,

$\overline{\sigma_{ij}}$ = stresses of the adjoint system caused by the load $\bar{1}$ applied to the point 1.

Similar relationship can be written for the system that contains the geogrid insertion as reinforcement. The reinforced system however shown in Figure 4.3 that generates deformations Δ_{iRI} (N) and Δ_{iRM} (N) given by Equations (3.39)–(3.41) and Equations (3.46)-(3.48) respectively differentiate itself from primary unreinforced pavement system in terms of material properties of the reinforced layers. It is conceivable that results of deformations defined by Equations (3.39)–(3.41) and Equations (3.46)–(3.48) can be achieved by unreinforced flexible pavement system (denoted as I in Figure 4.3) that has increased its thickness of base layer by the increment δt when single load application N is executed. The corresponding functional of the potential energy of permanent deformations of the equivalent unreinforced primary system I can be determined with the aid of the conjugated / adjoint system (denoted as II in Figure 4.3) based on the virtual work principle.

So the corresponding functional J_2 of the reinforced system R (for the geogrid insertion in the middle of the base and at the interface of base-subgrade layer) and associated adjoint system can be defined with the aid of equivalent unreinforced primary system I and the associated equivalent unreinforced adjoint system II (shown in Figure 4.3) based on the virtual work principle for a single number N of load repetition that is applied to the equivalent unreinforced primary system I (shown in Figure 4.3) subjected to load q. It is assessed based on permanent deformation of point 1 whereas the deformed system II is subjected to unit force $\bar{1}$ applied to point 1.

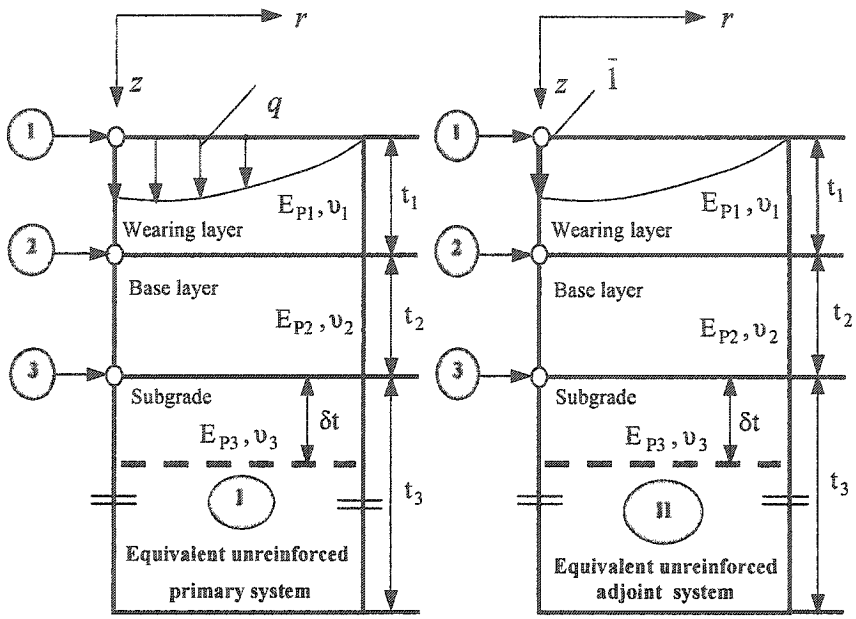

Figure 4.3. Sections of the equivalent primary system and the equivalent adjoint system

$$J_2(\Delta_1(N))_{EQ} = \bar{1} \bullet \Delta_{1R}(N) = \int_A [\int_0^{t_1} \varepsilon_{ij}\,\overline{\sigma_{ij}}\,dz + \int_{t_1}^{t_1+t_2+\delta t} \varepsilon_{ij}\,\overline{\sigma_{ij}}\,dz + \int_{t_1+t_2+\delta t}^{t_1+t_2+t_3} \varepsilon_{ij}\,\overline{\sigma_{ij}}\,dz]dA \qquad (4.17)$$

Comparison of Equations (4.16) and (4.17) reveals that their right hand sides represent the functional with moving ends for the same flexible pavement system. However, the subtraction of their left hand sides for arbitrary number of load repetition N is defined by Equation (3.49), Equation (3.52 – geogrid is at the interface of base –subgrade layer) and Equation (3.55 – for goegrid in the middle of the base layer). Thus, subtracting Equation (4.17) from Equation (4.16) results in:

$$\bar{1}.\Delta_{1R}(N) - \bar{1}.\Delta_{1U}(N) = -\bar{1}.\delta 1(N) \qquad (4.18)$$

However, $-\bar{1}.\delta 1(N)$ can be also expressed as:

$$-\bar{1}.\delta 1(N)=J_2(\Delta_1(N))_{EQ}-J_1(\Delta_1(N))=\delta J \tag{4.19}$$

For the axisymmetric problem in which the cross sectional area A is not subjected to any changes, Equation (4.14) can be written in the following fashion:

$$\delta J=\int_{x_0}^{x_1}(F_y-\frac{d}{dx}F_{y'})h(x)dxdA+\int_A F_{y'}\Big|_{x_1}(\delta y_1-y_{x_1}\delta_{x_1})dA-\int_A F_{y'}\Big|_{x_0}(\delta y_0-y_{x_0}\delta_{x_0})dA-\int_A F\Big|_{x_0}\delta x_0 dA+\int_A F\Big|_{x_1}\delta x_1 dA \tag{4.20}$$

It is easy to prove that in the investigated case ($-\delta 1(N)$) is equal to:

$$-\delta 1(N)=\int_A F\Big|_{x_1}\delta x_1 dA-\int_A F\Big|_{x_0}\delta x_0 dA \tag{4.21}$$

The minus sign in Equation (4.21) deserves a note of explanation. The decrease of potential means that it is subtracted from lower potential to higher potential, which gives as negative first variation of functional. Consequently, this implies an increase of stiffness. Thus the decrease of displacement (which means the decrease of potential) is associated with the increase of stiffness. For the constant load, the relationship between the displacements, potential and stiffness are shown in Figure 4.4.

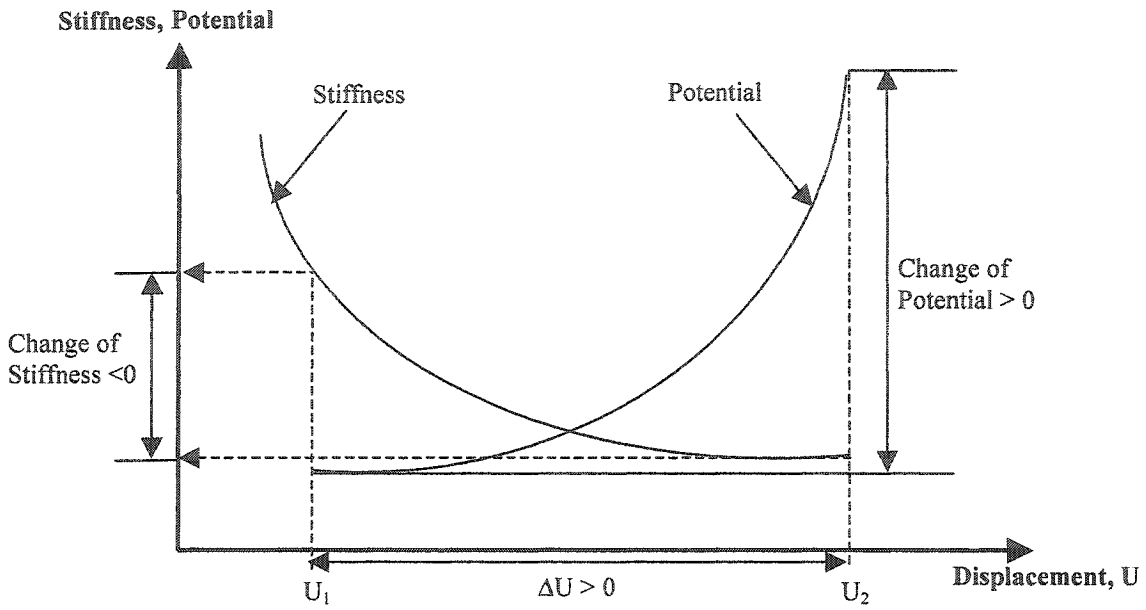

Figure 4. 4 Potential, Stiffness as a function of displacement (U)

For constant load potential is monotonically increase function of displacement whereas stiffness is the monotonically decreasing function of displacement.

It should be remembered in mind that in engineering applications, the potential (work = energy) for constant value of force is monotonically decreasing function of stiffness. For example:

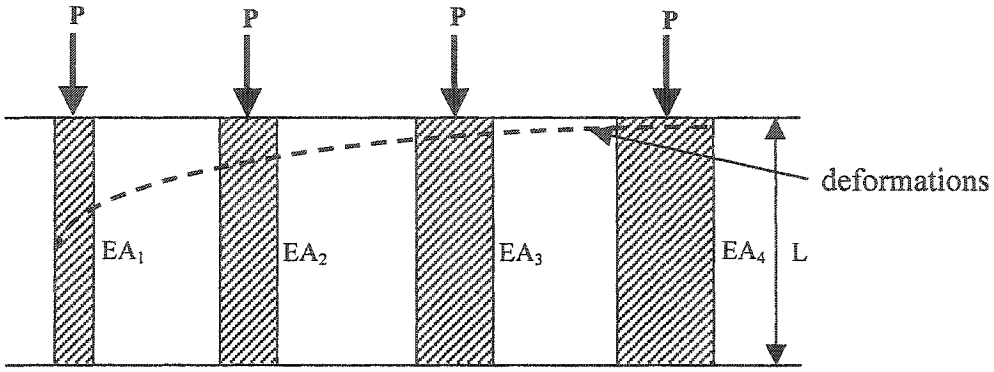

Figure 4.5 Potential as a decreasing function of deformation that is associated with increase of stiffness for columns (i.e., made of same material) subjected to the same applied load P

In the case discussed for constant value of modulus of permanent deformations E, stiffness is associated with thickness of the moving ends of functional. Thus the decrease of displacement (which means the decrease of potential) is associated with increase of stiffness. The decrease of potentials means that we should subtract from lower potential to higher potential. This gives us negative first variation of functional. Consequently, it gives positive increase of stiffness.

Multiplying both sides of Equation (4.21) by (-1) it is arrived at:

$$\bar{1}.\delta 1(N) = \int_A F \Big|_{x_0} \delta x_0 \, dA - \int_A F \Big|_{x_1} \delta x_1 \, dA \qquad (4.22)$$

In Equation (4.22) the left hand side represents the sensitivity of energy due to changes of boundaries δx_0 and δx_1. It is worth noting that in theoretical formulation resulted in Equation (4.22), it is postulated that δx_0 and δx_1 are constant values, although the variability of integrands F across area A can be of arbitrary type. Therefore, the variations of moving boundaries δx_0 and δx_1 in Equation (4.22) are taken in front of the integrals. In the analyzed case, the integrand F is defined as a work of vertical stresses acting on suitable permanent strains that are associated with corresponding areas (Budkowska, 1999 (16)). For our analysis it is postulated that the constitutive law for unrecoverable deformations is described by the relationships analogous to Hooke's law that contain modulus of permanent deformation E_P. The only stresses that work on vertical movements of boundaries are normal stress σ_z.

The strain vector $\{\varepsilon\}$ has the following components:

$$\{\varepsilon\}=\begin{Bmatrix}\varepsilon_z\\ \varepsilon_r\\ \varepsilon_\theta\\ \gamma_{rz}\end{Bmatrix}=\begin{Bmatrix}\dfrac{\partial v}{\partial z}\\ \dfrac{\partial u}{\partial z}\\ \dfrac{u}{r}\\ \dfrac{\partial u}{\partial z}+\dfrac{\partial v}{\partial r}\end{Bmatrix} \tag{4.23}$$

where v = displacement in z direction

u = displacement in r direction

ε_r, ε_z, ε_θ, γ_{rz} = the permanent strain components (radial, vertical and circumferential normal strains, shear strain respectively) of equivalent

unreinforced system generated by single number N of load q applied to the primary structure,

The corresponding stress vector $\{\sigma\}$ has the following components:

$$\{\sigma\}=\begin{Bmatrix}\sigma_z\\ \sigma_r\\ \sigma_\theta\\ \tau_{rz}\end{Bmatrix} \tag{4.24}$$

where σ_z, σ_r, σ_θ, τ_{rz} = the stress components (vertical, radial and circumferential normal stresses, shear strains respectively) generated by the single number N of load q.

For an axisymmetric problem the stress-strain relationships can be defined with the aid of Figure 4.6 and the Equations (4.25) – (4.28).

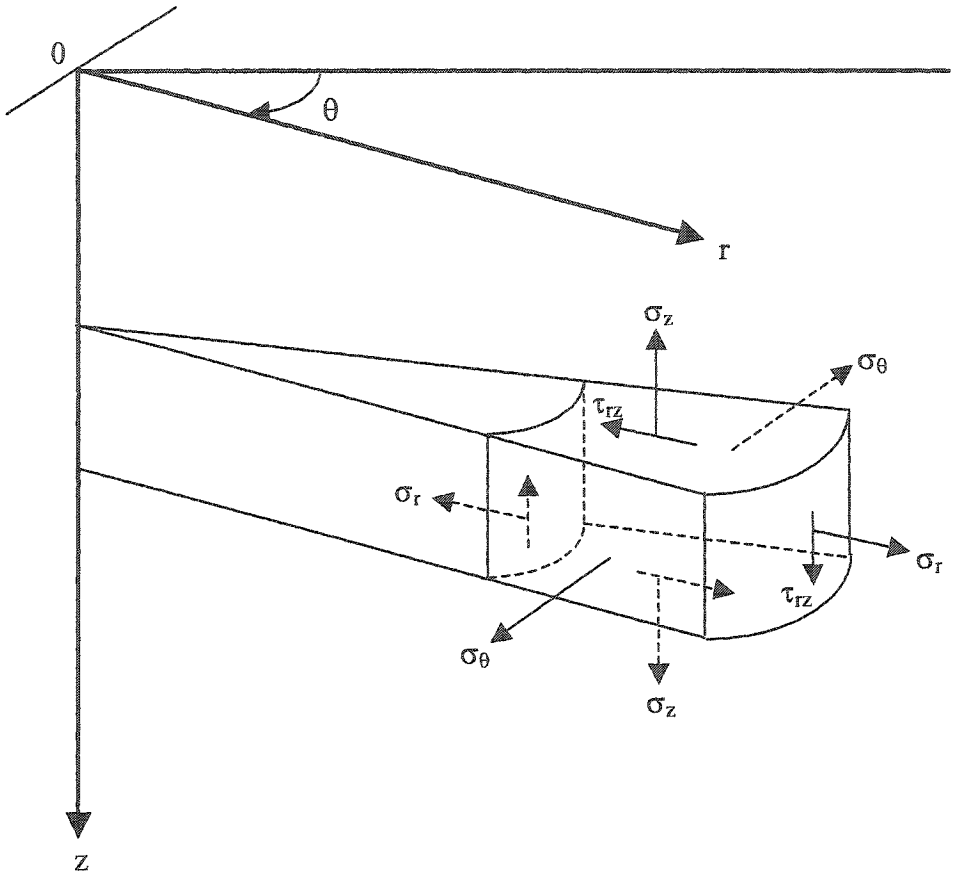

Figure 4.6 Stresses and strains acting on an axisymmetric element

$$\varepsilon_r = \frac{1}{E_p}[\sigma_r - \upsilon(\sigma_z + \sigma_\theta)] \tag{4.25}$$

$$\varepsilon_z = \frac{1}{E_p}[\sigma_z - \upsilon(\sigma_r + \sigma_\theta)] \tag{4.26}$$

$$\varepsilon_\theta = \frac{1}{E_p}[\sigma_\theta - \upsilon(\sigma_r + \sigma_z)] \tag{4.27}$$

$$\gamma_{rz} = \frac{\tau_{rz}}{G_p} \tag{4.28}$$

The integrand F of Equation (4.20) for axisymmetric problem is given as:

$$F = \varepsilon_r \overline{\sigma_r} + \varepsilon_z \overline{\sigma_z} + \varepsilon_\theta \overline{\sigma_\theta} + \gamma_{rz} \overline{\tau_{rz}} \tag{4.29}$$

where ε_r, ε_z, ε_θ, γ_{rz} = the permanent strain components (radial, vertical and circumferential normal strains, shear strain respectively) of equivalent unreinforced system generated by single number N of load q applied to the primary structure,

$\overline{\sigma_r}$, $\overline{\sigma_z}$, $\overline{\sigma_\theta}$, $\overline{\tau_{rz}}$ = the stresses generated by the load $\bar{1}$ applied at the point 1 to the deformed equivalent unreinforced adjoint system,

E_P = resilient modulus of permanent deformation,

G_P = shear modulus of permanent deformation.

Substitution of Equation (4.29) into Equation (4.22) shows that each term of the product $\varepsilon_{ij} \overline{\sigma_{ij}}$ combined with corresponding area, after integration should be multiplied by increment of moving boundaries, which are in vertical direction. Thus, the only stress and strain components that give the nonzero work are the normal stresses $\overline{\sigma_z}$ associated with the strains ε_z acting on the elementary area dA_z. This fact in reference to the specific problem investigated allows reshaping Equation (4.29) to its reduced form which when combined with Equation (4.26) results in:

$$F = \overline{\sigma_z} \varepsilon_z = \frac{\overline{\sigma_z}}{E_p} [\sigma_z - \upsilon(\sigma_r + \sigma_\theta)] \tag{4.30}$$

Substitution of Equation (4.30) into suitably modified Equation (4.21) gives:

$$\delta l(N) = \delta x_1 \int_A (\overline{\sigma_z}\, E_p)[\sigma_z - \upsilon(\sigma_r + \sigma_\theta)]dA - \delta x_0 \int_A (\overline{\sigma_z}\, E_p)[\sigma_z - \upsilon(\sigma_r + \sigma_\theta)]dA \tag{4.31}$$

More compact form of Equation (4.30) is the following:

$$\delta l\ (N) = \delta x_1 \int_A \overline{\sigma_z}\, \varepsilon_z dA - \delta x_0 \int_A \overline{\sigma_z}\, \varepsilon_z dA \tag{4.32}$$

For the axisymmetric problem the spatial discretization of the section by means of the eight nodal isoparametric quadrilateral elements generates in fact the discretization by means of toruses. The stresses and strains components act on the elementary area dA_z. So for the axisymmetric element, the infinitesimal area dA is the form of:

$$\int_A dA = \int_0^{2\pi} d\theta \int_{r_1}^{r_2} r dr = 2\pi \frac{r^2}{2}\Big|_{r_1}^{r_2} = \pi(r_2^2 - r_1^2) = \pi(r_2 + r_1)(r_2 - r_1) = 2\pi(\frac{r_1 + r_2}{2})\Delta r = 2\pi\pi(dr) \tag{4.33}$$

and this is shown in Figure 4.7.

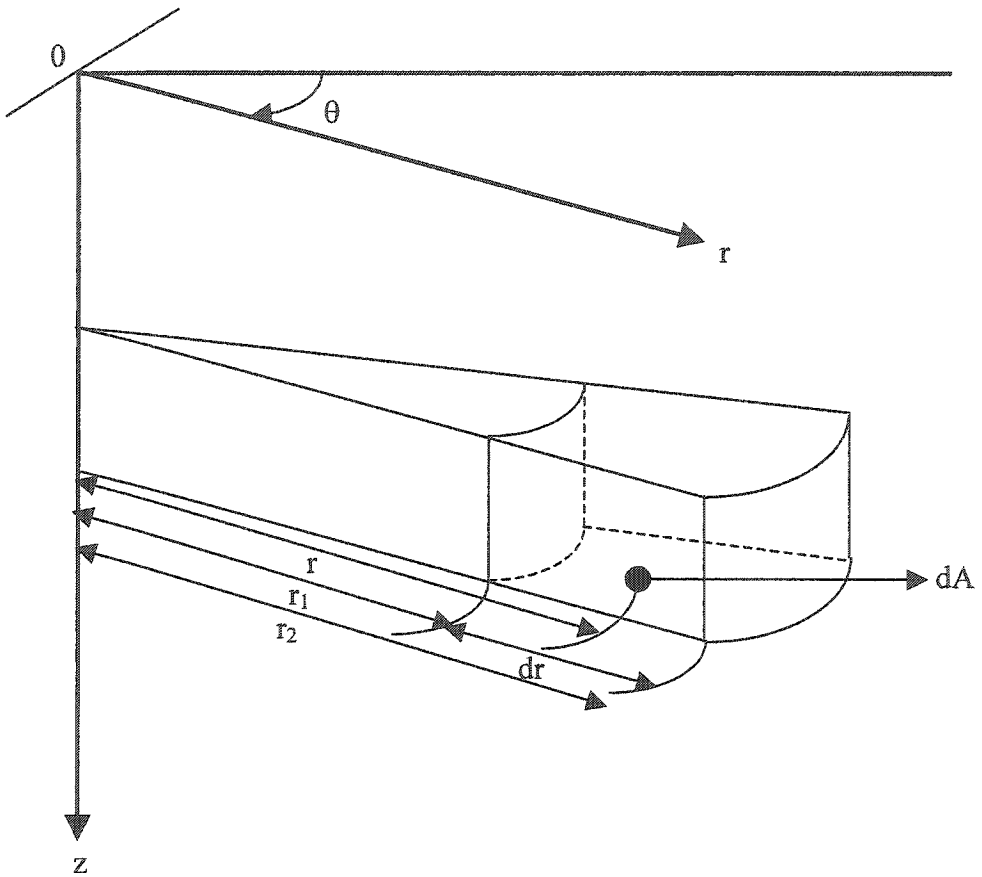

Figure 4.7 Infinitesimal area dA of an axisymmetric element

Thus the infinitesimal area dA in Equations (4.32) and (4.33) means $2\pi r(dr)$, where r defines the location of Gaussian point. It is worth noting that the purpose of Equation (4.32) is the determination of δt for the single value N of load application, whereas the values of remaining quantities are known.

The shifts of boundaries δx_1 and δx_0 are measured from the interface of base and subgrade layer. x_0 denotes the position of top boundary of subgrade layer and δx_0 means

shrinkage of subgrade's top boundary by δt downwards, whereas, x_1 stands for the bottom boundary of the base layer and δx_1 is the expansion of the base layer by δt downwards.

Further simplification of Equation (4.32) gives:

$$\delta 1(N) = \delta t \int_A [(\sigma_z \overline{\varepsilon_z})_{TOP} - (\sigma_z \overline{\varepsilon_z})_{BOTTOM}] dA \qquad (4.34)$$

Where subscript TOP refers to the stresses and strains located upwards of the base-subgrade interface, whereas the subscript BOTTOM is associated with the stresses and the strains components that appear below the base-subgrade interface. Therefore $\delta x_0 = \delta x_1 = \delta t$.

CHAPTER V

NUMERICAL ANALYSIS AND RESULT

5.1. Numerical Analysis

Numerical analysis and simulations of flexible pavements are important for understanding, extending and explaining the laboratory and field studies. The development of a numerical procedure involves many idealizations of the problem. They normally include (a) geometry, (b) loads, (c) material behavior or constitutive models of pavement materials, and (d) selection of the suitable numerical technique. The reliability of the numerical simulation/analysis largely depends on how closely the constitutive model represents the real material behavior and hence plays an important role. The main focus of this research is to identify the positive effect of this constitutive model for pavements materials on the prediction of the performance (performance check of permanent deformation) of flexible pavements of geogrid inclusion into the base layer as reinforcement.

The material properties and Finite Element Model assumptions used in the theoretical analysis are covered in this section. The potential benefits of geogrid reinforcement are also more clearly quantified in terms of the reduction in base thickness and the relative tendency to undergo rutting. In traditional analyses of flexible pavements the pavement materials are modeled as linear elastic material. However, pavement materials do not behave as linear elastic materials. They can be better modeled by non-linear elastic material or elasto-plastic constitutive models. Non-linear finite element sensitivity analysis is performed during this research.

Pavement geometries used in the sensitivity investigation for primary structure are shown in Figure 5.1. Sensitivity studies were also conducted to determine the effect of geogrid position (shown in Figure 5.2) and the potential beneficial effect of using geogrid.

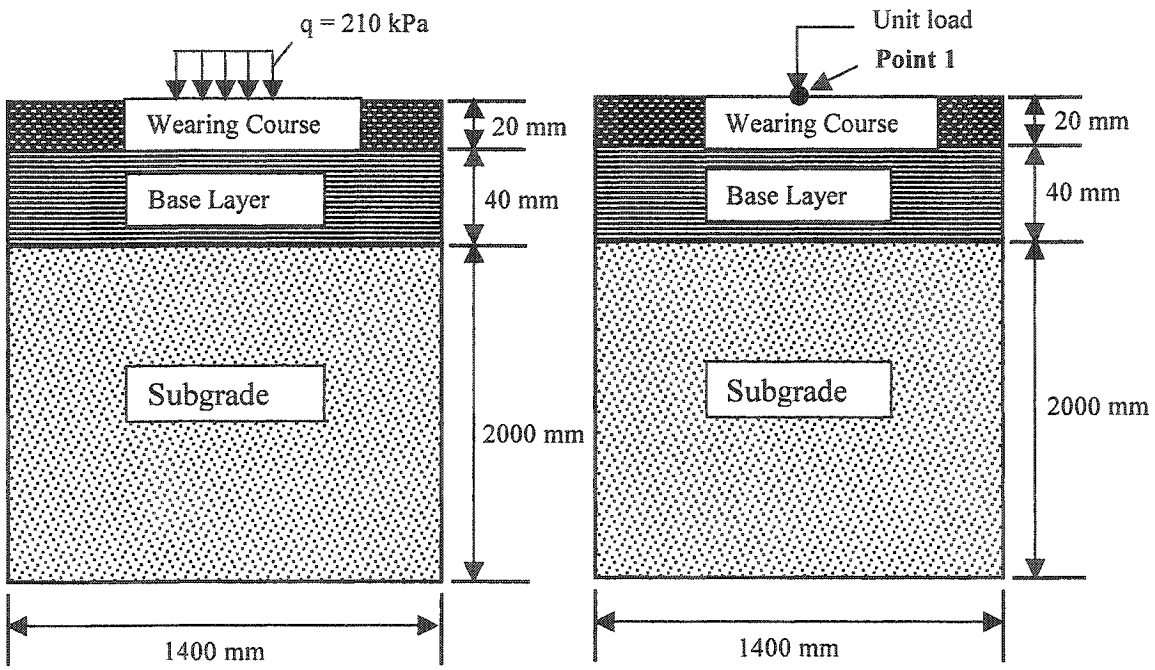

Primary Structure (Unreinforced) **Adjoint Structure (Unreinforced)**

Figure 5.1 Geometry of the pavement (unreinforced) tested in the laboratory

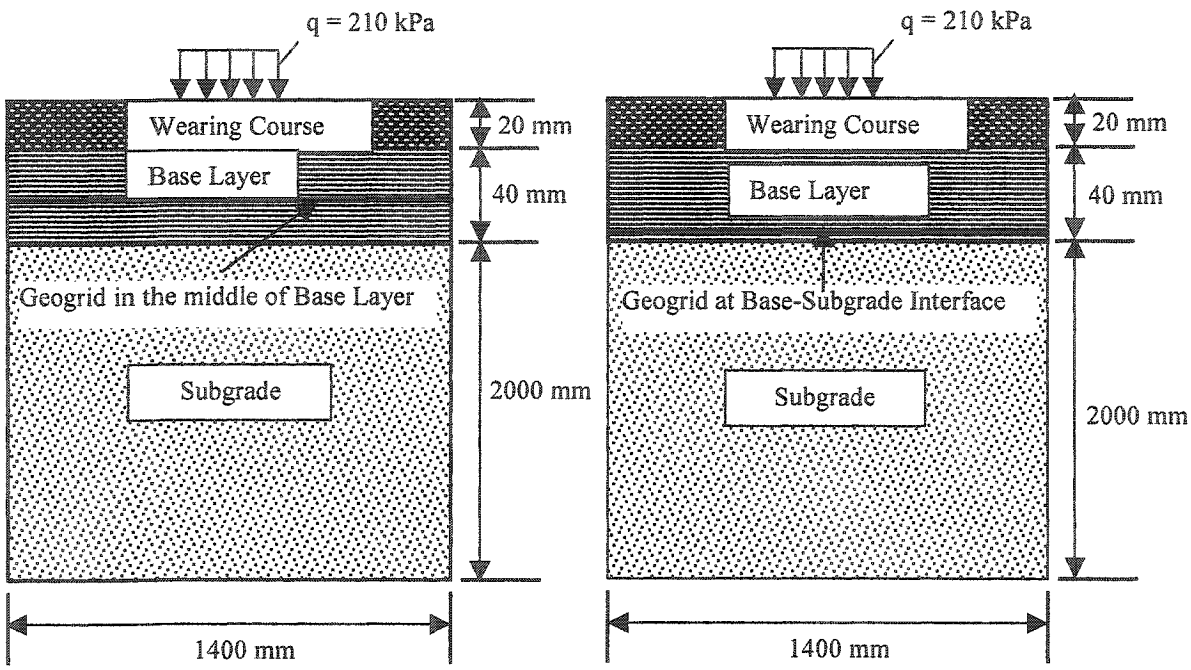

Figure 5.2 Geometry of the pavement (primary reinforced section) tested in the laboratory

An important objective of the sensitivity study was to establish pavement sections reinforced with a geogrid that structurally have the same strength or more as similar with un-reinforced section and vice versa. The beneficial effect was accounted for by establishing the reduction in base thickness due to reinforcement. Equivalent pavement section with and without reinforcement is hence identical except for the thickness of the base layer of the flexible pavement.

To perform the numerical analysis, the following assumption have been made:

1) The conventional flexible pavement in the study is a three-layer system (Surface layer followed by base layer and then followed by subgrade layer).

2) Each layer is considered to be homogeneous, isotropic and linearly elastic.

3) The properties of each layer are characterized by the permanent resilient modulus E and Poisson's ratio ν. The reason for using permanent resilient modulus instead of elastic modulus or resilient modulus is that permanent resilient modulus is associated with the permanent (unrecoverable) deformation.

4) The Poisson's ratio ν for surface, base and subgrade are 0.4,0.3 and 0.45 respectively and the value of ν would not be changed through the loading and unloading process during the numerical analysis.

5) A uniform pressure of q = 210 kPa (30 psi) is applied on the surface over a circular area of radius r = 27.22 mm acting on a circular area of 24.5 cm^2 on the primary structure. The passing tire generates this uniform pressure. In the studies performed, the dynamic effect is not taken into consideration. Therefore the load applied on the primary system can be considered either as a moving pressure or as a applying pressure q of " pumping type" that is slowly applied and with a constant value. Also the loading duration was not being considered.

On the other hand, concentrated unit load is applied on the adjoint structure (shown in Figure 5.1.). It is postulated here that the adjoint structure should be constructed in the same way as the primary structure i.e., it satisfies the same constitutive laws and deforms in the same way as the primary system does except for the loading condition.

6) In the numerical analysis, the geometry was considered as axisymmetric due to loading conditions.

7) In this study, the selection of optimal geogrid location into the base layer is assumed to be the middle of the base layer and also in the base-subgrade interface. For these two cases the equivalent base thickness is determined and related analysis are performed.

The numerical analysis in the study was divided into two stages. First one was to identify the permanent resilient modulus of each layer E_{Pi} as the function of number of load repetitions, N for the unreinforced section. The second one was to identify the equivalent base thickness δt when geogrid is inserted in the middle of the base layer and at the base subgrade interface as the function of N number of load repetitions. Actually E_{Pi} for each layer are incorporated into the theoretical formulation of δt.

5.2 Finite Element Method (FEM)

The Finite Element Method (FEM) is a very useful method for " Numerical solutions of field problems" where a field problem is described by differential equations or by the variational calculus (Cook, R.D. et al, 2001 (20)). In FEM method the structure or geometry of the field problem is divided into small pieces, called elements and are connected by the nodes. Assembly of entire elements and nodes is called a mesh, and boundary conditions are applied to the mesh to model the real-world situation. The mesh is designed and analyzed in the Finite Element (FE) software package. In this case ABAQUS is the most suitable Finite Element software to analyses the non-linear problem of this research.

In most of the Finite Element Analysis (FEA), soil is represented by means of quadrilateral continuum elements. According to the ABAQUS Standard User's Manual, 2002 (1), continuum elements are solid elements that may either be linear or quadratic (non-linear) A linear four-sided continuum element has four nodes at which displacements are calculated and four interior integration points (Gaussissan point) at which the stresses and strains are calculated. A first-order differential equation is used to solve this type of linear elements.

On the other hand, a quadratic element has eight nodes and nine Gaussissan points and a second order differential equation is used to solve the problem. The two types are shown in Figure 5.3.

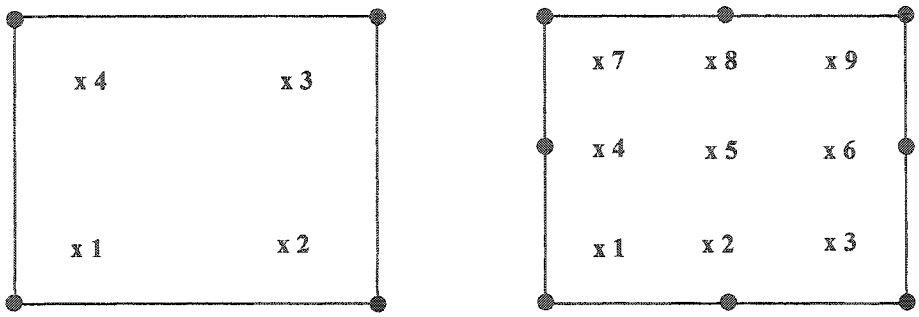

Figure 5. 3 Linear and quadratic continuum elements [ABAQUS 2002]

ABAQUS requires two parts of data to build up its source code. They are: (1) Model data and (2) History data. Model data contains geometry (i.e., nodal coordinates, element connectivity and element properties) and material properties (i.e., elastic modulus E, Poisson's ratio, ν). On the other hand history data consists of the type of simulation (i.e., static, dynamic etc), the loads and boundary conditions as well as the output required.

5.2.1 Model Set-up

The element used in the ABAQUS analysis is CAX8 that means continuum (solid) axisymmetric eight-noded isoparametric quadrilateral element. So the system can be analyzed by half because of the axisymmetric feature of geometry and load. Thus the initial 3-D problem can be simplified into 2-D problem. The area of interest can be restricted within 250 mm x 2060 mm. Inside this area axisymmmetric elements are employed. The number of elements used for each material is as follows: 70 elements for surface layer; 56 elements for base and 112 elements for subgrade layer. No special interface elements were used. The each layer (3 layer system) in the model to be considered as elastic which has been incorporated to permanent deformation associated

with each application of load through the elastic half space (i.e., axisymmetric model) which deformed in unrecoverable fashion. To preserve the unrecoverable features of the systems investigated, the geometry of the problem is to be updated after each pressure load application q for primary system as well as for adjoint system after each unit concentrated load application. The model is set up as shown in Figure 5.4 and the related assumption to build up this model are described in section 5.1

5.2.2 History Description

5.2.2.1 Boundary Conditions

The boundary conditions of flexible pavement are as follows: fixed at the bottom of the subgrade (both in the horizontal and vertical direction) and fixed in the horizontal direction, allowing for vertical displacements along the sides. The pavement surface is unrestrained (i.e., not fixed).

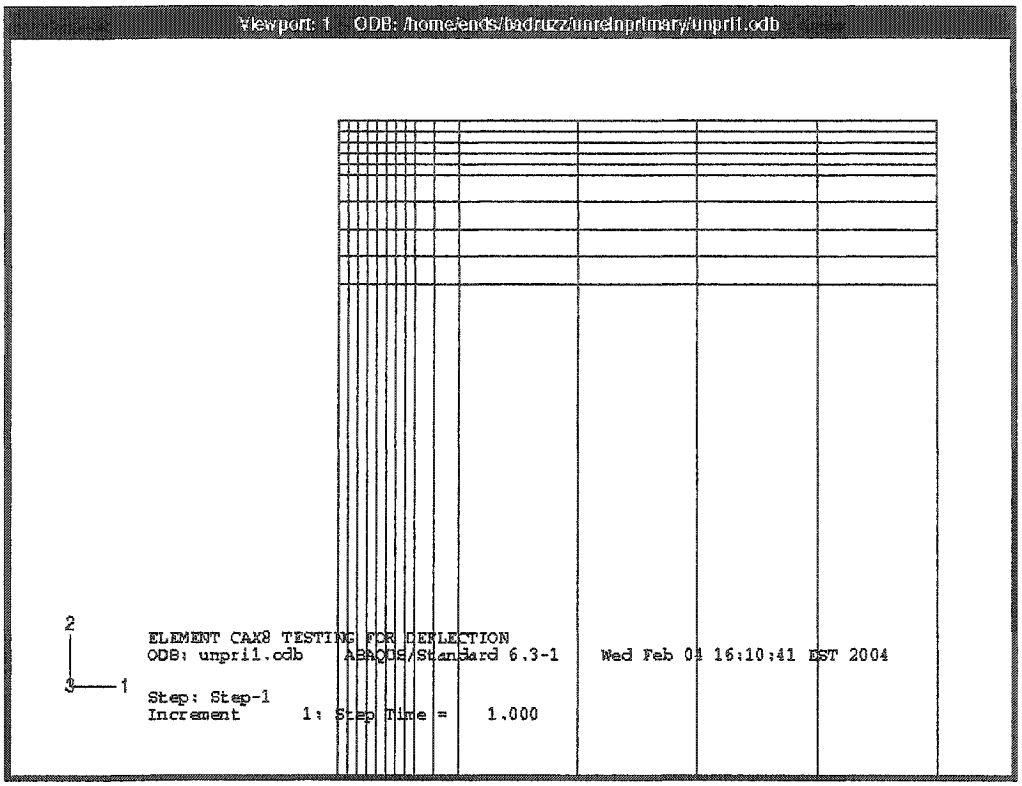

Figure 5. 4 Mesh of 3-layer flexible pavement (Model set- up)

Figure 5.4 portrays a typical mesh of the problem's geometry analyzed in ABAQUS. After a closer look of Figure 5.4, it can be seen that the mesh is denser at the loading place (beginning) and coarser at points away from the loading place. The ABAQUS input file of the mesh is provided in Appendix B1 for the primary system, and in Appendix B2 for adjoint system. Discussion and explanation of the elements of the input file is given in Appendix B3.

5.2.2.2 Loading

In ABAQUS, loading is somewhat complex. Therefore, it is necessary to familiarize the reader with the loading terms. The loading terms are defined and described in the ABAQUS Standard User's Manual, 2002 (1).

In the studies performed, the dynamic effect (inertia force) is not taken into consideration. Therefore, the load q applied on the primary system can be considered as a moving pressure or as an applying pressure q of "pumping type" that is slowly applied and removed with a constant value. Therefore for the primary system a uniform pressure of q = 210 kPa is applied on the pavement surface over a circular area of radius r = 27.22 mm. The moving wheels generated this pressure. The loading waveform, which might be triangular, rectangular or haversine shaped, was not taken into consideration. Also the loading duration was not being taken or step analysis was not being considered.

On the other hand, for the purpose of sensitivity analysis to be performed in the virtual work principle, a temporary system called adjoint system is introduced. It is constructed in the same way as the primary structure except the loading condition. In adjoint system concentrated unit load is applied instead of pressure load, however it satisfies the same constitutive laws and deforms in the same way as the primary system does.

A sample of a typical input file in Appendix B1 demonstrates the loading sequence, which is found at the very end of the input file.

5.3. Methodology or Formulation

The numerical analysis was performed by means of the Finite Element Method (FEM) program ABAQUS, 2002 (1). In practical applications by the FEM the stresses are calculated at Gausssian points. In discussed case $(\sigma_z \overline{\varepsilon_z})_{TOP}$ products are determined at the lower Gaussian points of the upper layer whereas $(\sigma_z \overline{\varepsilon_z})_{BOTTOM}$ are considered at the upper Gaussian points of the bottom layer. For the axisymmetric problem the spatial discretization is done by means of the eight nodal isoparametric quadrilateral elements. The infinitesimal area dA in Equation (4.33) means $2\pi r$ (dr), where r defines the location of Guassian point. The final form of equation that allows determining δt is the following:

$$\delta t = \frac{\delta 1(N)}{\int_A [(\sigma_z \overline{\varepsilon_z})_{TOP} - (\sigma_z \overline{\varepsilon_z})_{BOTTOM}]_N \, dA} \tag{5.1}$$

The determined δt is for only one load application. Final Δh = total equivalent thickness of base layer = $\sum_{i=1}^{3400} \delta t_i$. Each $(\delta t)_i$ is determined for updated geometry of primary unreinforced system, for which E_{P1}, E_{P2} ,E_{P3} as a function of N are already done. For each N, $\delta 1(N)$ is also given as the difference between permanent deformations of unreinforced section and permanent deformations of reinforced section with the aid of Equations (3.49) - (3.51). To preserve the unrecoverable features of the systems investigated; the geometry of the problem was updated after each load q application on the primary structure and each unit load $\bar{1}$ application on the adjoint structure.

5.4 Results and Discussions

In the numerical analysis we postulate that the constitutive model employed in the analysis is the modified Hooke's law that involves to its description the resilient modulus E_P that represents permanent deformations and depends on number of passes N. This means that in each layer i there is:

$$E_{Pi} = E_{Pi}(N)$$

It is also postulated that each layer is homogeneous. Again the regression analysis was employed to derive the equations of moduli of permanent deformation E_{Pi} as the function of number of passes N.

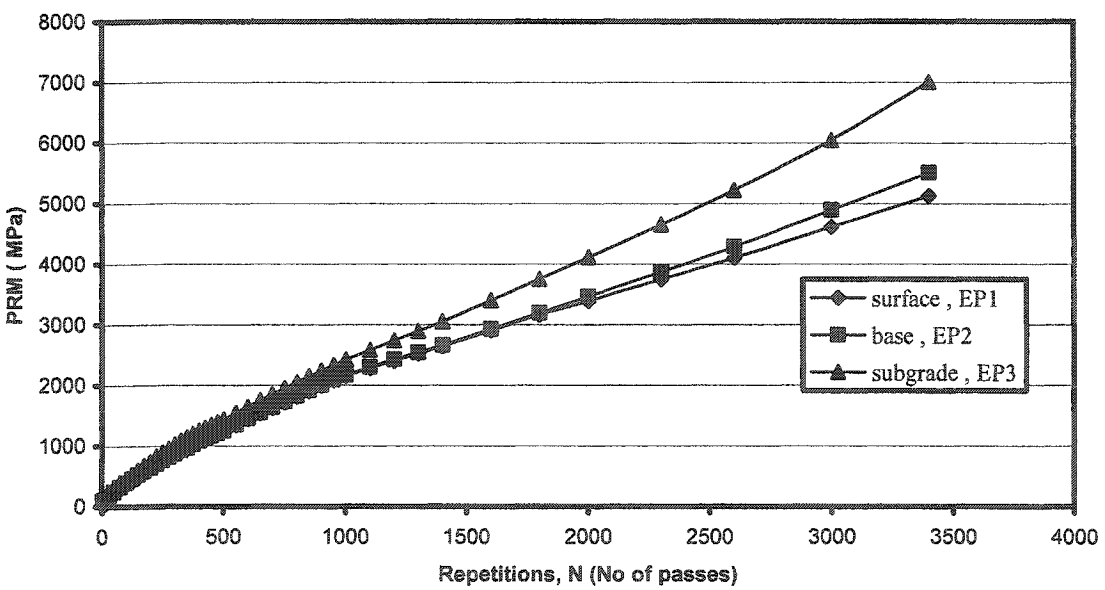

Figure 5. 5. Distribution of moduli of permanent deformation E_{Pi} determined for layer i = 1, 2 and 3 as the function of load applications N for the unreinforced pavement system.

The moduli E_{Pi} identified numerically (shown in Figure 5.5) for each layer are incorporated into the theoretical formulation for the δt. The results presented in Figure 5.5 and provided by δ1(N) (shown in Figure 3.7) when implemented in Equation (5.1) allows us to determine the δt (N) which are shown in Figure 5.6.

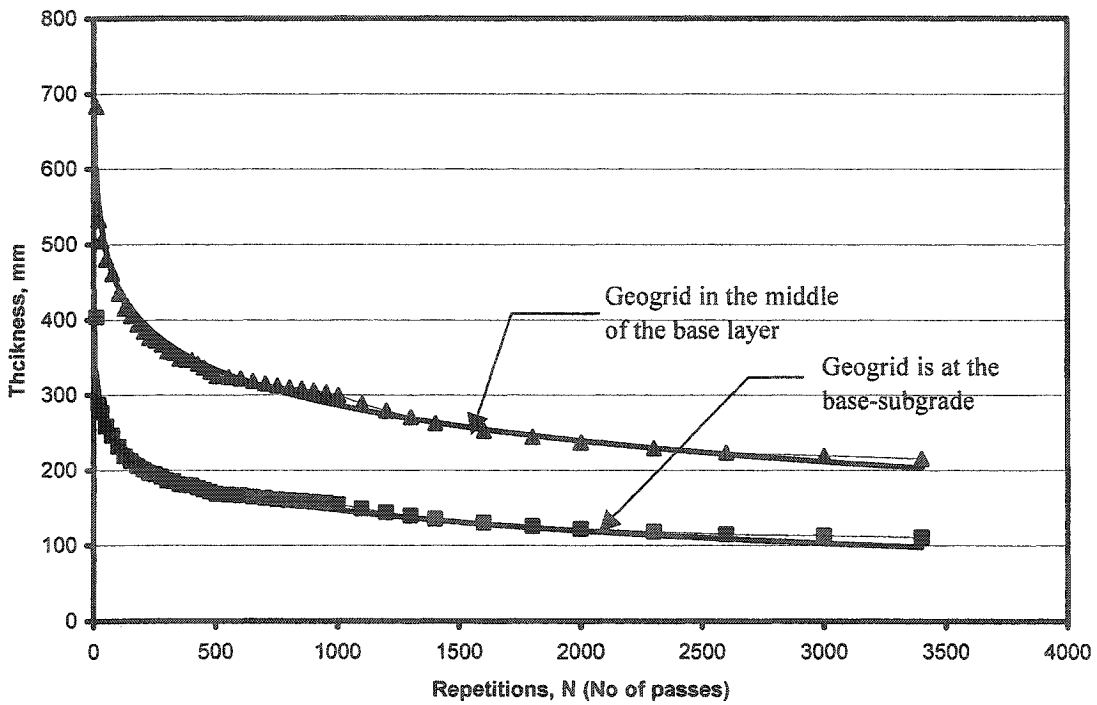

Figure 5. 6. Distribution of increments of base layer δt (N) related to each number N of load application.

From Figure 5.6 it can be stated that cost can be decreased when geogrid is in the middle of the base layer compared to geogrid at the base-subgrade interface because this cost savings depend on the material of base layer, labor and transport. Each $(\delta t)_i$ is determined for updated geometry of primary system.

In addition, Appendix C (Figure C.1 to C.23) will bring some ideas of the response of system (contour of strain, stress and displacement) for certain number of repetitions.

CHAPTER VI

CONCLUSIONS AND RECOMMENDATIONS

6.1 Conclusions

The following conclusions can be drawn from this research:

1) The beneficial effect of geogrid insertion into a base layer is a very effective way of decreasing of permanent deformations (i.e., short–term rutting), which can be achieved by the combined effects of interlocking and stiffening that are developed around a geogrid.

2) The objective of numerical investigations was to identify the optimal position of geogrid insertion into the granular base layer and to find the equivalent base thickness for the estimation of cost savings. Also it was the quantitative evaluation of the performance of unreinforced and two geogrid-reinforced sections of flexible pavement.

3) From Figure 5.6 it can be stated that in terms of effectiveness cost can be decreased when geogrid is in the middle of the base layer compared to geogrid at the base-subgrade interface.

4) A closer look at the results presented in Figures (3.2)-(3.4) shows that geogrid reinforced section results in much smaller permanent deformations that is translated to longer durability of the system, safer conditions of driving and better economy of the system. Another advantage of application of geogrid can be

associated with reduction of the thickness of the base layer that is considered to be thinner when compared with the unreinforced section thus allowing the determination of the equivalent thickness of the homogeneous unreinforced base layer.

5) In this thesis, it is postulated that the difference of permanent deformations of unreinforced and reinforced system can be compensated by increasing the thickness of the base layer of unreinforced system.

6) Finally it can be easily concluded that the optimal location of a geogrid insertion in a flexible pavement system produces the best interlocking, highest stiffness and maximum value of modulus of permanent deformation E_P of the composite layer.

6.2 Recommendations for Further Study

More research would be required to study the following: (1) multilayer of geogrid insertion into the flexible pavement, (2) placement of geogrids in the middle of the base layer and at the interface of base-subgrade layer at the same time and hence find the equivalent thickness of unreinforced base layer and related other structural benefits, and (3) finally introduce a design method with optimal geogrid inclusion into the base layer of flexible pavement.

It is necessary to test the pavement materials in triaxial tests with volume change measurements or in true triaxial equipment, so that they can be used to calibrate advanced

constitutive models or to develop suitable ones. Then the proposed numerical procedure can be used to analyze the complete behavior of geosynthetic–reinforced flexible pavements. The quantitative as well as qualitative results obtained from these numerical analyses can be validated against field or laboratory observations.

Since FEA demonstrated significant improvement in our numerical analysis, it would be beneficial to carry out a study on a full-scale model. Also, in order to understand the effect of the stiffness of geosynthetics on resilient and permanent deformations of soils using geogrids having various stiffness, further testing would have to be carried out.

REFERENCES

[1] ABAQUS Standard Users Manual, (2002), Version 6.3, Habbitt, Karlson & Sorenson, Inc.

[2] Abdel Halim, A.O. (1993)."Geogrid reinforcement of asphalt pavements." *Ph.D Thesis,* University of Waterloo.

[3] Al-Qadi, I.L., Brandon, T.L., Valentine, R.J., Lacina, B.A., and Smith, T.E. (1994) " Laboratory evaluation of geosysnthetic reinforced pavement section", *Transportation Research Board, preprint, Paper No. 94-049, 73rd Annual Meeting, Washington DC,* pp.143.

[4] Al-Qadi, I.L., Brandon, T.L., Smith, T.E., and Lacina, B.A. (1994)."How do geosynthetics improve pavement's performance", *Proceedings of the third Materials Engineering Conference, San Diego, C.A., USA, No. 804, Oct, 1994, Infrastructure: New Materials and Methods of Repair*, pp. 606-616.

[5] American Association of State Highway and Transportation Officials (AASHTO), (1993). "AASHTO guide for design of pavement structures." Washington D.C., pp 256.

[6] Anderson, P. and Killeavy, M. (1989)."Geotextiles and geogrids: cost effective alternate materials for pavement design and construction." *Geosynthetics '89 Conference, San Diego,* pp. 353-360.

[7] Bardet, J.P. (1997). "Experimental soil mechanics." Prentice-Hall, Inc., New Jersey, USA.

[8] Barker, W.R. (1987). "Open-graded bases for airfield pavements." *USAE Waterways Experiment Station, Misc. paper GL-87-16.*

[9] Barksdale, R.D. (1972). "Repeated load test evaluation of base course materials." *Georgia Highway Department, Research Project 7002, School of Civil Engineering, Georgia Institute of Technology, Atlanta.*

[10] Barksdale, R.D., and Brown, S.F. (1988)."Potential benefits of geosynthetics in flexible pavements." *NCHRP Report No-315: Transportation Research Board, Washington, DC.*

[11] Barksdale, R.D., Brown, S.F. and Chan, F. (1989)."Potential benefits of geosynthetics in flexible pavement systems, Supplement to NCHRP Report No. 315." *National Cooperative Highway Research Program Supplement to Report No. 315, Transportation Research Board, National Research Council, Washington D.C.*, pp 150.

[12] Brown, S.F., and Brodrick, B.V (1981)."Nottingham pavement test facility." *Transportation Research Record 810*, pp. 67-72.

[13] Brown, S.F., Jones, C.D.P., and Brodrick, B.V. (1982)."Use of non-woven fabrics in permanent road pavements." *In proceedings of the Constitution of Civil Engineers, Part 2,* Vol. 73, pp. 541-563.

[14] Brown, S.F., and Pappin, J.W. (1981)."Analysis of pavements with granular bases." *Transportation Research Record 810,* pp.17-22.

[15] Brown, S.F., and Pappin, J.W. (1981)."Modeling of granular materials in pavements." *Transportation Research Record 1022*, pp. 45-51.

[16] Budkowska, B.B. (1999). "Effect of variable thickness of soil layers on the behavior of laterally loaded piles–sensitivity analysis", *Computers and Geotechnics*, 25(1), pp. 25-43.

[17] Budkowska, B.B. and J.Yu (2002). "Mitigation of short term rutting by interlocking layer developed around a geogrid-sensitivity analysis." *Computer and Geotechnics*, 30, pp. 61-79.

[18] Carroll, R.G., Walls, J.C, and Haas, R (1987). "Granular base reinforcement of flexible pavements using geogrids." *Geosynthetic Conference, New Orleans, Lousiana.*

[19] Chan, F., Barksdale, R.D., and Brown, S.F. (1989). "Aggregate base reinforcement of surface pavements" *Geotextiles and Geomembranes,* 8, pp. 165-189.

[20] Cook, R.D. et al (2001). "Concepts and Applications of Finite Element Analysis" (4th Ed.), New York: John Wiley & Sons, Inc.

[21] Dimaggio, J.A., and Cribbs, M.M (1996). "The role of geosynthetics on USA highways." *Geotextiles and Geomembranes*, 14, pp. 243-251.

[22] Gelfand, I.M. and Fomin, S.W. (1963). "Calculus of Variations", Prentice–Hall, Englewood Cliffs, N.J., U.S.A.

[23] Giroud, J.P., Ah-Line, C., and Bonaparte, R. (1985)."Design of unpaved roads and trafficked areas with geogrids." *Proc., Symp. Polymer Grid Reinforcement, Science and Engineering Research Council and Netlon Ltd.*, London, pp. 116-127.

[24] Haas, R.G. (1984). "Structural behavior of Tensar Reinforced pavements and some field applications." *Proc. Symp. Polymer Grid Reinforcement in Civil Engineering, Institution of Civil Engineers, London.*

[25] Hass, R., Walls, J., and Carroll, R.G. (1988). "Geogrid reinforcement of granular bases in flexible pavements." *Transportation Research Record, 1188, Transportation Research Board, Washington, DC,* pp.19-27.

[26] Huang, Y.H. (1993). "Pavement Analysis and Design." Prentice Hall, Englewood Cliffs, New Jersey.

[27] Koerner, R.M. (1990). "Designing with geosynthetics." Englewood Cliff, Prentice-Hall, New Jersey, pp. 167.

[28] Miura, N. (1988). "Use of polymer grid against settlement under cyclic loading" *Research Report, Saga Prefectural Office.*

[29] Miura, N., Sakai, A., and Taesiri, Y (1990). "Polymer grid reinforced pavement on soft clay grounds." *Geotextiles and Geomembranes,* 9, pp. 99-123.

[30] Moghaddas-Nejad, F. and Small, J.C (1996) "Effect of geogrid reinforcement in model track tests on pavements." *Journal of Transportation Engineering, ASCE,* 122(6), pp. 468-474.

[31] Moghaddas-Nejad, F. and Small, J.C. (2003)."Resilient and Permanent Characteristics of reinforced granular materials by repeated load triaxial tests" *Geotechnical Testing Journal,* 26(2), pp.1-15.

[32] Omoto, S., Kawabata, K., and Mizobuchi, M. (1992). "Reinforcement effect of geotextiles on pavements with weak subgrade." *Earth Reinforcement Practice, Rotterdam,* pp. 671-676.

[33] Pappin, J.W. (1975). "Pavement evaluation project." *Griffith, NSW, CSIRO, Division of Applied Geomechanics, Project Report 2, Melbourne.*

[34] Penner, R., Haas, R., Walls, J. and Kennepohl, J. (1985). "Geogrid reinforcement of granular bases." *Paper presented at the Roads and Transportation Association of Canada Annual Conference, Vancouver.*

[35] Perkins, S. (1995). "Feasibility of the use of existing analytical models and experimental data to assess current design methods for pavement geogrid-reinforced base layers", *Report No. FHWA/MT-94/8116, U.S. Department of Transportation, Federal Highway Administration, Washington, DC,* pp. 39.

[36] Perkins, S. and Ismeik, M. (1997). "A synthesis and evaluation of geosynthetic reinforced base course layers in flexible pavements: Part I ", *Geosynthetics International,* V.4, No.6, pp. 549-604.

[37] Perkins, S. and Ismeik, M. (1997). "A synthesis and evaluation of geosynthetic reinforced base course layers in flexible pavements: Part II", *Geosynthetics International,* V.4, No.6, pp. 605-621.

[38] Rigo, J.M. (1993). "General introduction, main conclusions of the 1989 Conference on reflecting cracking in pavements, and further prospectus." *Proceedings of the Second International RILEM Conference, Liege, Belgium, March 10-12,* pp. 3-20.

[39] Ruddock, E.C., Potter, J.F., and McAvoy, A.R. (1982). "A full-scale experiment on granular and bituminous road pavements laid on fabrics." *In Proceedings of the Second International Conference on Geotextiles, Vol. II, Las Vegas,* pp. 365-370.

[40] Smith, T.E., Brandon, T.L, Al-Qadi, I.L and Lacina, B.A (1994). "Laboratory performance of geotextile and geogrid reinforced flexible pavements", *the Via Department of Civil Engineering, Virginia Tech, Blacksburg, VA.*

[41] Tensar Cooperation (1986). "Granular base reinforcement of flexible pavements using Tensar geogrids", *Tensar Technical Note TTN: BR1, Morrow, Georgia,* pp. 21.

[42] Tensar Cooperation (1987). "Design guideline for flexible pavements with Tensar geogrid reinforced bases." *Tensar Technical Note, TTN: BR2, Morrow, Georgia,* pp. 28.

[43] http: // www.tensarcorp.com

[44] Wathugala, W.G., Baoshan, H., and Surajit, P. (1996)."Numerical simulation of geosynthetic reinforced flexible pavements". *Transportation research record 1534, Nov, 1996*, pp. 58-65.

[45] Webster, Steve L. (1991). "Geogrid reinforced base courses for flexible pavements or light aircraft", *Report No-GL-93-6, Report for U.S Department of Transportation, Vicksburg, Mississippi.*

[46] Wong, H., and Small, J.C. (1994). "Effect of orientation of approach slabs on pavement deformation." *Journal of Transportation Engineering, ASCE*, 120(4), pp. 590-602.

[47] Yoder, E.J., Witeczak, M.W. (1975). "Principles of pavement design" 2nd Edition, New York, John Wiley & Sons.

[48] Zaghloul, S., and T. White. (1993). "Use of a three-dimensional dynamic Finite Element program for analysis of flexible pavement." *In Transportation Research Record 1388, TRB, National Research Council, Washington, D.C.*, pp. 60-69.

APPENDIX A

SAMPLE CALCULATION AND METHODS FOR DETERMINATION OF REGRESSION EQUATION

APPENDIX A

SAMPLE CALCULATION AND METHODS FOR DETERMINATION OF REGRESSION EQUATION

A.1. Retrieving the deflection data from laboratory results by scanning

1) For Unreinforced Section:

Preliminary data for permanent deformation for unreinforced section (by scan)			
X	Y1	Y2	Y3
Step (No of Passes)	Deflection of surface (mm)	Deflection of Base (mm)	Deflection of subgrade (mm)
2	-0.3	-0.5	-0.01
10	-2.1	-1	-0.1
20	-3.3	-1.5	-0.35
30	-4.1	-2.25	-0.65
40	-4.75	-2.7	-0.9
50	-5.3	-3	-1.1
60	-5.75	-3.4	-1.3
70	-6.1	-3.7	-1.5
80	-6.4	-4	-1.6
90	-6.75	-4.2	-1.75
100	-7	-4.4	-1.8
200	-9	-5.75	-2.5
300	-10.25	-6.75	-3.1
400	-11.25	-7.5	-3.5
500	-12	-8	-3.75
600	-12.5	-8.5	-3.9
700	-13.1	-8.9	-4.1
800	-13.6	-9.25	-4.25
900	-14	-9.5	-4.4
1000	-14.5	-9.8	-4.5
1500	-15.75	-10.9	-5
2000	-17	-11.75	-5.5
2500	-17.75	-12.3	-5.75
3000	-18.5	-12.75	-6.25
3400	-19	-13	-6.4

A.2. Calculation for obtaining the G Matrix

A) Surface of Unreinforced Section:

X	X=log10x	Y	X^2	X^3	X^4	X^5	X^6	X^Y	(X^2)*Y	(X^3)*Y
2	0.30103	-0.3	0.09062	0.02728	0.00821	0.00247	0.00074	-0.09031	-0.02719	-0.00818
10	1	-2.1	1	1	1	1	1	-2.1	-2.1	-2.1
20	1.30103	-3.3	1.69268	2.20223	2.86516	3.72766	4.8498	-4.2934	-5.58584	-7.26735
30	1.47712	-4.1	2.18189	3.22291	4.76063	7.03203	10.3872	-6.0562	-8.94574	-13.2139
40	1.60206	-4.75	2.5666	4.11184	6.58742	10.5534	16.9072	-7.60978	-12.1913	-19.5312
50	1.69897	-5.3	2.8865	4.90408	8.33188	14.1556	24.05	-9.00454	-15.2984	-25.9916
60	1.77815	-5.75	3.16182	5.6222	9.99712	17.7764	31.6091	-10.2244	-18.1805	-32.3276
70	1.8451	-6.1	3.40439	6.28143	11.5898	21.3844	39.4563	-11.2551	-20.7668	-38.3167
80	1.90309	-6.4	3.62175	6.89252	13.1171	24.963	47.5068	-12.1798	-23.1792	-44.1121
90	1.95424	-6.75	3.81906	7.46338	14.5852	28.5031	55.702	-13.1911	-25.7787	-50.3778
100	2	-7	4	8	16	32	64	-14	-28	-56
200	2.30103	-9	5.29474	12.1834	28.0343	64.5077	148.434	-20.7093	-47.6527	-109.65
300	2.47712	-10.25	6.13613	15.1999	37.6521	93.2688	231.038	-25.3905	-62.8953	-155.799
400	2.60206	-11.25	6.77072	17.6178	45.8426	119.285	310.387	-29.2732	-76.1706	-198.2
500	2.69897	-12	7.28444	19.6605	53.0631	143.216	386.535	-32.3876	-87.4133	-235.926
600	2.77815	-12.5	7.71812	21.4421	59.5694	165.493	459.764	-34.7269	-96.4766	-268.026
700	2.8451	-13.1	8.09458	23.0299	65.5223	186.417	530.375	-37.2708	-106.039	-301.691
800	2.90309	-13.6	8.42793	24.467	71.03	206.207	598.636	-39.482	-114.62	-332.752
900	2.95424	-14	8.72755	25.7833	76.1701	225.025	664.778	-41.3594	-122.186	-360.966
1000	3	-14.5	9	27	81	243	729	-43.5	-130.5	-391.5
1500	3.17609	-15.75	10.0876	32.039	101.759	323.195	1026.5	-50.0234	-158.879	-504.614
2000	3.30103	-17	10.8968	35.9707	118.74	391.965	1293.89	-56.1175	-185.246	-611.501
2500	3.39794	-17.75	11.546	39.2326	133.31	452.979	1539.2	-60.3134	-204.941	-696.379
3000	3.47712	-18.5	12.0904	42.0397	146.177	508.276	1767.34	-64.3267	-223.672	-777.734
24	**54.7727**	**-231.1**	**140.5**	**385.394**	**1106.71**	**3283.93**	**9981.34**	**-624.885**	**-1776.74**	**-5233.99**

A.3. Determination of Polynomial Coefficient by MATHLAB

```
G=[24,54.77273858,140.5002393,385.3937261;
   54.77273858,140.5002393,385.3937261,1106.71259;
 140.5002393,385.3937261,1106.71259,3283.932316;
 385.3937261,1106.71259,3283.932316,9981.335964]


G =

  1.0e+003 *

    0.0240   0.0548   0.1405   0.3854
    0.0548   0.1405   0.3854   1.1067
    0.1405   0.3854   1.1067   3.2839
    0.3854   1.1067   3.2839   9.9813

>> B=inv (G)

B =

    2.6343  -4.4444   2.2252  -0.3410
   -4.4444   9.2845  -5.2007   0.8532
    2.2252  -5.2007   3.0891  -0.5256
   -0.3410   0.8532  -0.5256   0.0916

>> H=[-231.05; -624.885; -1776.74; -5233.99]

H =

  1.0e+003 *

   -0.2311
   -0.6249
   -1.7767
   -5.2340

>> A=B*H

A =

   -0.0491
   -0.3431
   -1.7791
    0.1009
```

Formula (permanent deformation as a function of number of passes n) for the point at the top of surface:

$$F(n) = -0.0491 - 0.3431 \times \log_{10}(n) - 1.7791 \times \log_{10}^{2}(n) + 0.1009 \times \log_{10}^{3}(n) \qquad (3.19)$$

Thus the other polynomial equations of deflections can be found in this similar way.

APPENDIX B

ABAQUS INPUT FILE

B1. ABAQUS Input File for Primary Structure

The following is a typical ABAQUS input file for the Primary Structure with a pressure load of q = 210 kPa at the 1st pass. The input file is divided into specific important sections and they are briefly summarized at the Appendix B3. The corresponding mesh is shown in Figure 5.4.

```
*****ABAQUS INPUT FILE FOR PRIMARY STRUCTURE*********
*****PRIMARY STRUCTURE: LOAD 210 Kpa: STEP 1:********
*HEADING
ELEMENT CAX8 TESTING FOR DEFLECTION
*PREPRINT, ECHO=YES, HISTORY=NO, MODEL=NO

****** SECTION 1:************
***** NODE INPUT*********

*NODE
101,0,0
102,0,125
103,0,250
104,0,375
105,0,500
106,0,625
107,0,750
108,0,875
109,0,1000
110,0,1125
111,0,1250
112,0,1375
113,0,1500
114,0,1625
115,0,1750
116,0,1875
117,0,2000
118,0,2005
119,0,2010
120,0,2015
121,0,2020
122,0,2025
123,0,2030
124,0,2035
130,0,2050
131,0,2052
132,0,2054
133,0,2056
134,0,2058
135,0,2060
**
201,2,0
203,2,250
```

```
205,2,500
207,2,750
209,2,1000
211,2,1250
213,2,1500
215,2,1750
217,2,2000
219,2,2010
221,2,2020
223,2,2030
225,2,2040
227,2,2044
229,2,2048
231,2,2052
233,2,2056
235,2,2060
**
301,4,0
302,4,125
303,4,250
304,4,375
305,4,500
306,4,625
307,4,750
308,4,875
309,4,1000
310,4,1125
311,4,1250
312,4,1375
313,4,1500
314,4,1625
315,4,1750
316,4,1875
317,4,2000
318,4,2005
319,4,2010
320,4,2015
321,4,2020
322,4,2025
323,4,2030
324,4,2035
325,4,2040
326,4,2042
327,4,2044
328,4,2046
329,4,2048
330,4,2050
331,4,2052
332,4,2054
333,4,2056
334,4,2058
335,4,2060
**
401,6,0
403,6,250
405,6,500
407,6,750
```

```
409,6,1000
411,6,1250
413,6,1500
415,6,1750
417,6,2000
419,6,2010
421,6,2020
423,6,2030
425,6,2040
427,6,2044
429,6,2048
431,6,2052
433,6,2056
435,6,2060
**
501,8,0
502,8,125
503,8,250
504,8,375
505,8,500
506,8,625
507,8,750
508,8,875
509,8,1000
510,8,1125
511,8,1250
512,8,1375
513,8,1500
514,8,1625
515,8,1750
516,8,1875
517,8,2000
518,8,2005
519,8,2010
520,8,2015
521,8,2020
522,8,2025
523,8,2030
524,8,2035
525,8,2040
526,8,2042
527,8,2044
528,8,2046
529,8,2048
530,8,2050
531,8,2052
532,8,2054
533,8,2056
534,8,2058
535,8,2060
**
601,10,0
603,10,250
605,10,500
607,10,750
609,10,1000
611,10,1250
```

```
613,10,1500
615,10,1750
617,10,2000
619,10,2010
621,10,2020
623,10,2030
625,10,2040
627,10,2044
629,10,2048
631,10,2052
633,10,2056
635,10,2060
**
701,12,0
702,12,125
703,12,250
704,12,375
705,12,500
706,12,625
707,12,750
708,12,875
709,12,1000
710,12,1125
711,12,1250
712,12,1375
713,12,1500
714,12,1625
715,12,1750
716,12,1875
717,12,2000
718,12,2005
719,12,2010
720,12,2015
721,12,2020
722,12,2025
723,12,2030
724,12,2035
725,12,2040
726,12,2042
727,12,2044
728,12,2046
729,12,2048
730,12,2050
731,12,2052
732,12,2054
733,12,2056
734,12,2058
735,12,2060
**
801,14,0
803,14,250
805,14,500
807,14,750
809,14,1000
811,14,1250
813,14,1500
815,14,1750
```

```
817,14,2000
819,14,2010
821,14,2020
823,14,2030
825,14,2040
827,14,2044
829,14,2048
831,14,2052
833,14,2056
835,14,2060
**
901,16,0
902,16,125
903,16,250
904,16,375
905,16,500
906,16,625
907,16,750
908,16,875
909,16,1000
910,16,1125
911,16,1250
912,16,1375
913,16,1500
914,16,1625
915,16,1750
916,16,1875
917,16,2000
918,16,2005
919,16,2010
920,16,2015
921,16,2020
922,16,2025
923,16,2030
924,16,2035
925,16,2040
926,16,2042
927,16,2044
928,16,2046
929,16,2048
930,16,2050
931,16,2052
932,16,2054
933,16,2056
934,16,2058
935,16,2060
**
1001,18,0
1003,18,250
1005,18,500
1007,18,750
1009,18,1000
1011,18,1250
1013,18,1500
1015,18,1750
1017,18,2000
1019,18,2010
```

```
1021,18,2020
1023,18,2030
1025,18,2040
1027,18,2044
1029,18,2048
1031,18,2052
1033,18,2056
1035,18,2060
**
1101,20,0
1102,20,125
1103,20,250
1104,20,375
1105,20,500
1106,20,625
1107,20,750
1108,20,875
1109,20,1000
1110,20,1125
1111,20,1250
1112,20,1375
1113,20,1500
1114,20,1625
1115,20,1750
1116,20,1875
1117,20,2000
1118,20,2005
1119,20,2010
1120,20,2015
1121,20,2020
1122,20,2025
1123,20,2030
1124,20,2035
1125,20,2040
1126,20,2042
1127,20,2044
1128,20,2046
1129,20,2048
1130,20,2050
1131,20,2052
1132,20,2054
1133,20,2056
1134,20,2058
1135,20,2060
**
1201,22,0
1203,22,250
1205,22,500
1207,22,750
1209,22,1000
1211,22,1250
1213,22,1500
1215,22,1750
1217,22,2000
1219,22,2010
1221,22,2020
1223,22,2030
```

```
1225,22,2040
1227,22,2044
1229,22,2048
1231,22,2052
1233,22,2056
1235,22,2060
**
1301,24,0
1302,24,125
1303,24,250
1304,24,375
1305,24,500
1306,24,625
1307,24,750
1308,24,875
1309,24,1000
1310,24,1125
1311,24,1250
1312,24,1375
1313,24,1500
1314,24,1625
1315,24,1750
1316,24,1875
1317,24,2000
1318,24,2005
1319,24,2010
1320,24,2015
1321,24,2020
1322,24,2025
1323,24,2030
1324,24,2035
1325,24,2040
1326,24,2042
1327,24,2044
1328,24,2046
1329,24,2048
1330,24,2050
1331,24,2052
1332,24,2054
1333,24,2056
1334,24,2058
1335,24,2060
**
1401,26,0
1403,26,250
1405,26,500
1407,26,750
1409,26,1000
1411,26,1250
1413,26,1500
1415,26,1750
1417,26,2000
1419,26,2010
1421,26,2020
1423,26,2030
1425,26,2040
1427,26,2044
```

```
1429,26,2048
1431,26,2052
1433,26,2056
1435,26,2060
**
1501,28,0
1502,28,125
1503,28,250
1504,28,375
1505,28,500
1506,28,625
1507,28,750
1508,28,875
1509,28,1000
1510,28,1125
1511,28,1250
1512,28,1375
1513,28,1500
1514,28,1625
1515,28,1750
1516,28,1875
1517,28,2000
1518,28,2005
1519,28,2010
1520,28,2015
1521,28,2020
1522,28,2025
1523,28,2030
1524,28,2035
1525,28,2040
1526,28,2042
1527,28,2044
1528,28,2046
1529,28,2048
1530,28,2050
1531,28,2052
1532,28,2054
1533,28,2056
1534,28,2058
1535,28,2060
**
1601,30,0
1603,30,250
1605,30,500
1607,30,750
1609,30,1000
1611,30,1250
1613,30,1500
1615,30,1750
1617,30,2000
1619,30,2010
1621,30,2020
1623,30,2030
1625,30,2040
1627,30,2044
1629,30,2048
1631,30,2052
```

```
1633,30,2056
1635,30,2060
**
1701,32,0
1702,32,125
1703,32,250
1704,32,375
1705,32,500
1706,32,625
1707,32,750
1708,32,875
1709,32,1000
1710,32,1125
1711,32,1250
1712,32,1375
1713,32,1500
1714,32,1625
1715,32,1750
1716,32,1875
1717,32,2000
1718,32,2005
1719,32,2010
1720,32,2015
1721,32,2020
1722,32,2025
1723,32,2030
1724,32,2035
1725,32,2040
1726,32,2042
1727,32,2044
1728,32,2046
1729,32,2048
1730,32,2050
1731,32,2052
1732,32,2054
1733,32,2056
1734,32,2058
1735,32,2060
1801,36,0
1803,36,250
1805,36,500
1807,36,750
1809,36,1000
1811,36,1250
1813,36,1500
1815,36,1750
1817,36,2000
1819,36,2010
1821,36,2020
1823,36,2030
1825,36,2040
1827,36,2044
1829,36,2048
1831,36,2052
1833,36,2056
1835,36,2060
1901,40,0
```

```
1902,40,125
1903,40,250
1904,40,375
1905,40,500
1906,40,625
1907,40,750
1908,40,875
1909,40,1000
1910,40,1125
1911,40,1250
1912,40,1375
1913,40,1500
1914,40,1625
1915,40,1750
1916,40,1875
1917,40,2000
1918,40,2005
1919,40,2010
1920,40,2015
1921,40,2020
1922,40,2025
1923,40,2030
1924,40,2035
1925,40,2040
1926,40,2042
1927,40,2044
1928,40,2046
1929,40,2048
1930,40,2050
1931,40,2052
1932,40,2054
1933,40,2056
1934,40,2058
1935,40,2060
2001,45,0
2003,45,250
2005,45,500
2007,45,750
2009,45,1000
2011,45,1250
2013,45,1500
2015,45,1750
2017,45,2000
2019,45,2010
2021,45,2020
2023,45,2030
2025,45,2040
2027,45,2044
2029,45,2048
2031,45,2052
2033,45,2056
2035,45,2060
2101,50,0
2102,50,125
2103,50,250
2104,50,375
2105,50,500
```

```
2106,50,625
2107,50,750
2108,50,875
2109,50,1000
2110,50,1125
2111,50,1250
2112,50,1375
2113,50,1500
2114,50,1625
2115,50,1750
2116,50,1875
2117,50,2000
2118,50,2005
2119,50,2010
2120,50,2015
2121,50,2020
2122,50,2025
2123,50,2030
2124,50,2035
2125,50,2040
2126,50,2042
2127,50,2044
2128,50,2046
2129,50,2048
2130,50,2050
2131,50,2052
2132,50,2054
2133,50,2056
2134,50,2058
2135,50,2060
2201,75,0
2203,75,250
2205,75,500
2207,75,750
2209,75,1000
2211,75,1250
2213,75,1500
2215,75,1750
2217,75,2000
2219,75,2010
2221,75,2020
2223,75,2030
2225,75,2040
2227,75,2044
2229,75,2048
2231,75,2052
2233,75,2056
2235,75,2060
2301,100,0
2302,100,125
2303,100,250
2304,100,375
2305,100,500
2306,100,625
2307,100,750
2308,100,875
2309,100,1000
```

```
2310,100,1125
2311,100,1250
2312,100,1375
2313,100,1500
2314,100,1625
2315,100,1750
2316,100,1875
2317,100,2000
2318,100,2005
2319,100,2010
2320,100,2015
2321,100,2020
2322,100,2025
2323,100,2030
2324,100,2035
2325,100,2040
2326,100,2042
2327,100,2044
2328,100,2046
2329,100,2048
2330,100,2050
2331,100,2052
2332,100,2054
2333,100,2056
2334,100,2058
2335,100,2060
2401,125,0
2403,125,250
2405,125,500
2407,125,750
2409,125,1000
2411,125,1250
2413,125,1500
2415,125,1750
2417,125,2000
2419,125,2010
2421,125,2020
2423,125,2030
2425,125,2040
2427,125,2044
2429,125,2048
2431,125,2052
2433,125,2056
2435,125,2060
2501,150,0
2502,150,125
2503,150,250
2504,150,375
2505,150,500
2506,150,625
2507,150,750
2508,150,875
2509,150,1000
2510,150,1125
2511,150,1250
2512,150,1375
2513,150,1500
```

```
2514,150,1625
2515,150,1750
2516,150,1875
2517,150,2000
2518,150,2005
2519,150,2010
2520,150,2015
2521,150,2020
2522,150,2025
2523,150,2030
2524,150,2035
2525,150,2040
2526,150,2042
2527,150,2044
2528,150,2046
2529,150,2048
2530,150,2050
2531,150,2052
2532,150,2054
2533,150,2056
2534,150,2058
2535,150,2060
2601,175,0
2603,175,250
2605,175,500
2607,175,750
2609,175,1000
2611,175,1250
2613,175,1500
2615,175,1750
2617,175,2000
2619,175,2010
2621,175,2020
2623,175,2030
2625,175,2040
2627,175,2044
2629,175,2048
2631,175,2052
2633,175,2056
2635,175,2060
2701,200,0
2702,200,125
2703,200,250
2704,200,375
2705,200,500
2706,200,625
2707,200,750
2708,200,875
2709,200,1000
2710,200,1125
2711,200,1250
2712,200,1375
2713,200,1500
2714,200,1625
2715,200,1750
2716,200,1875
2717,200,2000
```

```
2718,200,2005
2719,200,2010
2720,200,2015
2721,200,2020
2722,200,2025
2723,200,2030
2724,200,2035
2725,200,2040
2726,200,2042
2727,200,2044
2728,200,2046
2729,200,2048
2730,200,2050
2731,200,2052
2732,200,2054
2733,200,2056
2734,200,2058
2735,200,2060
2801,225,0
2803,225,250
2805,225,500
2807,225,750
2809,225,1000
2811,225,1250
2813,225,1500
2815,225,1750
2817,225,2000
2819,225,2010
2821,225,2020
2823,225,2030
2825,225,2040
2827,225,2044
2829,225,2048
2831,225,2052
2833,225,2056
2835,225,2060
2901,250,0
2902,250,125
2903,250,250
2904,250,375
2905,250,500
2906,250,625
2907,250,750
2908,250,875
2909,250,1000
2910,250,1125
2911,250,1250
2912,250,1375
2913,250,1500
2914,250,1625
2915,250,1750
2916,250,1875
2917,250,2000
2918,250,2005
2919,250,2010
2920,250,2015
2921,250,2020
```

```
2922,250,2025
2923,250,2030
2924,250,2035
2925,250,2040
2926,250,2042
2927,250,2044
2928,250,2046
2929,250,2048
2930,250,2050
2931,250,2052
2932,250,2054
2933,250,2056
2934,250,2058
2935,250,2060

**** SECTION 2: *********
**** DEFINE ELEMENTS*****

*ELEMENT,TYPE=CAX8
1,101,301,303,103,201,302,203,102
*ELGEN,ELSET=SUBGRADE
1,14,200,1,8,2,14
*ELEMENT,TYPE=CAX8
113,117,317,319,119,217,318,219,118
*ELGEN,ELSET=BASE
113,14,200,1,4,2,14
*ELEMENT,TYPE=CAX8
169,125,325,327,127,225,326,227,126
*ELGEN,ELSET=SURFACE
169,14,200,1,5,2,14

***** DEFINE 3-LAYER OF PAVEMENT SYSTEM ***********

*SOLID SECTION,MATERIAL=A1,ELSET=SUBGRADE
*SOLID SECTION,MATERIAL=A2,ELSET=BASE
*SOLID SECTION,MATERIAL=A3,ELSET=SURFACE

***** SECTION 3:*****************
***** DEFIME MATERIALS***********

*MATERIAL,NAME=A1
*ELASTIC,TYPE=ISOTROPIC
100.0,0.45
*MATERIAL,NAME=A2
*ELASTIC,TYPE=ISOTROPIC
85.0,0.3
*MATERIAL,NAME=A3
*ELASTIC,TYPE=ISOTROPIC
23.0,0.4

***** SECTION 4:**************************
***** DEFINE BOUNDARY CONDITIONS***********

*BOUNDARY
101,ENCASTRE
201,ENCASTRE
```

```
301,ENCASTRE
401,ENCASTRE
501,ENCASTRE
601,ENCASTRE
701,ENCASTRE
801,ENCASTRE
901,ENCASTRE
1001,ENCASTRE
1101,ENCASTRE
1201,ENCASTRE
1301,ENCASTRE
1401,ENCASTRE
1501,ENCASTRE
1601,ENCASTRE
1701,ENCASTRE
1801,ENCASTRE
1901,ENCASTRE
2001,ENCASTRE
2101,ENCASTRE
2201,ENCASTRE
2301,ENCASTRE
2401,ENCASTRE
2501,ENCASTRE
2601,ENCASTRE
2701,ENCASTRE
2801,ENCASTRE
2901,ENCASTRE
101,1
102,1
103,1
104,1
105,1
106,1
107,1
108,1
109,1
110,1
111,1
112,1
113,1
114,1
115,1
116,1
117,1
118,1
119,1
120,1
121,1
122,1
123,1
124,1
125,1
126,1
127,1
128,1
129,1
130,1
```

```
131,1
132,1
133,1
134,1
135,1
2901,1
2902,1
2903,1
2904,1
2905,1
2906,1
2907,1
2908,1
2909,1
2910,1
2911,1
2912,1
2913,1
2914,1
2915,1
2916,1
2917,1
2918,1
2919,1
2920,1
2921,1
2922,1
2923,1
2924,1
2925,1
2926,1
2927,1
2928,1
2929,1
2930,1
2931,1
2932,1
2933,1
2934,1
2935,1

****** SECTION 5:**********
****** DEFINE LOADING CONDITION*******

*STEP
*STATIC
*DLOAD
225,P3,0.21
226,P3,0.21
227,P3,0.21
228,P3,0.21
229,P3,0.21
230,P3,0.21
231,P3,0.21
```

```
******* SECTION 6:********************
******* DEFINE OUTPUT GENERATION******

*EL FILE
S,
COORD,
E,
LOADS
*ENERGY FILE
*NODE FILE
U,COORD
*NODE PRINT
U,COORD
*EL PRINT
S,
COORD,
E,
LOADS,
*END STEP
```

B2. ABAQUS Input File for Adjoint Structure

The following is a typical ABAQUS input file for the Adjoint Structure with a unit concentrated load at the 1st pass. The input file is divided into specific important sections and they are briefly summarized at the Appendix B3.

```
*ABAQUS INPUT FILE FOR ADJOINT STRUCTURE
*HEADING
ELEMENT CAX8 TESTING FOR DEFLECTION
*PREPRINT, ECHO=YES, HISTORY=NO, MODEL=NO

****** SECTION 1:*****************
****** NODE INPUT*****************

*NODE
101,0,0
102,0,125
103,0,250
104,0,375
105,0,500
106,0,625
107,0,750
108,0,875
109,0,1000
110,0,1125
111,0,1250
112,0,1375
113,0,1500
114,0,1625
115,0,1750
116,0,1875
117,0,2000
118,0,2005
119,0,2010
120,0,2015
121,0,2020
122,0,2025
123,0,2030
124,0,2035
125,0,2040
126,0,2042
127,0,2044
128,0,2046
129,0,2048
130,0,2050
131,0,2052
132,0,2054
133,0,2056
134,0,2058
135,0,2060
**
201,2,0
```

```
203,2,250
205,2,500
207,2,750
209,2,1000
211,2,1250
213,2,1500
215,2,1750
217,2,2000
219,2,2010
221,2,2020
223,2,2030
225,2,2040
227,2,2044
229,2,2048
231,2,2052
233,2,2056
235,2,2060
**
301,4,0
302,4,125
303,4,250
304,4,375
305,4,500
306,4,625
307,4,750
308,4,875
309,4,1000
310,4,1125
311,4,1250
312,4,1375
313,4,1500
314,4,1625
315,4,1750
316,4,1875
317,4,2000
318,4,2005
319,4,2010
320,4,2015
321,4,2020
322,4,2025
323,4,2030
324,4,2035
325,4,2040
326,4,2042
327,4,2044
328,4,2046
329,4,2048
330,4,2050
331,4,2052
332,4,2054
333,4,2056
334,4,2058
335,4,2060
**
401,6,0
403,6,250
405,6,500
```

```
407,6,750
409,6,1000
411,6,1250
413,6,1500
415,6,1750
417,6,2000
419,6,2010
421,6,2020
423,6,2030
425,6,2040
427,6,2044
429,6,2048
431,6,2052
433,6,2056
435,6,2060
**
501,8,0
502,8,125
503,8,250
504,8,375
505,8,500
506,8,625
507,8,750
508,8,875
509,8,1000
510,8,1125
511,8,1250
512,8,1375
513,8,1500
514,8,1625
515,8,1750
516,8,1875
517,8,2000
518,8,2005
519,8,2010
520,8,2015
521,8,2020
522,8,2025
523,8,2030
524,8,2035
525,8,2040
526,8,2042
527,8,2044
528,8,2046
529,8,2048
530,8,2050
531,8,2052
532,8,2054
533,8,2056
534,8,2058
535,8,2060
**
601,10,0
603,10,250
605,10,500
607,10,750
609,10,1000
```

```
611,10,1250
613,10,1500
615,10,1750
617,10,2000
619,10,2010
621,10,2020
623,10,2030
625,10,2040
627,10,2044
629,10,2048
631,10,2052
633,10,2056
635,10,2060
**
701,12,0
702,12,125
703,12,250
704,12,375
705,12,500
706,12,625
707,12,750
708,12,875
709,12,1000
710,12,1125
711,12,1250
712,12,1375
713,12,1500
714,12,1625
715,12,1750
716,12,1875
717,12,2000
718,12,2005
719,12,2010
720,12,2015
721,12,2020
722,12,2025
723,12,2030
724,12,2035
725,12,2040
726,12,2042
727,12,2044
728,12,2046
729,12,2048
730,12,2050
731,12,2052
732,12,2054
733,12,2056
734,12,2058
735,12,2060
**
801,14,0
803,14,250
805,14,500
807,14,750
809,14,1000
811,14,1250
813,14,1500
```

```
815,14,1750
817,14,2000
819,14,2010
821,14,2020
823,14,2030
825,14,2040
827,14,2044
829,14,2048
831,14,2052
833,14,2056
835,14,2060
**
901,16,0
902,16,125
903,16,250
904,16,375
905,16,500
906,16,625
907,16,750
908,16,875
909,16,1000
910,16,1125
911,16,1250
912,16,1375
913,16,1500
914,16,1625
915,16,1750
916,16,1875
917,16,2000
918,16,2005
919,16,2010
920,16,2015
921,16,2020
922,16,2025
923,16,2030
924,16,2035
925,16,2040
926,16,2042
927,16,2044
928,16,2046
929,16,2048
930,16,2050
931,16,2052
932,16,2054
933,16,2056
934,16,2058
935,16,2060
**
1001,18,0
1003,18,250
1005,18,500
1007,18,750
1009,18,1000
1011,18,1250
1013,18,1500
1015,18,1750
1017,18,2000
```

```
1019,18,2010
1021,18,2020
1023,18,2030
1025,18,2040
1027,18,2044
1029,18,2048
1031,18,2052
1033,18,2056
1035,18,2060
**
1101,20,0
1102,20,125
1103,20,250
1104,20,375
1105,20,500
1106,20,625
1107,20,750
1108,20,875
1109,20,1000
1110,20,1125
1111,20,1250
1112,20,1375
1113,20,1500
1114,20,1625
1115,20,1750
1116,20,1875
1117,20,2000
1118,20,2005
1119,20,2010
1120,20,2015
1121,20,2020
1122,20,2025
1123,20,2030
1124,20,2035
1125,20,2040
1126,20,2042
1127,20,2044
1128,20,2046
1129,20,2048
1130,20,2050
1131,20,2052
1132,20,2054
1133,20,2056
1134,20,2058
1135,20,2060
**
1201,22,0
1203,22,250
1205,22,500
1207,22,750
1209,22,1000
1211,22,1250
1213,22,1500
1215,22,1750
1217,22,2000
1219,22,2010
1221,22,2020
```

```
1223,22,2030
1225,22,2040
1227,22,2044
1229,22,2048
1231,22,2052
1233,22,2056
1235,22,2060
**
1301,24,0
1302,24,125
1303,24,250
1304,24,375
1305,24,500
1306,24,625
1307,24,750
1308,24,875
1309,24,1000
1310,24,1125
1311,24,1250
1312,24,1375
1313,24,1500
1314,24,1625
1315,24,1750
1316,24,1875
1317,24,2000
1318,24,2005
1319,24,2010
1320,24,2015
1321,24,2020
1322,24,2025
1323,24,2030
1324,24,2035
1325,24,2040
1326,24,2042
1327,24,2044
1328,24,2046
1329,24,2048
1330,24,2050
1331,24,2052
1332,24,2054
1333,24,2056
1334,24,2058
1335,24,2060
**
1401,26,0
1403,26,250
1405,26,500
1407,26,750
1409,26,1000
1411,26,1250
1413,26,1500
1415,26,1750
1417,26,2000
1419,26,2010
1421,26,2020
1423,26,2030
1425,26,2040
```

```
1427,26,2044
1429,26,2048
1431,26,2052
1433,26,2056
1435,26,2060
**
1501,28,0
1502,28,125
1503,28,250
1504,28,375
1505,28,500
1506,28,625
1507,28,750
1508,28,875
1509,28,1000
1510,28,1125
1511,28,1250
1512,28,1375
1513,28,1500
1514,28,1625
1515,28,1750
1516,28,1875
1517,28,2000
1518,28,2005
1519,28,2010
1520,28,2015
1521,28,2020
1522,28,2025
1523,28,2030
1524,28,2035
1525,28,2040
1526,28,2042
1527,28,2044
1528,28,2046
1529,28,2048
1530,28,2050
1531,28,2052
1532,28,2054
1533,28,2056
1534,28,2058
1535,28,2060
**
1601,30,0
1603,30,250
1605,30,500
1607,30,750
1609,30,1000
1611,30,1250
1613,30,1500
1615,30,1750
1617,30,2000
1619,30,2010
1621,30,2020
1623,30,2030
1625,30,2040
1627,30,2044
1629,30,2048
```

```
1631,30,2052
1633,30,2056
1635,30,2060
**
1701,32,0
1702,32,125
1703,32,250
1704,32,375
1705,32,500
1706,32,625
1707,32,750
1708,32,875
1709,32,1000
1710,32,1125
1711,32,1250
1712,32,1375
1713,32,1500
1714,32,1625
1715,32,1750
1716,32,1875
1717,32,2000
1718,32,2005
1719,32,2010
1720,32,2015
1721,32,2020
1722,32,2025
1723,32,2030
1724,32,2035
1725,32,2040
1726,32,2042
1727,32,2044
1728,32,2046
1729,32,2048
1730,32,2050
1731,32,2052
1732,32,2054
1733,32,2056
1734,32,2058
1735,32,2060
1801,36,0
1803,36,250
1805,36,500
1807,36,750
1809,36,1000
1811,36,1250
1813,36,1500
1815,36,1750
1817,36,2000
1819,36,2010
1821,36,2020
1823,36,2030
1825,36,2040
1827,36,2044
1829,36,2048
1831,36,2052
1833,36,2056
1835,36,2060
```

```
1901,40,0
1902,40,125
1903,40,250
1904,40,375
1905,40,500
1906,40,625
1907,40,750
1908,40,875
1909,40,1000
1910,40,1125
1911,40,1250
1912,40,1375
1913,40,1500
1914,40,1625
1915,40,1750
1916,40,1875
1917,40,2000
1918,40,2005
1919,40,2010
1920,40,2015
1921,40,2020
1922,40,2025
1923,40,2030
1924,40,2035
1925,40,2040
1926,40,2042
1927,40,2044
1928,40,2046
1929,40,2048
1930,40,2050
1931,40,2052
1932,40,2054
1933,40,2056
1934,40,2058
1935,40,2060
2001,45,0
2003,45,250
2005,45,500
2007,45,750
2009,45,1000
2011,45,1250
2013,45,1500
2015,45,1750
2017,45,2000
2019,45,2010
2021,45,2020
2023,45,2030
2025,45,2040
2027,45,2044
2029,45,2048
2031,45,2052
2033,45,2056
2035,45,2060
2101,50,0
2102,50,125
2103,50,250
2104,50,375
```

```
2105,50,500
2106,50,625
2107,50,750
2108,50,875
2109,50,1000
2110,50,1125
2111,50,1250
2112,50,1375
2113,50,1500
2114,50,1625
2115,50,1750
2116,50,1875
2117,50,2000
2118,50,2005
2119,50,2010
2120,50,2015
2121,50,2020
2122,50,2025
2123,50,2030
2124,50,2035
2125,50,2040
2126,50,2042
2127,50,2044
2128,50,2046
2129,50,2048
2130,50,2050
2131,50,2052
2132,50,2054
2133,50,2056
2134,50,2058
2135,50,2060
2201,75,0
2203,75,250
2205,75,500
2207,75,750
2209,75,1000
2211,75,1250
2213,75,1500
2215,75,1750
2217,75,2000
2219,75,2010
2221,75,2020
2223,75,2030
2225,75,2040
2227,75,2044
2229,75,2048
2231,75,2052
2233,75,2056
2235,75,2060
2301,100,0
2302,100,125
2303,100,250
2304,100,375
2305,100,500
2306,100,625
2307,100,750
2308,100,875
```

```
2309,100,1000
2310,100,1125
2311,100,1250
2312,100,1375
2313,100,1500
2314,100,1625
2315,100,1750
2316,100,1875
2317,100,2000
2318,100,2005
2319,100,2010
2320,100,2015
2321,100,2020
2322,100,2025
2323,100,2030
2324,100,2035
2325,100,2040
2326,100,2042
2327,100,2044
2328,100,2046
2329,100,2048
2330,100,2050
2331,100,2052
2332,100,2054
2333,100,2056
2334,100,2058
2335,100,2060
2401,125,0
2403,125,250
2405,125,500
2407,125,750
2409,125,1000
2411,125,1250
2413,125,1500
2415,125,1750
2417,125,2000
2419,125,2010
2421,125,2020
2423,125,2030
2425,125,2040
2427,125,2044
2429,125,2048
2431,125,2052
2433,125,2056
2435,125,2060
2501,150,0
2502,150,125
2503,150,250
2504,150,375
2505,150,500
2506,150,625
2507,150,750
2508,150,875
2509,150,1000
2510,150,1125
2511,150,1250
2512,150,1375
```

```
2513,150,1500
2514,150,1625
2515,150,1750
2516,150,1875
2517,150,2000
2518,150,2005
2519,150,2010
2520,150,2015
2521,150,2020
2522,150,2025
2523,150,2030
2524,150,2035
2525,150,2040
2526,150,2042
2527,150,2044
2528,150,2046
2529,150,2048
2530,150,2050
2531,150,2052
2532,150,2054
2533,150,2056
2534,150,2058
2535,150,2060
2601,175,0
2603,175,250
2605,175,500
2607,175,750
2609,175,1000
2611,175,1250
2613,175,1500
2615,175,1750
2617,175,2000
2619,175,2010
2621,175,2020
2623,175,2030
2625,175,2040
2627,175,2044
2629,175,2048
2631,175,2052
2633,175,2056
2635,175,2060
2701,200,0
2702,200,125
2703,200,250
2704,200,375
2705,200,500
2706,200,625
2707,200,750
2708,200,875
2709,200,1000
2710,200,1125
2711,200,1250
2712,200,1375
2713,200,1500
2714,200,1625
2715,200,1750
2716,200,1875
```

```
2717,200,2000
2718,200,2005
2719,200,2010
2720,200,2015
2721,200,2020
2722,200,2025
2723,200,2030
2724,200,2035
2725,200,2040
2726,200,2042
2727,200,2044
2728,200,2046
2729,200,2048
2730,200,2050
2731,200,2052
2732,200,2054
2733,200,2056
2734,200,2058
2735,200,2060
2801,225,0
2803,225,250
2805,225,500
2807,225,750
2809,225,1000
2811,225,1250
2813,225,1500
2815,225,1750
2817,225,2000
2819,225,2010
2821,225,2020
2823,225,2030
2825,225,2040
2827,225,2044
2829,225,2048
2831,225,2052
2833,225,2056
2835,225,2060
2901,250,0
2902,250,125
2903,250,250
2904,250,375
2905,250,500
2906,250,625
2907,250,750
2908,250,875
2909,250,1000
2910,250,1125
2911,250,1250
2912,250,1375
2913,250,1500
2914,250,1625
2915,250,1750
2916,250,1875
2917,250,2000
2918,250,2005
2919,250,2010
2920,250,2015
```

```
2921,250,2020
2922,250,2025
2923,250,2030
2924,250,2035
2925,250,2040
2926,250,2042
2927,250,2044
2928,250,2046
2929,250,2048
2930,250,2050
2931,250,2052
2932,250,2054
2933,250,2056
2934,250,2058
2935,250,2060

********* SECTION 2: *****************
********* DEFINE ELEMENTS ************

*ELEMENT, TYPE=CAX8
1,101,301,303,103,201,302,203,102
*ELGEN, ELSET=SUBGRADE
1,14,200,1,8,2,14
*ELEMENT, TYPE=CAX8
113,117,317,319,119,217,318,219,118
*ELGEN, ELSET=BASE
113,14,200,1,4,2,14
*ELEMENT, TYPE=CAX8
169,125,325,327,127,225,326,227,126
*ELGEN, ELSET=SURFACE
169,14,200,1,5,2,14

********* DEFINE 3-LAYER OF PAVEMENT SYSTEM ****

*SOLID SECTION, MATERIAL=A1, ELSET=SUBGRADE
*SOLID SECTION, MATERIAL=A2, ELSET=BASE
*SOLID SECTION, MATERIAL=A3, ELSET=SURFACE

********* SECTION 3: *************
********* DEFINE MATERIALS *******

*MATERIAL, NAME=A1
*ELASTIC, TYPE=ISOTROPIC
100.0,0.45
*MATERIAL, NAME=A2
*ELASTIC, TYPE=ISOTROPIC
85.0,0.3
*MATERIAL, NAME=A3
*ELASTIC, TYPE=ISOTROPIC
23.0,0.4

******* SECTION 4: **********************
******* DEFINE BOUNDARY CONDITIONS ******

*BOUNDARY
101,ENCASTRE
```

```
201,ENCASTRE
301,ENCASTRE
401,ENCASTRE
501,ENCASTRE
601,ENCASTRE
701,ENCASTRE
801,ENCASTRE
901,ENCASTRE
1001,ENCASTRE
1101,ENCASTRE
1201,ENCASTRE
1301,ENCASTRE
1401,ENCASTRE
1501,ENCASTRE
1601,ENCASTRE
1701,ENCASTRE
1801,ENCASTRE
1901,ENCASTRE
2001,ENCASTRE
2101,ENCASTRE
2201,ENCASTRE
2301,ENCASTRE
2401,ENCASTRE
2501,ENCASTRE
2601,ENCASTRE
2701,ENCASTRE
2801,ENCASTRE
2901,ENCASTRE
101,1
102,1
103,1
104,1
105,1
106,1
107,1
108,1
109,1
110,1
111,1
112,1
113,1
114,1
115,1
116,1
117,1
118,1
119,1
120,1
121,1
122,1
123,1
124,1
125,1
126,1
127,1
128,1
129,1
```

```
130,1
131,1
132,1
133,1
134,1
135,1
2901,1
2902,1
2903,1
2904,1
2905,1
2906,1
2907,1
2908,1
2909,1
2910,1
2911,1
2912,1
2913,1
2914,1
2915,1
2916,1
2917,1
2918,1
2919,1
2920,1
2921,1
2922,1
2923,1
2924,1
2925,1
2926,1
2927,1
2928,1
2929,1
2930,1
2931,1
2932,1
2933,1
2934,1
2935,1

********* SECTION 5: ************************
********* DEFINE LOADING CONDITION **********

*STEP
*STATIC
*CLOAD
135,2,-1

******** SECTION 6: ************************
******** DEFINE OUTPUT GENERATION **********

*EL FILE
S,
COORD,
E,
```

```
LOADS
*ENERGY FILE
*NODE FILE
U, COORD
*NODE PRINT
U, COORD
*EL PRINT
S,
COORD,
E,
LOADS,
*END STEP
```

B3. Explanation of the ABAQUS input File

The above input file is divided into six sections and each one briefly explained here. The six sections are:

(1) Node definition;

(2) Element definition;

(3) Material definition;

(4) Boundary conditions;

(5) Loading sequence; and

(6) Output request.

First, ABAQUS generates the nodes of the geometry. The nodes may be inputted from the same text file or from the different text file. Either way the nodes require an identifying number according to x, y, z coordinates. In ABAQUS these are specified as coordinates 1, 2 and 3 respectively. Because of the axisymmetric feature of geometry and load condition the problem is specified in r, z coordinates of 2-D space problem. In the present case, the input file contains the specified nodes for the three layer pavement system as well as to preserve the unrecoverable features of the system investigated, the geometry of the problem to be updated after each load application.

Second, ABAQUS forms elements from the defined nodes from the previous section. The element used in the ABAQUS analysis is CAX8 that means continuum (solid) axisymmetric eight-node isoparametric quadrilateral element. The elements are generated by means of the * ELGEN command. Three layers of pavement are included in the

analysis, therefore each are specified by the *ELSET command by the SUBGRADE, BASE and SURFACE respectively. The number of elements used for each layer is as follows: 112 elements for subgrade, 56 elements for base layer and 70 elements for surface layer.

Third, the material properties for each element must be specified. The first material is well-graded sand (specified as A1 in the ABAQUS input file) for subgrade, the second material is uniform fine gravel (specified as A2 in the ABAQUS input file) for base layer and the third material is bitumen (specified as A3 in the ABAQUS input file) for the top surface layer. Each material is defined by the different modulus of elasticity (E) and Poisson's ration (ν) for each load of application and they will behave as isotropic material. The value of E will be changed but the value of ν will be remain unchanged for subsequent each load of application.

Fourth, the boundary conditions are identified. The command * ENCASTRE means that the nodes are fixed (i.e., allowing zero displacements) in any direction, *1 means that the nodes are restrained in only one direction i.e. horizontal direction (i.e., allowing the vertical displacement only) and if there is no specification means that the nodes are not restrained in any direction (i.e., not fixed). In our case, the bottom nodes are fixed (i.e., ENCASTRE) in the horizontal and vertical direction, while the right and left hand side of the geometry are fixed only in the horizontal direction, allowing for the only vertical displacement and the top nodes are unrestrained (i.e., not fixed), modeling the real world scenario.

Fifth, is the loading criterion. The loading definitions are outlined in 5.2.2b and the ABAQUS terms are explained here. Static and constant pressure load of q = 210 kPa (0.21 MPa) as DLOAD is applied on the elements 225 to 231 of the top of the surface layer for the primary structure. On the other hand, the concentrated load, *CLOAD is applied at node 135 in the vertical (2) downward (negative) direction with the magnitude of one unit load for the adjoint structure.

Sixth and final is the output request that will be generated in the ABAQUS output file. For the output request, S means stress, E means strains, U means displacement that are to be displayed in the output file as per request.

Deformed contour plots and many other graphical advantages can be obtained through the ABAQUS CAE option.

APPENDIX C

ABAQUS CAE RESULTS

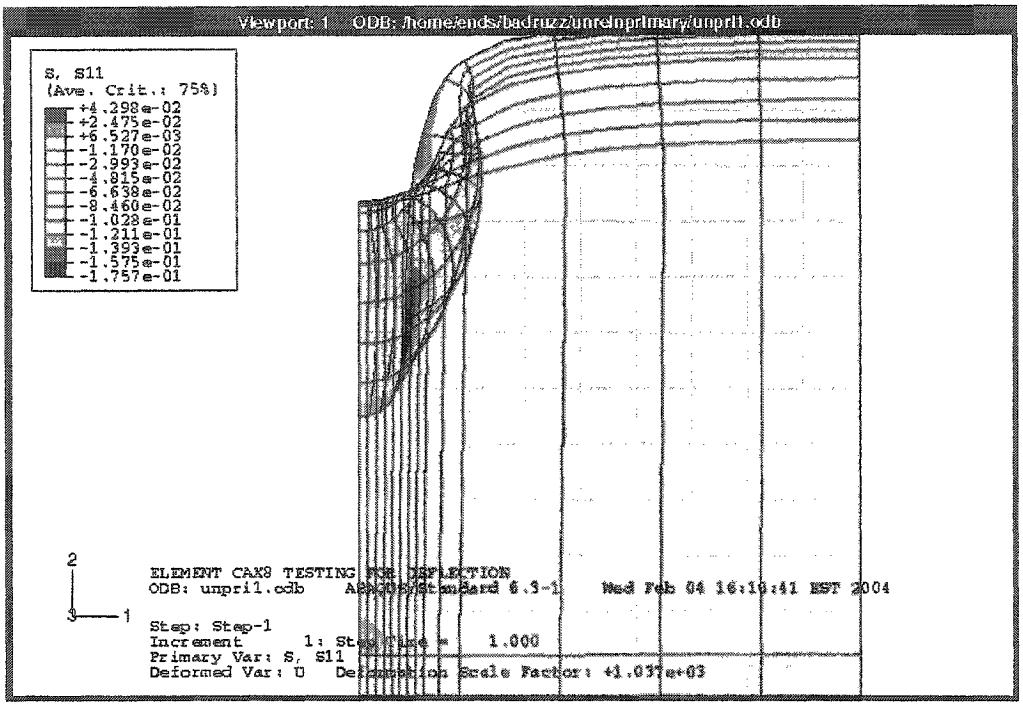

Figure C.1 Contour of normal stress in the radial direction (S11) at 1st pass for primary structure

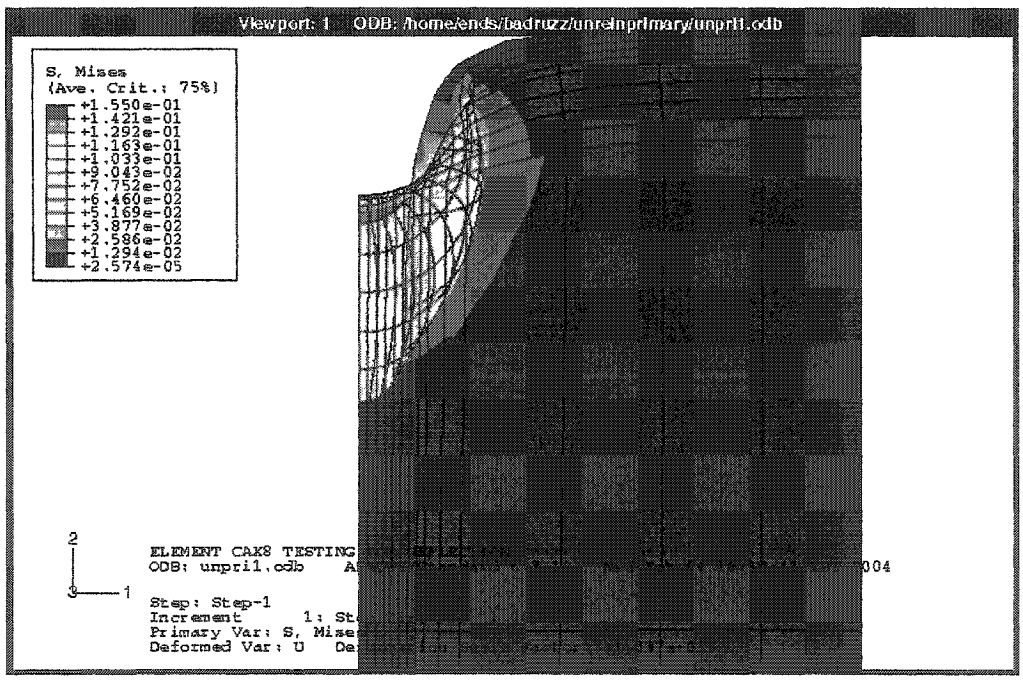

Figure C.2 Contour of Von Mises stress at 1st pass for primary structure

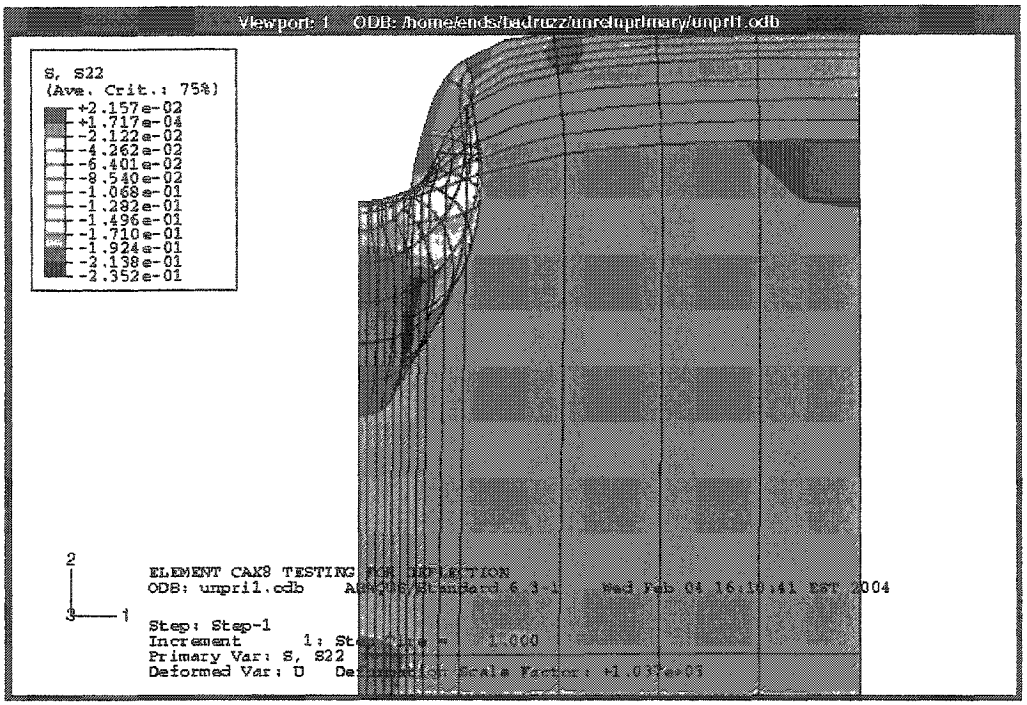

Figure C.3 Contour of normal stress in the vertical direction (S22) at 1st pass for primary structure

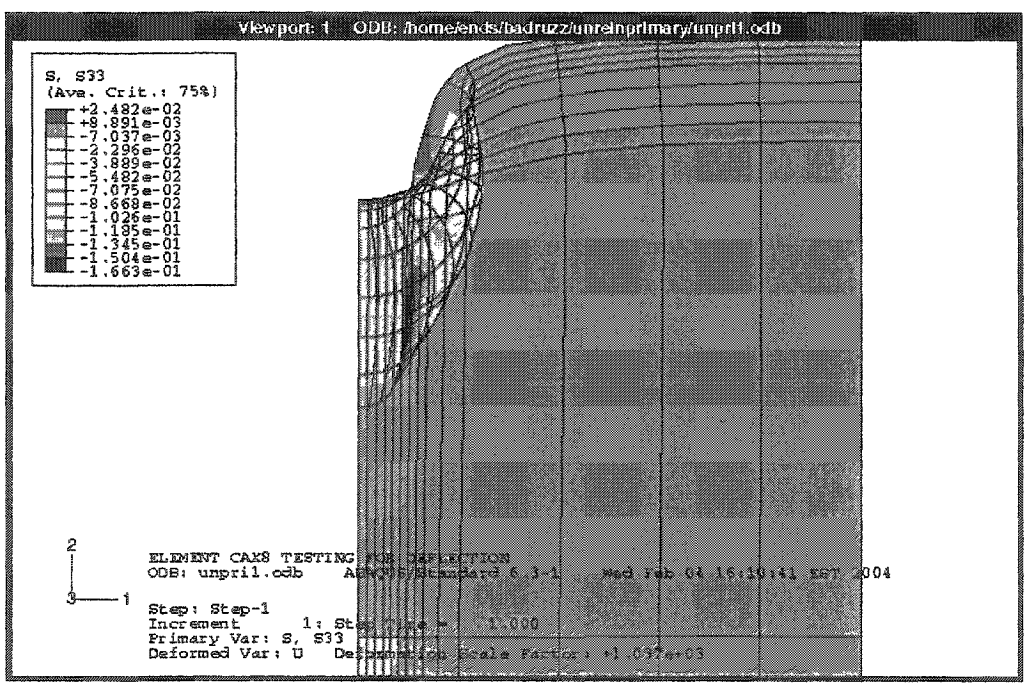

Figure C.4 Contour of normal stress in the circumferential direction (S33) at 1st pass for primary structure

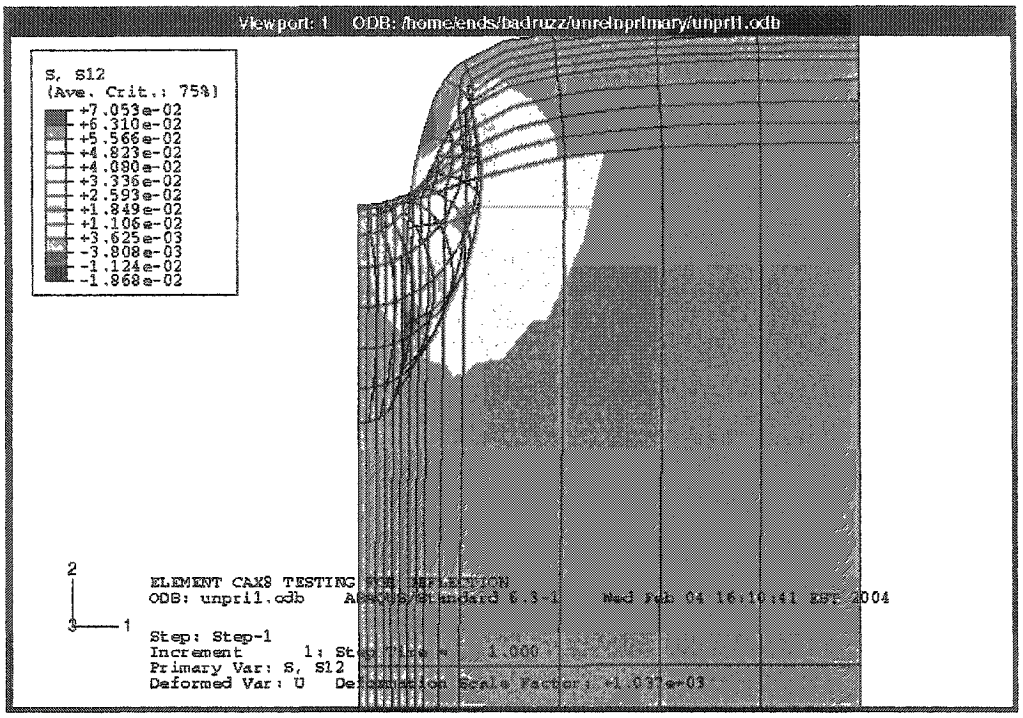

Figure C.5 Contour of shear stress in vertical - radial plane (S12) at 1st pass for primary structure

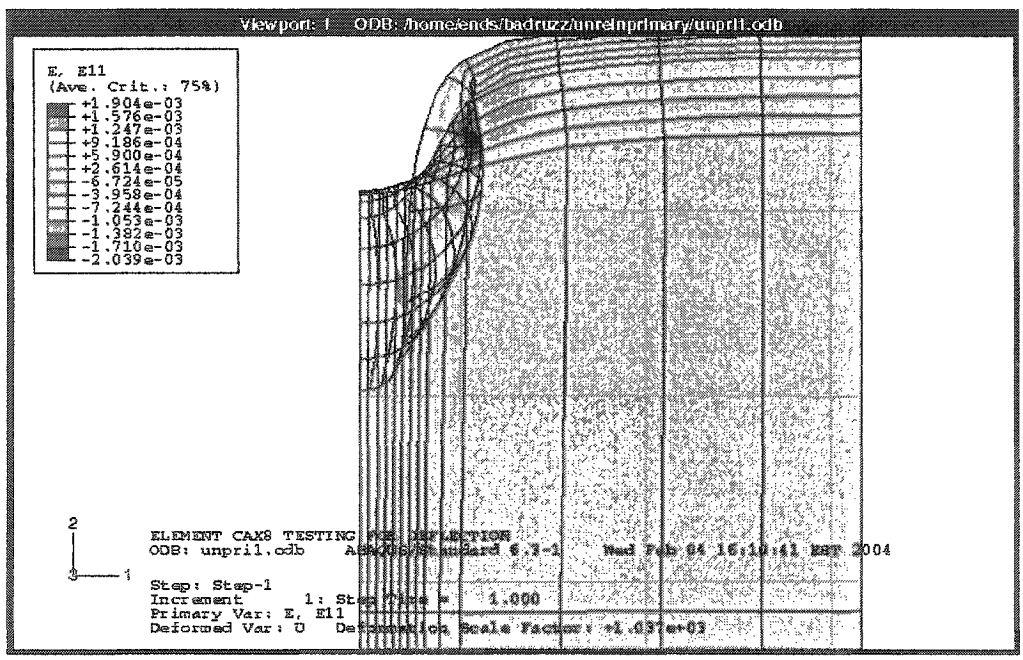

Figure C.6 Contour of normal strain in the radial direction (E11) at 1st pass for primary structure

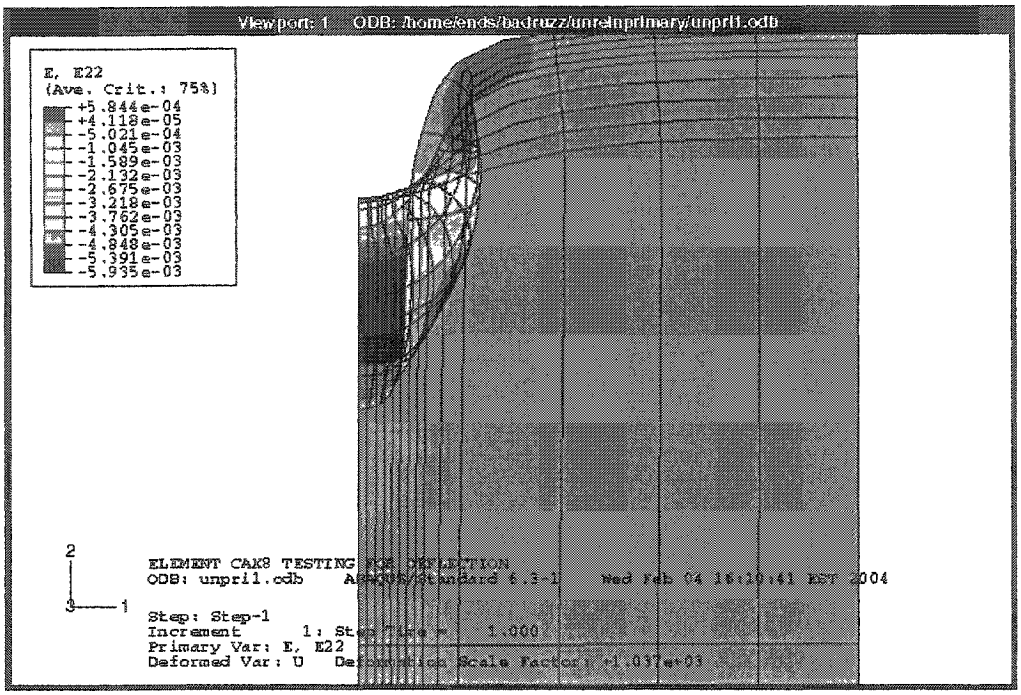

Figure C.7 Contour of normal strain in the vertical direction (E22) at 1st pass for primary structure

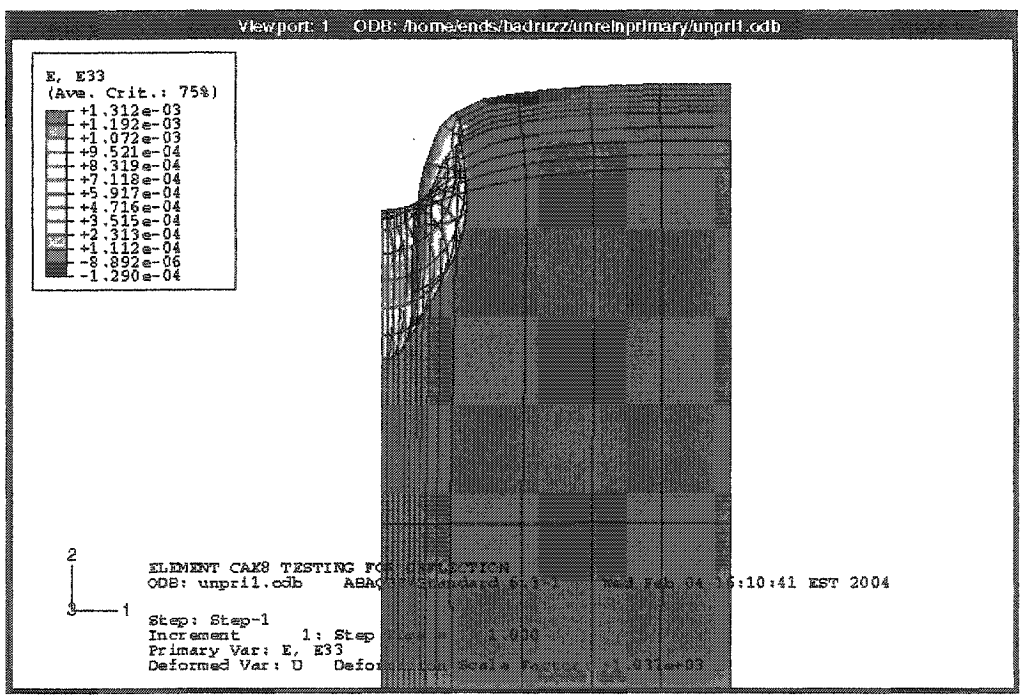

Figure C.8 Contour of normal strain in the circumferential direction (E33) at 1st pass for primary structure.

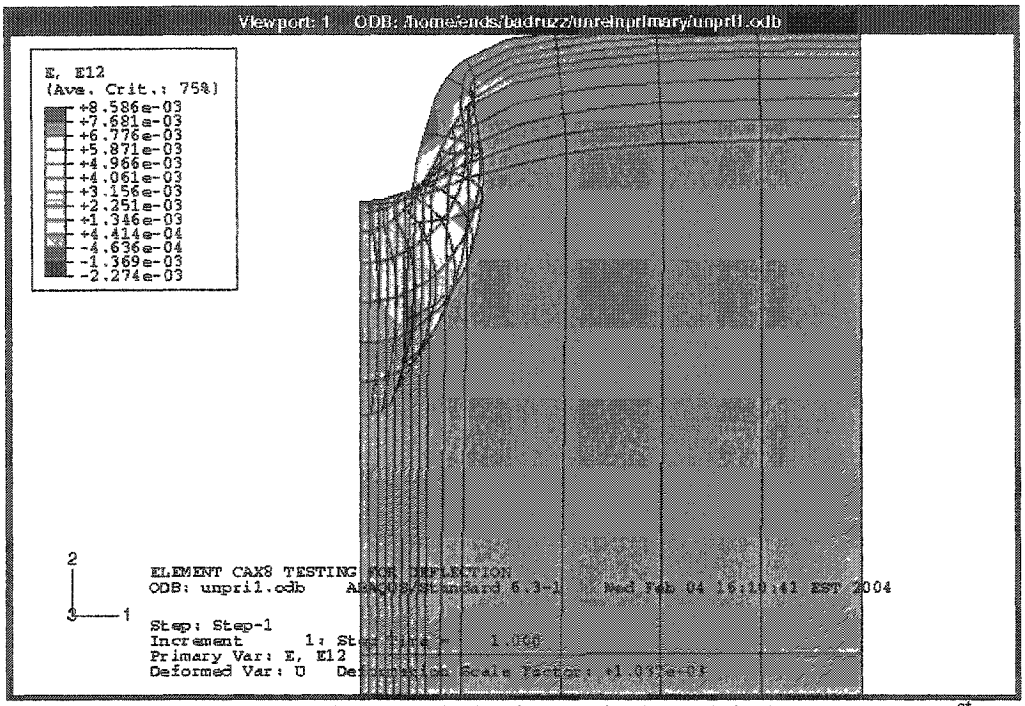

Figure C.9 Contour of shear strain in the vertical- radial plane (E12) at 1st pass for primary structure

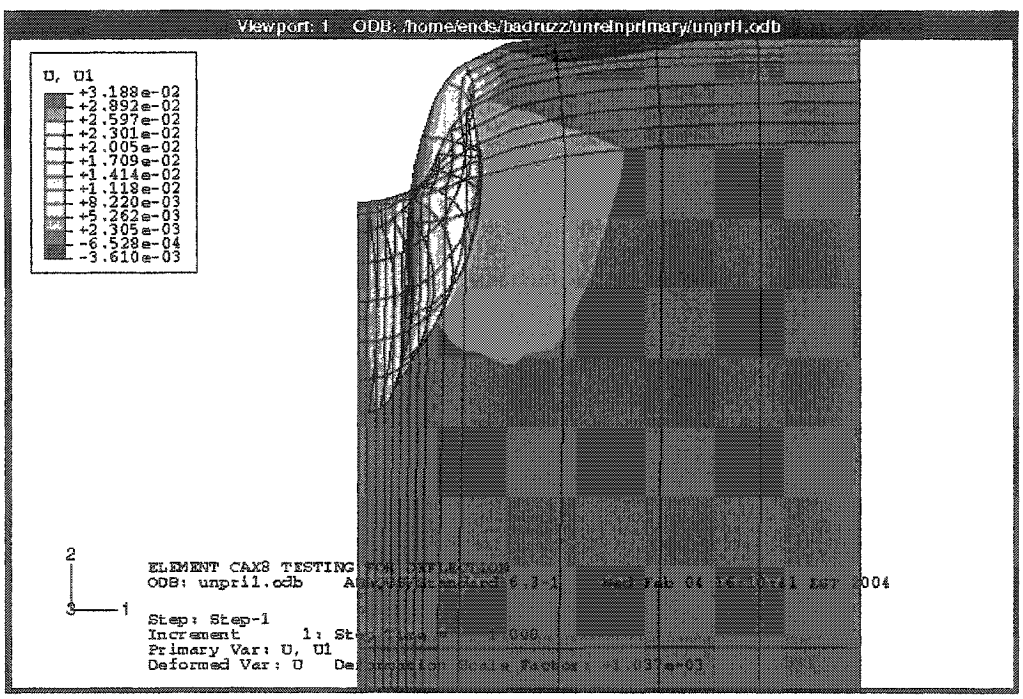

Figure C.10 Contour of deflections in the radial direction (U1) at 1st pass for primary structure

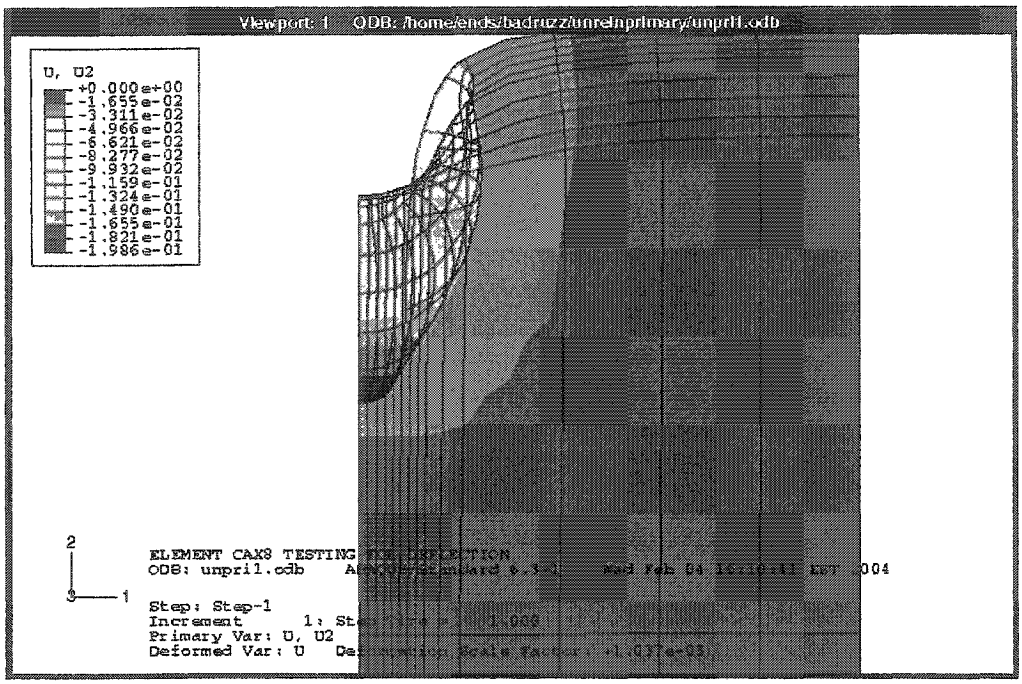

Figure C.11 Contour of deflections in the vertical direction (U2) at 1st pass for primary structure

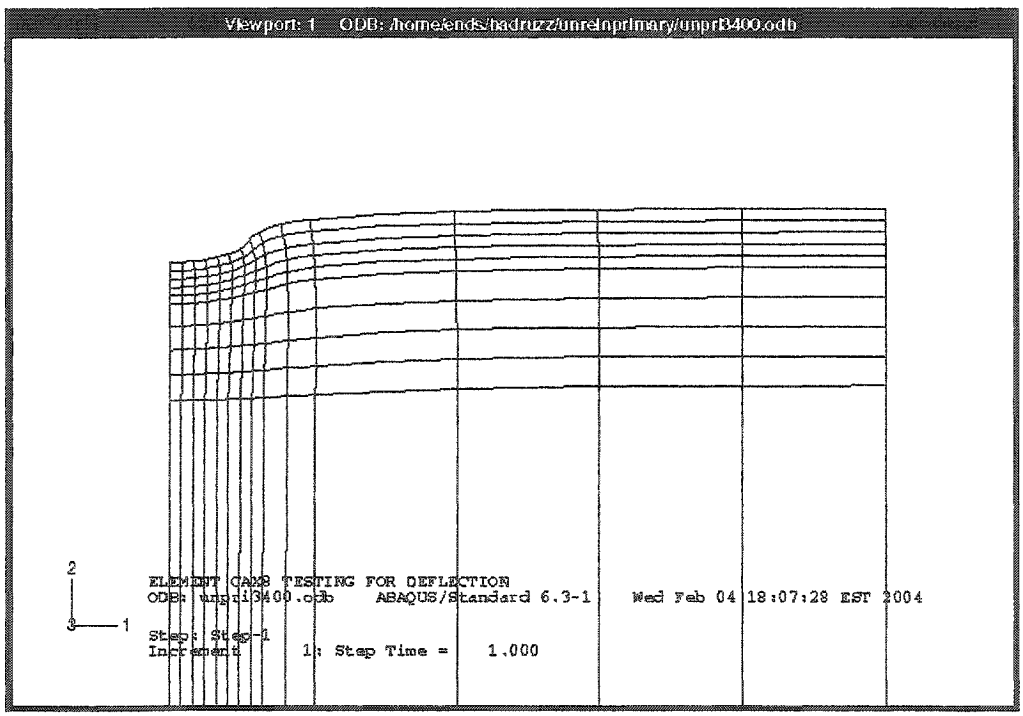

Figure C.12 Contour of deformed mesh at 3400th pass for primary structure

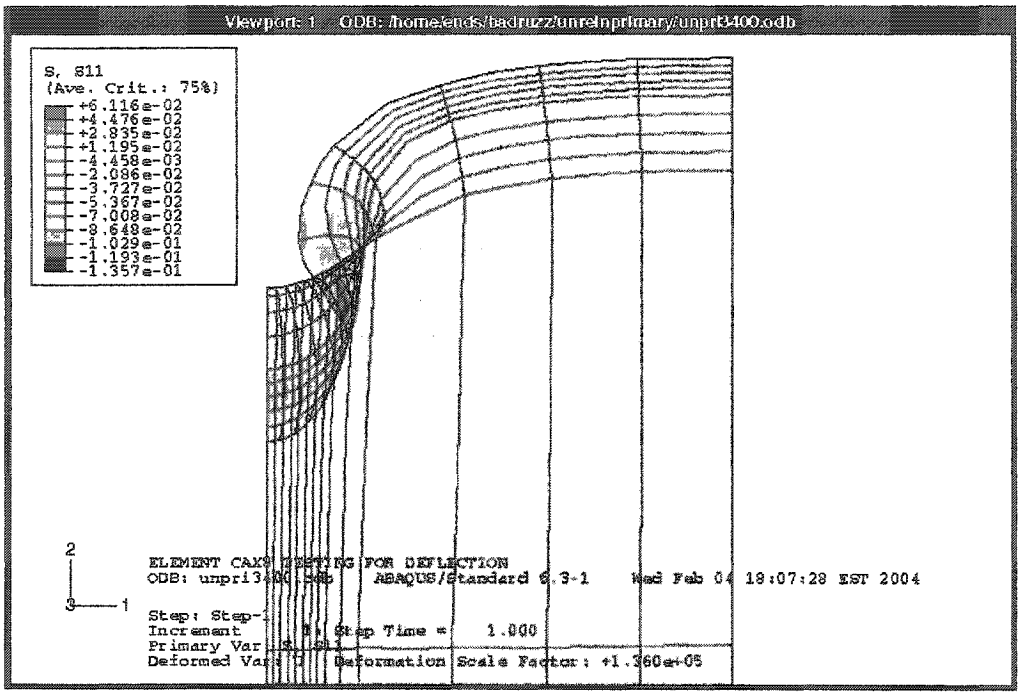

Figure C.13 Contour of normal stress in the radial direction (S11) at 3400th pass for primary structure

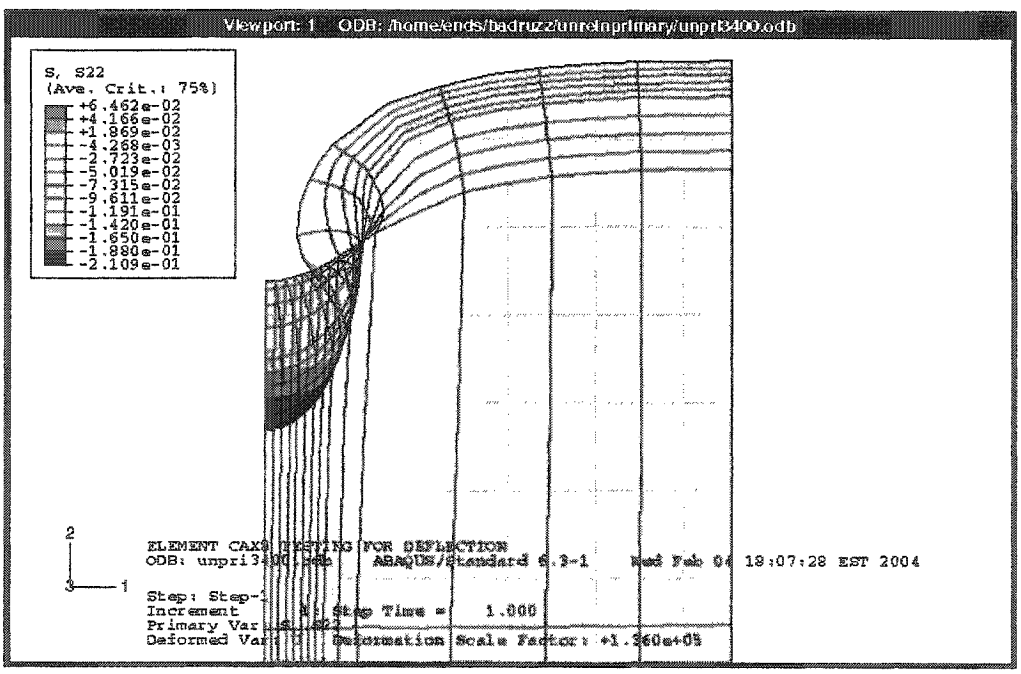

Figure C.14 Contour of normal stress in the vertical direction (S22) at 3400th pass for primary structure

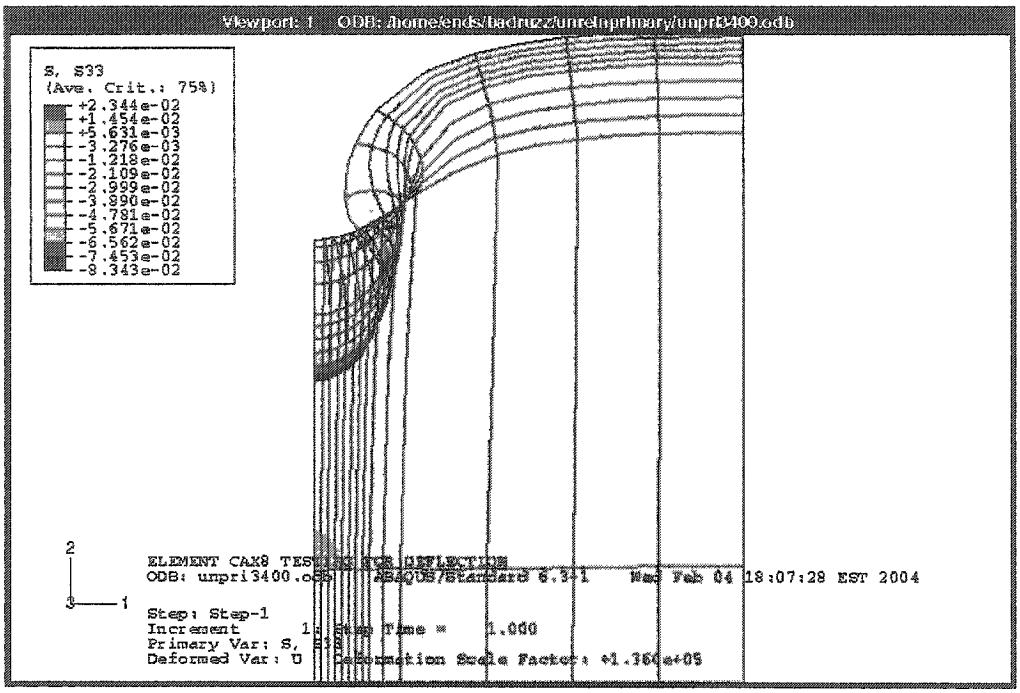

Figure C.15 Contour of normal stress in the circumferential direction (S33) at 3400th pass for primary structure

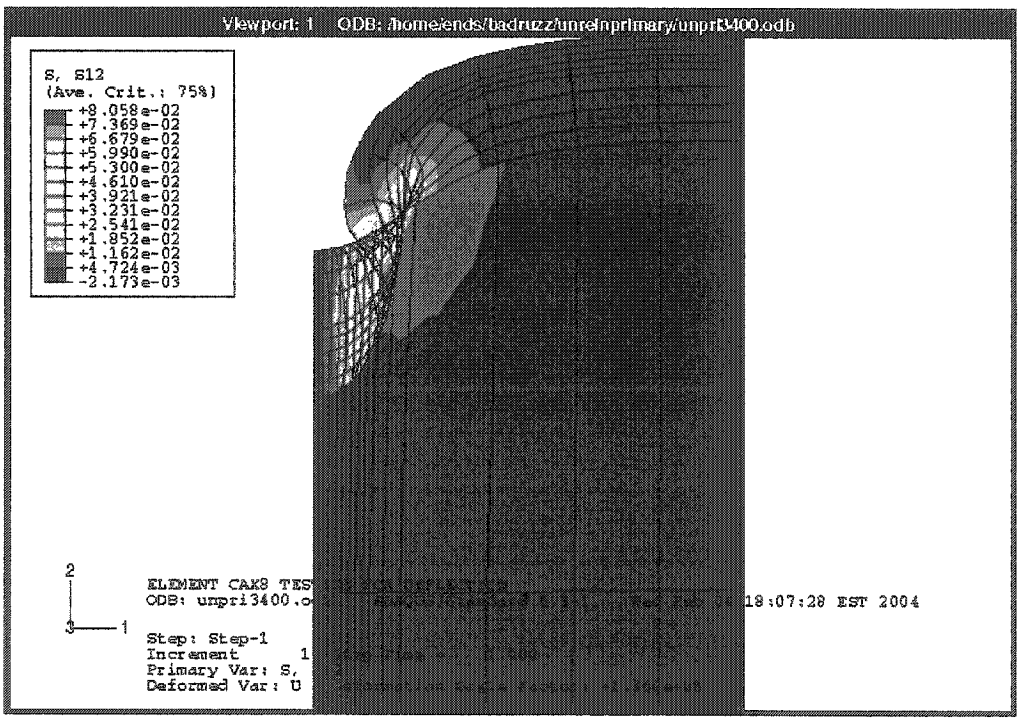

Figure C.16 Contour of shear stress in the vertical- radial plane (S12) at 3400th pass for primary structure.

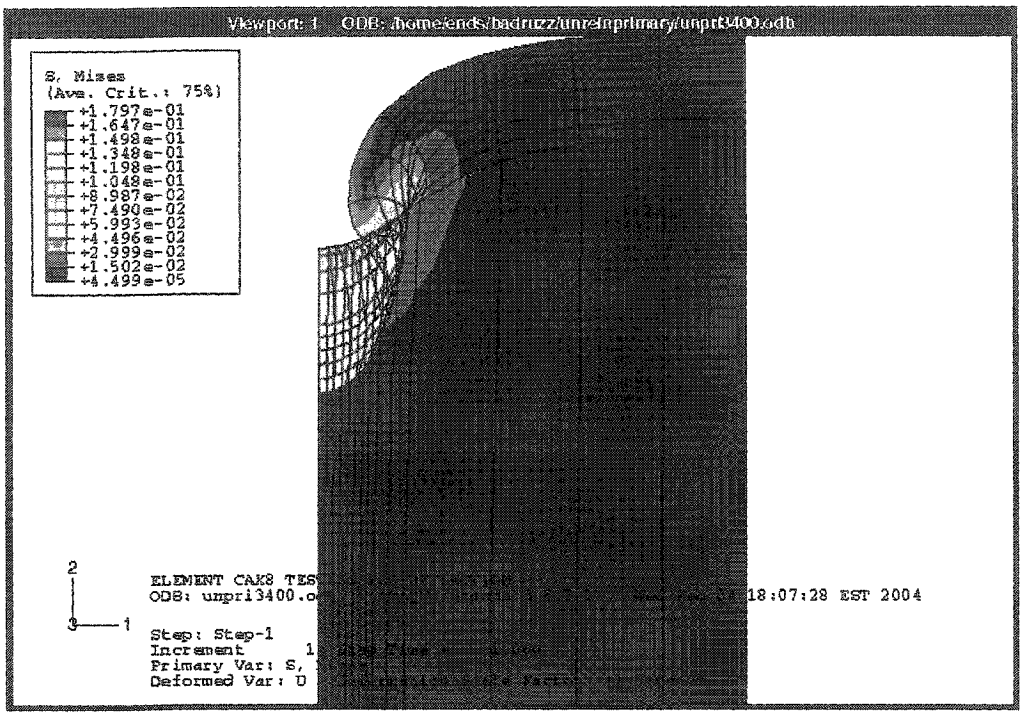

Figure C.17 Contour of Von Mises stress at 3400th pass for primary structure

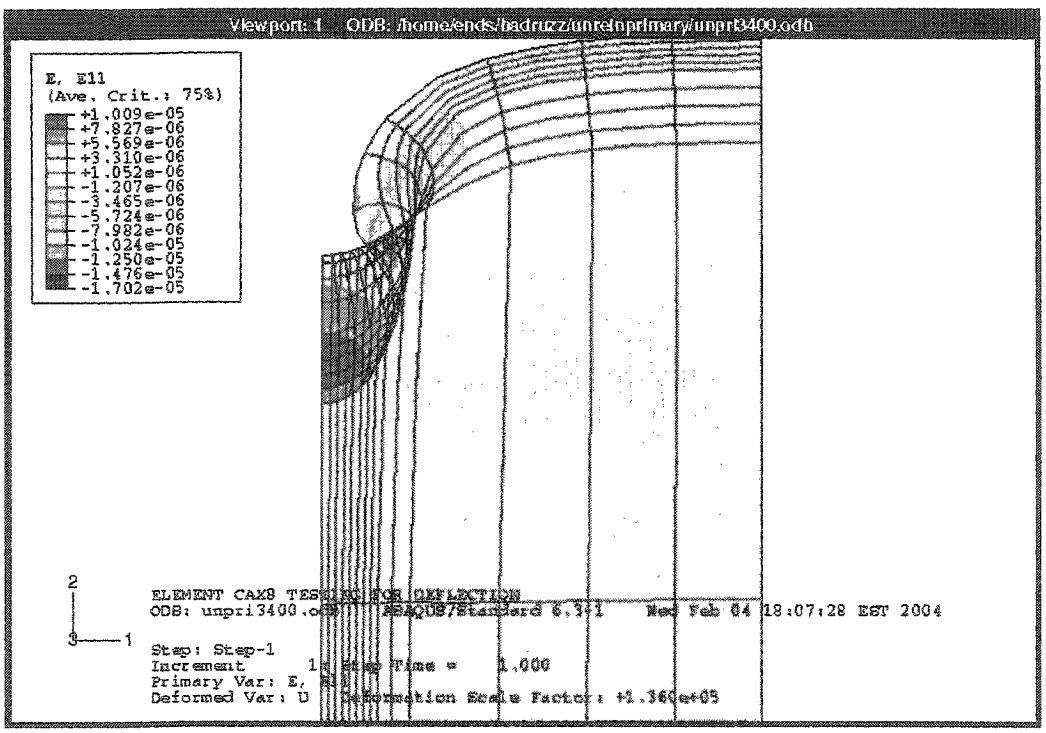

Figure C.18 Contour of normal strain in the radial direction (E11) at 3400th pass for primary structure

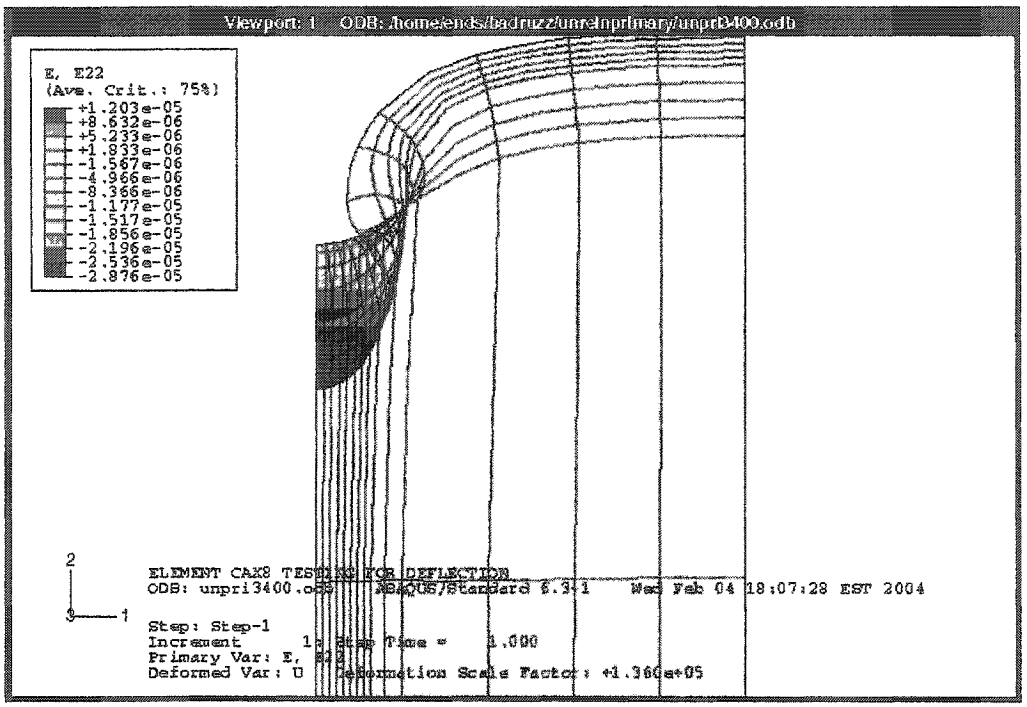

Figure C.19 Contour of normal strain in the vertical direction (E22) at 3400th pass for primary structure

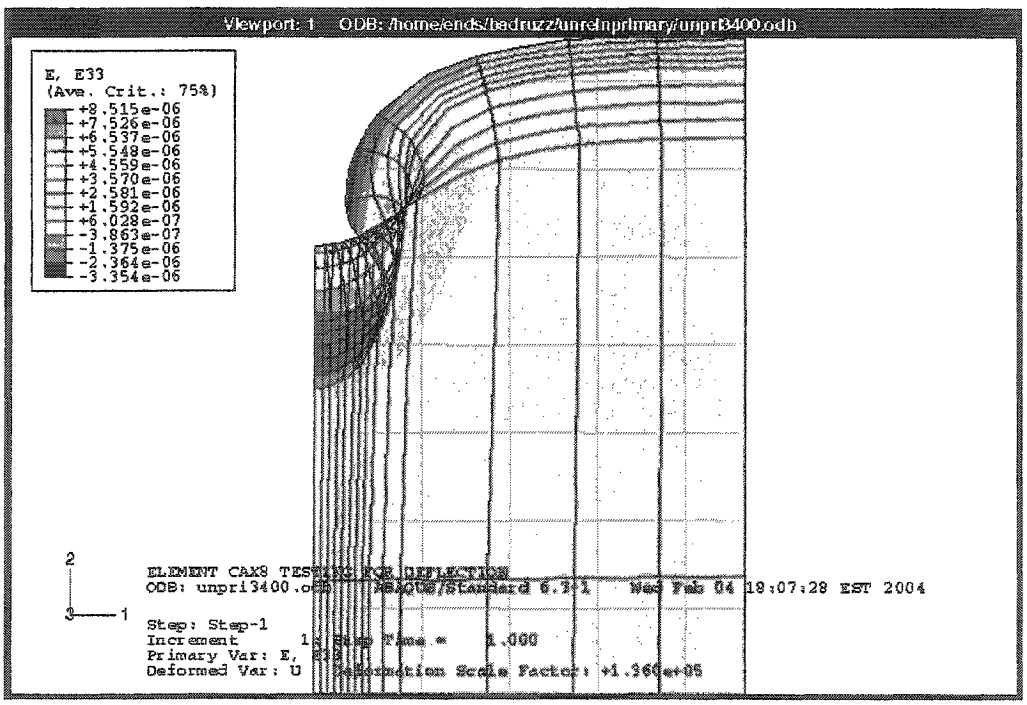

Figure C.20 Contour of normal strain in the circumferential direction (E33) at 3400th pass for primary structure

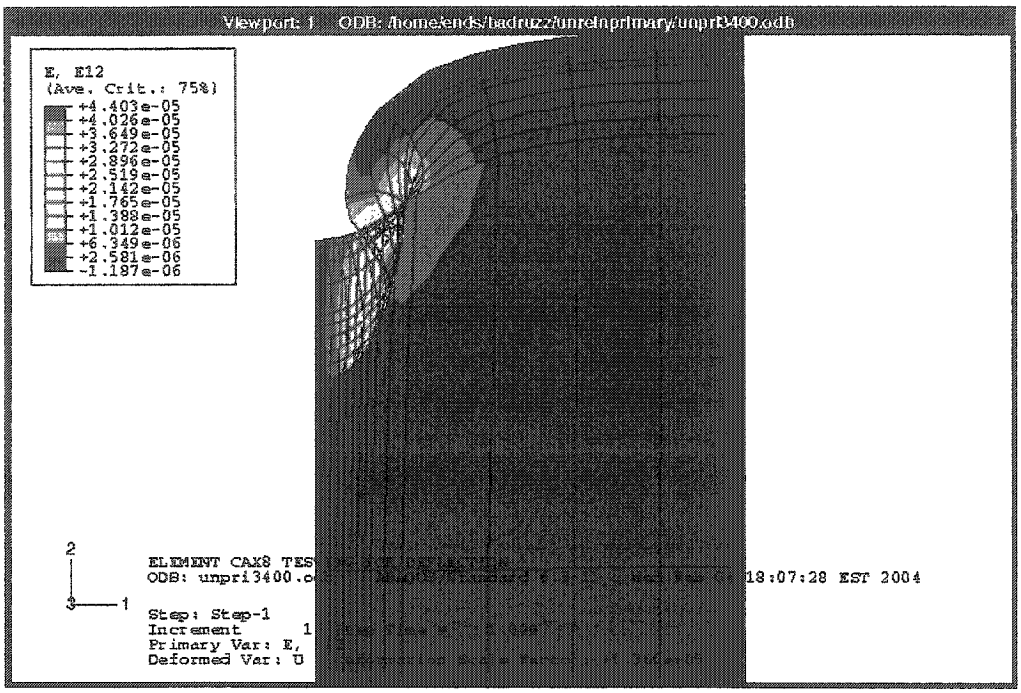

Figure C.21 Contour of shear strain in the vertical- radial plane (E12) at 3400th pass for primary structure

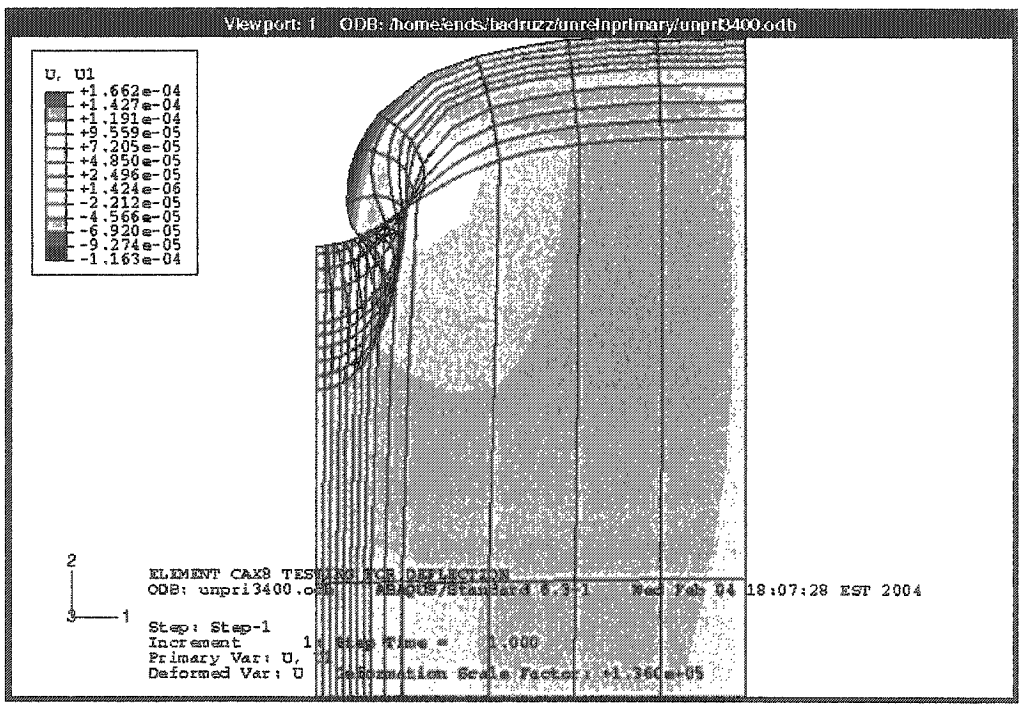

Figure C.22 Contour of deflections in the radial direction (U1) at 3400th pass for primary structure

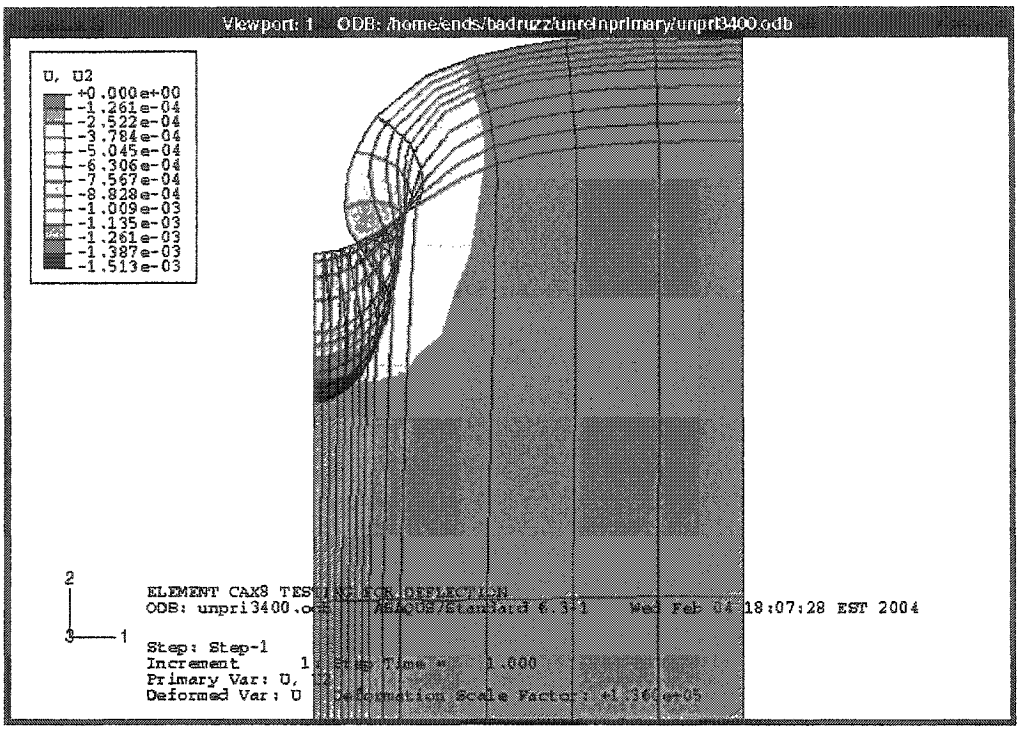

Figure C.23 Contour of deflections in the vertical direction (U2) at 3400th pass for primary structure

VITA AUCTORIS

Md. Badruzzaman was born on October 02, 1976 in Dhaka, Bangladesh. He graduated on June 2000 with B.Sc Degree in the Department of Civil Engineering from Bangladesh University of Engineering and Technology (BUET).

After graduation, he worked in Hivertech Limited, a local reputed Construction and Design Company as a Civil Engineer for 1½ years. After that he got admission at University of Windsor and started his M.A.Sc (thesis based) Program from September 2002. He is currently a candidate for the Master of Applied Science Degree in Civil Engineering at University of Windsor. He hopes to complete the degree requirement in April 2004.